Bendix **Guidance Systems Division**

FINAL SUMMARY REPORT

ADVANCED

CONTROL MOMENT GYRO

DEVELOPMENT

MSFC CONTRACT:

NAS8-25756

1974

PREPARED BY:

THE BENDIX

CORPORATION

GUIDANCE SYSTEMS

DIVISION

TETERBORO,

NEW JERSEY 07608

PREPARED BY:

J. M. Kolvek

J. M. KOLVEK

APPROVED BY:

R. F. CARLISLE

TABLE OF CONTENTS

TABLE OF CONTENTS (CONTINUED)

TABLE OF CONTENTS (CONTINUED)

PAGE NO.

INTRODUCTION

During the 4 year period from 1970 to 1973 the Bendix Guidance Systems Division (BGSD) of the Bendix Corporation developed and delivered to Marshall Space Flight Center (MSFC) several items of advanced Control Moment Gyro (CMG) prototype and breadboard equipment for MSFC evaluation under Contract NAS8-25756. The equipment developed addressed the following goals as desired improvements over the existing Skylab ATM CMG;

1. Useful life of 2 years without repairs.

2. Useful life of 5 to 10 years with minimum parts replacement.

3. Repairability in minimum time and with low order skills.

4. Improved wheel spin up time.

5. Wheel Speed Control.

6. Increased torque output. (T_O)

7. Increased bandwidth. (BW)

8. Brushless D C (BDC) Spin Motors, Gimbal Torquers and Gimbal Tachometers with associated Pulse Width Modulated (PWM) electronics.

9. Unlimited Gimbal freedom.

10. Increased Angular Momentum.(H)

The development effort resulted in the following evaluation test articles which are reported upon in the ensuing sections of this report;

1. A complete 2000FT-LB-SEC Double Gimballed CMG (DG CMG) incorporating all of the desired improvements. This CMG, with test equipment, was delivered on consignment to MSFC in June, 1972 for MSFC evaluation. Section 1 reports on this effort.

2. A 6000FT-LB-SEC Inner Gimbal and Rotor Assembly (IGRA) and associated breadboard spin control electronics incorporating 3 phase A-C spin motors with variable voltage and frequency spin control electronics. This IGRA was to have been consigned to MSFC at the end of 1973 for evaluation. A new outer gimbal and frame was constructed to support this IGRA during a possible future construction and assembly of other CMG subassemblies necessary to provide a full DGCMG for evaluation. The equipment was destroyed in an explosion accident on October 25, 1973 when the rotor experienced a burst failure. Section 2 reports on this effort.

3. Space Replaceable Spin Bearings were developed and incorporated in the above test articles. Section 3 reports on this effort.

4. An electronic breadboard was designed and constructed to demonstrate feasibility of electronic replacement for Flex

Leads or Slip Rings to provide unlimited CMG gimbal freedom. This breadboard was delivered to MSFC for evaluation in February, 1973. Section 4 reports on this effort.

During the contract, BGSD also delivered documentation in the form of Monthly Progress Reports, Technical Memorandums, copies of Viewgraph Design Review Presentations and Engineering Drawings. This report is the Final Contract Summary Report.

Acknowledgement is given to the following Bendix personnel for their design and development efforts during the conduct of this program and for their contributions to this report.

R. Abramowitz	C. Gurrisi	H. Schulien
J. Bertini	S. Haddad	M. Seitzman
P. Burke	P. Imbeninato	T. Sheppard
A. Carriero	H. Kalfaian	S. Stein
P. Dubas	S. Lamberski	W. Teimer
G. Edson	G. Metz	J. Ukstins
A. Esser	J. Pierry	R. Weiss
S. Froman	L. Pursiano	T. Wheelock

SECTION 1

ADVANCED CMG DEVELOPMENT

2000H DG CMG
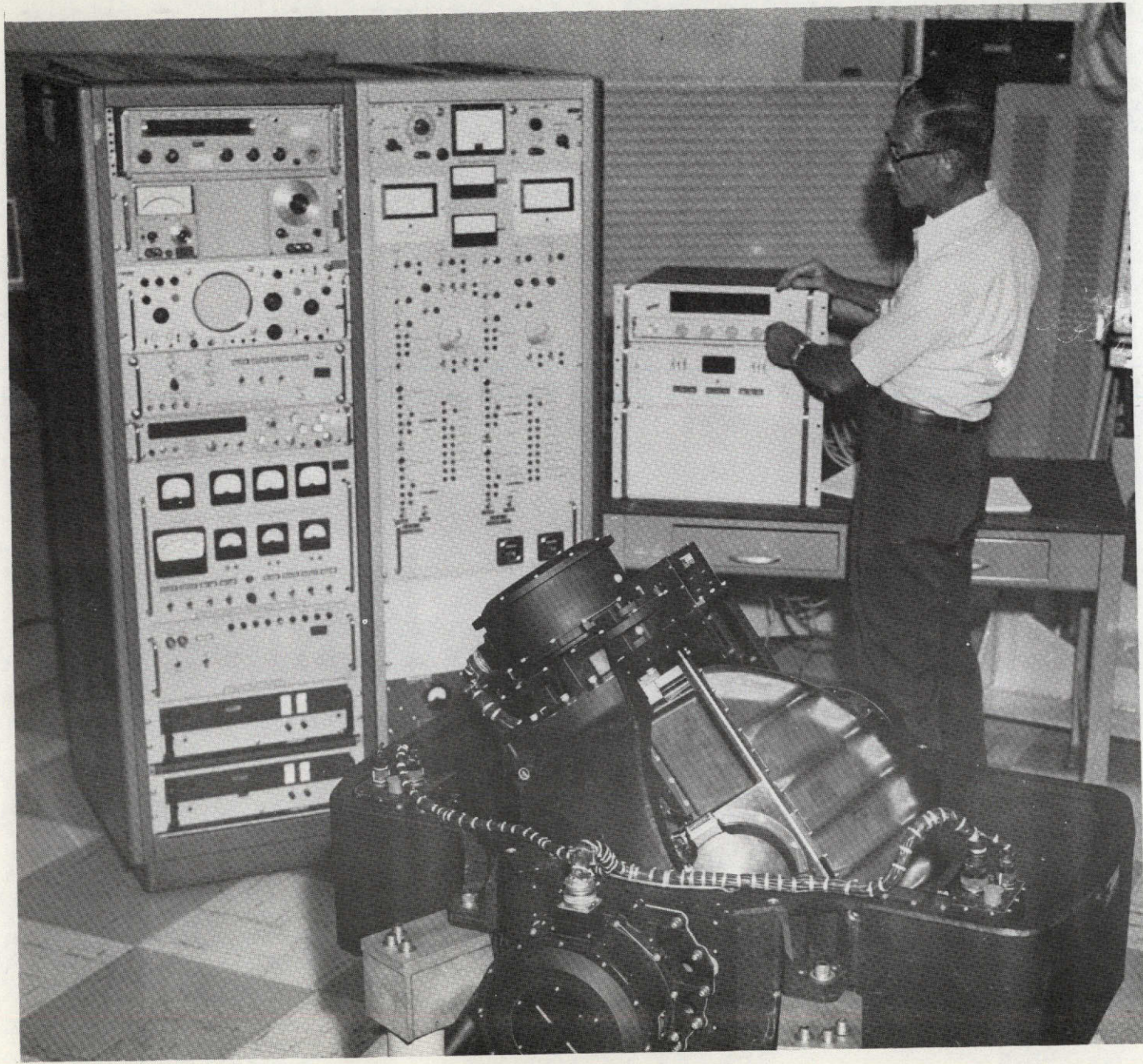
2000 FPS DGCMG

FIGURE 1.1-1

1.1 GENERAL

The advanced 2000FT-LB-SEC. Double Gimballed Control Moment Gyro (2000FPS DG CMG) developed under this contract is shown in Figure 1.1-1, under evaluation test at MSFC. The CMG and its test panels and cables were delivered to MSFC in June, 1972 for MSFC evaluation. All goals were met with the exception of the gimbal rate loop bandwidth and cross coupling between gimbals as a function of frequency.

The basic concept for this CMG was to use the desirable features of the Skylab ATM CMG and incorporate new features based on new technology as well as provide for new and changing Pointing Control System requirements for potential future missions. As a result, the following design philosophy was adopted for the various subassemblies of the DG CMG;

a. Inner Gimbal and Rotor Assembly (IGRA)

Use the same wheel (rotor), gimbal, strut, covers, performance monitors and wheel suspension system as that employed in the Skylab ATM CMG. The wheel suspension system consists of the spin bearings, their lubrication technique, the lubricant sealing technique and the bearing preload technique. The desired changes included Brushless D-C Spin Motors and replaceable spin

bearings. Since the desired angular momentum was essentially the same as that of the ATM CMG, MSFC provided a full ATM CMG engineering IGRA as GFE to be reworked and used as the IGRA for this DGCMG. The reworks that were provided included:

1. Replacing the A-C spin motors with BDC spin motors.

2. Incorporating replaceable spin bearings. This required internal IGRA harness and connector re-design to allow bearing replacement without soldering operations.

3. Provisions to mount the electronics, for BDC spin motor control, on the gimbal of the IGRA.

b. Outer Gimbal (O.G.)

Since an ATM Type IGRA was to be used, MSFC also furnished, as GFE, an available ATM CMG O.G. to be reworked as required for use in this CMG assembly.

c. Frame

A new frame had to be designed and built to provide for O.G. swing due to the size of the new gimbal actuator and sensor pivot assemblies. The frame was also designed so that the full CMG would fit and be capable of mounting on the existing ATM CMG Torque Measurement Fixture.

d. Frame Covers

These covers were not required for this prototype development unit.

e. Actuator Pivot Assemblies (O.G. and I.G.)

These assemblies were new designs incorporating BDC Torquers, BDC Tachometers and improved gearing of the ATM CMG actuator type. Their mounting to the CMG gimbals is identical to that provided in the ATM CMG.

f. Sensor Pivot Assemblies (O.G. and I.G.)

These assemblies were new designs incorporating slip rings for unlimited gimbal freedom, a resolver for gimbal angle readout and a brush type tachometer operating at gimbal speed for engineering evaluation measurements. Their mounting to the CMG gimbals is identical to that provided in the ATM CMG.

g. Electronics

All electronics required for wheel control and gimbal control was mounted on the CMG. i.e. The wheel control electronics is mounted on the inner gimbal (on the IGRA); the inner gimbal control electronics is mounted on the outer gimbal; the outer gimbal control electronics is mounted on the frame. The electronic design provided high efficiency Pulse Width Modulated (PWM) drivers for the spin motors and gimbal torquers and

all power supplies, regulators, control loop circuits, monitor conditioners and interfacing circuits required. Although the circuits were provided on printed circuits boards, high density packaging was not desired or provided in order to allow for ease of engineering circuit development measurements and changes in this prototype DGCMG.

h. Wheel Control

Wheel speed (and therefore H) control is provided closed loop by the spin motor and its control electronics. To provide a range of angular momentum (H) for engineering evaluation, the electronics provides the ability to set the wheel operating speed at 4,000 rpm (H=1000 FT-LB-SEC.), 8,000 rpm (H=2000 FT-LB-SEC.) or 12,000 rpm (H=3000 FT-LB-SEC.). The nominal design point for the complete system was chosen to be 8000 rpm (H=2000 FT-LB-SEC.) operation. Speed control is provided to an accuracy of less than 0.1 percent, within the torque capabilities of the spin motors, and wheel spin up time to 8,000 rpm is nominally 2 hours.

i. Gimbal Control (O.G. and I.G.)

Unlimited gimbal freedom is provided on both gimbals by virtue of slip rings in the sensor pivot assemblies. The gimbal rate control loops provide for a nominal peak gimbal rate

of 5 deg/sec with the ability to command 30 deg/sec O.G. maximum
rate as a function of relative gimbal angle. For simplicity
and identicality of circuits, both the IG and OG command rate
limit was set at 30 deg/sec. Gimbal angle is measured by the
sensor pivot assembly resolvers for use as test monitors and/or
data for momentum management. The peak CMG output torque was
set at 175 FT-LB for each axis at 2000 FT-LB-SEC. (8,000 rpm)
angular momentum operation.

    j.   Environmental Guidelines

        The DG CMG design provides for operation in the
same environments as the ATM CMG. The detail guidelines imposed
are defined in MSFC document 50M22162.

1.2 SYSTEM DESCRIPTION

1.2.1   Physical and Performance Characteristics

The advanced 2,000 FPS DG CMG depicted in Figure 1.1-1 (Bendix Part No. 2123625) has the following major physical and performance characteristics;

PHYSICAL

Configuration: Similar to the ATM CMG, but all electronics is mounted on the gimbals and frame.

Weight: 558 Lbs.

Mounting: Four point C.G.

External Finish: Black (anodized parts and painted parts)

PERFORMANCE

Stored Angular Momentum (H), FPS: Nominal 2000 (8000 RPM)

Set   1000 (4000 RPM)

Set   3000 (12000 RPM)

Max. Output Torque (To), FP: 175 simultaneous on both gimbals.

200 minimum on one gimbal.

Threshold Moment, FP: 0.0175

Degrees of Freedom: two-unlimited rotation (no stops)

Max. Gimbal Rates (Wg), deg./sec.: 5 nominal each gimbal.

PERFORMANCE (Continued)

Max. Gimbal rates (Wg), deg./sec.: (continued)

> O.G. can be driven
> at 30 max. as a
> function of relative
> gimbal angle.

Threshold Rate, deg./sec.: 0.0005

Bandwidth: 5HZ to 30 HZ at 2000 FPS. (over the gimbal

range and from 0.25 to 5 deg./sec. command

rate range).

Wheel Spin Up Time, hours: 2.5 to 2000 FPS (8000 RPM)

Wheel Deceleration Time, hours: 1.75 to 1000 RPM from

8000 RPM (Regenerative

Braking).

Wheel Speed Control: less than 0.1 percent.

Power at nominal 28 V. D-C Line and 2000 FPS (8000 RPM)

operation:

Wheel Control System

> Spin Up Peak (2 motors): 400 W. (Just before synch.
> speed).

> Running (1 motor): 50 W.

Gimbal Control System

> Peak: 450 W. (At simultaneous 5 deg./sec. or

> 175 FP from each gimbal).

Spin Bearing Heaters: 48 W. or 120 W. Available (24 W.

or 60 W. each Bearing).

OTHER KEY CHARACTERISTICS

IGRA: Rotor   Rimmed disc of 18 Ni 300 Maraging Steel.

Rotor Diameter   22 inches

Rotor Weight   145 pounds

Rotor operating speed   4000 to 12000 RPM

Spin Motor   2 Two Phase BDC (Hall Commutated)

Monitors: Redundant Bearing Thermisters - 2 per bearing.

Redundant Speed Measurement

Cavity Pressure for ground test use.
Bearing Vibration for ground test use.
Manually Operated Evacuation Valve.

Each Actuator Pivot Assembly:

Gear Ratio   28 to 1

Torque Motor: 1 Two Phase BDC (Hall Commutated)

Tachometer: 1 Two Phase BDC (Hall Commutated)

Provision to increase torque motor inertia for Eng'g. test.

Each Sensor Pivot Assembly:

Slip Ring Assembly

Gimbal Position Pickoff   1 Resolver

Gimbal Tachometer (Eng'g. Test)   TG 4401B, 3.9V/rad./sec.

1.2.2 System Block Diagram

Figure 1.2-1 is a block diagram of the electromechanical functional elements of the DGCMG. The control of the DGCMG is shown divided into 3 independent control subsystems, namely Wheel Control (Inner Gimbal and Rotor Assy.), Inner Gimbal Control and Outer Gimbal control. The DGCMG was constructed to provide independent wiring for these three control subsystems. Power, command and monitoring was provided on a manually operated test panel such that each control subsystem could be operated alone or in combination for engineering development flexibility.

The Wheel Control subsystem is made up of two 2 phase BDC Spin Motors and their associated Hall Commutation and speed control electronics, one for each phase. Each phase electronics package is independent of the other three (including wiring) for separate external CMG control during engineering studies. With this arrangement, wheel run-up can be accomplished with any two phases with an increase in run-up time. In addition, having attained speed, any one phase will hold speed to a degraded accuracy. Normal run-up is accomplished with two complete spin motor control channels (4 phases) and normal operation at speed is provided by one of the two spin motors and its two phases of electronics. External CMG manual monitoring provisions includes redundant IGRA cavity vacuum sensors, redundant spin bearing

ADV. 2000H DGCMG BLOCK DIAGRAM
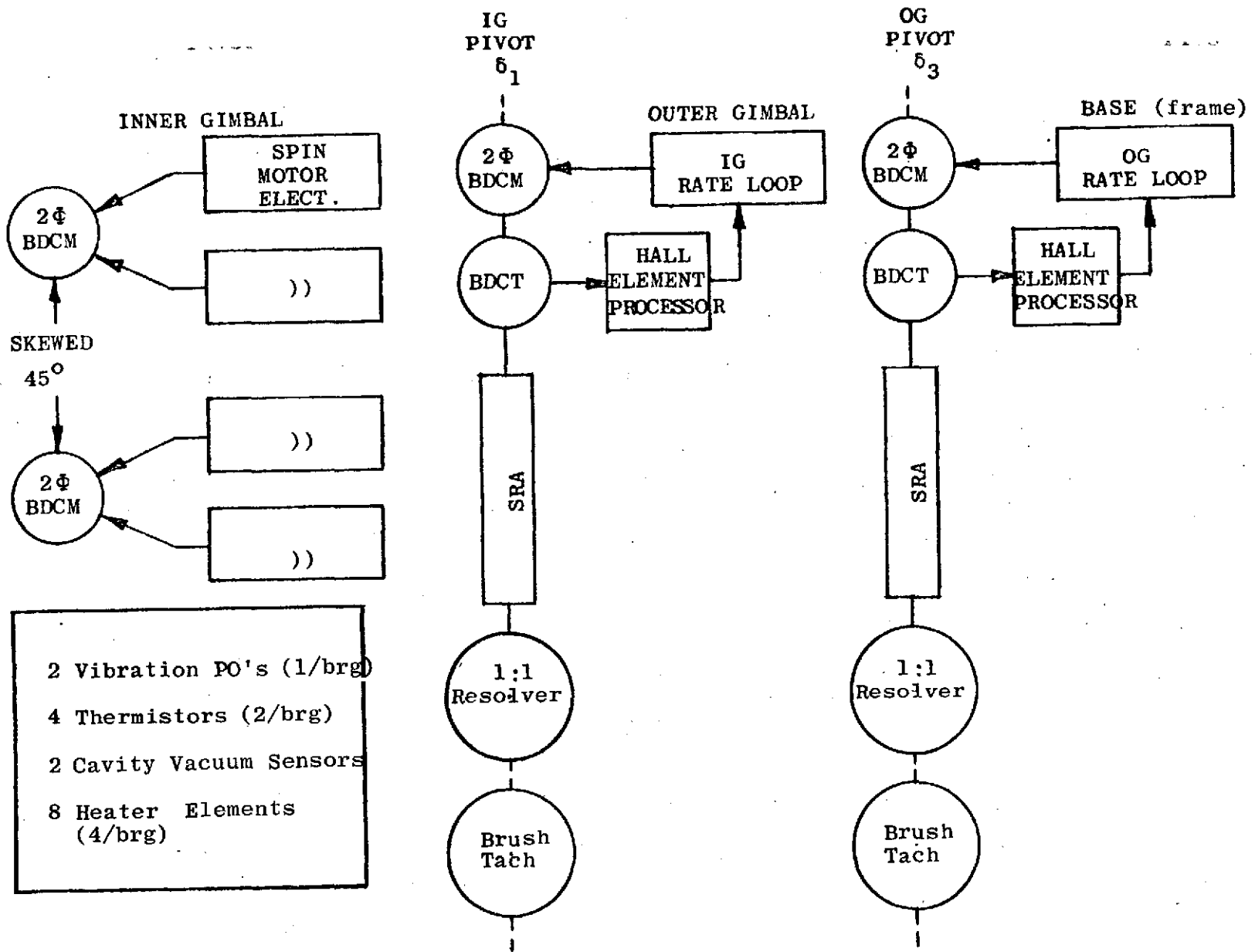
FIGURE 1.2-1

thermisters, spin bearing vibration pickoffs and speed measurement from the Hall element electronics. Speed selection is externally set by application of one of the three set frequencies for H=1000, 2000, 3000 FPS (Speed = 4000, 8000, 12000 RPM). Heater excitation is also externally applied as desired for engineering testing. Provision for rapid wheel run down (rather than a long power off coast down) was made in the manual test and control panel furnished with the DGCMG. The DC Brake switch disconnects the spin notor electronics 28V. DC power lines from their power sources and connects the lines across power resistors located in the test panel. Procedurally, at 1000 RPM the DC brake is to be turned off.

Each Gimbal Control subsystem is made up of a two phase BDC Torquer and Tachometer, with their associated Hall commutation and gimbal rate control electronics. External CMG manual monitoring capability includes gimbal angle provided by the resolvers, gimbal rate provided by a brush type Tachometer (for engineering test) and motor rate from the BDC Tachometer electronics. Gimbal rate command is externally applied by the application of an analog $\pm$ 10V. D-C signal to the rate loop electronics.

The slip ring assemblies (SRA) provide for the trans-

mission of all power and signal data across the gimbal pivots thereby allowing unlimited gimbal freedom.

1.2.3   System Electrical Interfaces

The system electrical interfaces are shown in Figures 1.2-2 through 1.2-5 representing five external cable connectors.

+28V. DC Side 1 ⌀A   A,C,E
   OV. DC   B,D,F
   Pwr. Shield   G   IGRA Side 1
+28V. DC Side 1 ⌀B   H,K,M   Spin Motor Pwr.
   OV. DC   J,L,N
   Pwr. Shield   P

+28V. DC Side 2 ⌀A   R,T,V
   OV. DC   S,U,W
   Pwr. Shield   X   IGRA Side 2
+28V. DC Side 2 ⌀B   Y,a,c   Spin Motor Pwr.
   OV. DC   Z,b,d
   Pwr. Shield   e

120W. Brg. Htr Side 1   f,g
  24W. Brg. Htr Side 1   h
       Htr. Low Side 1   i,j   IGRA Spin Brg.
120W. Brg. Htr Side 2   k,m   Heater Pwr.
24W. Brg. Htr Side 2   n
       Htr. Low Side 2   p,q

+28V. DC I.G. Actuator   r,t,v,x   I.G. Rate Servo Pwr.
   OV. DC   s,u,w,y
   Pwr. Shield   z
   Wired Spares   AA,CC,EE,GG
   Wired Spares   BB,DD,FF,HH

O.G. Sensor Pivot Connector
JT 02 RE-22-55P

Electrical Interface

FIGURE 1.2-2

I.G.R.A. Side 1

Pin Nos.		Pin Nos.
1,2	Brg. Thermistor	33,34
3,4	Brg. Thermistor	35,36
5	Vac. Gauge Input	37
6	Vac. Gauge Input	38
7	Spare	39
8	+28V. DC Vib. Mon.	40
9	0V. DC	41
10	Vib. Mon. Self Test	42
11	Vib. Mon. Output	43
12	Shield	44
13	Int./Ext. Freq. ØA	45
14	Ext. Freq. Input ØA	46
15	Speed Meas. ØA	47
16	Speed Comm. ØA	48
17	-5V. DC Brake ØA	49
18,19	Motor I Mon. ØA	50,51
20	Sig. Gnd. ØA	52
21	Sig. Shield ØA	53
22	Int./Ext.Freq. ØB	54
23	Ext. Freq. Input ØB	55
24	Speed Meas. ØB	56
25	Speed Comm. ØB	57
26	-5V. DC Brake ØB	58
27,28	Motor I Mon. ØB	59,60
29	Sig. Gnd. ØB	61
30	Sig. Shield ØB	62
31,63	+28V. DC Sig. Cond.	32,64
	Spare	65

I.G.R.A. Side 2

O.G. Sensor Pivot Connector JT02RE-20-2P

Electrical Interface

FIGURE 1.2-3

Signal	Pin	Group
I.G. Rate Comm. (Diff.)	1	
I.G. Rate Comm. (Diff.)	2	
I.G. Motor Tach. (Test)	3	
I.G. Error Rate	4	I.G. Rate
I.G. Motor Tach. (Monitor)	5	Servo Sig's.
Spare	6	
I.G. Servo Sig. Gnd.	7	
Sig. Shield	8	
I.G. Gimbal Tach.	9	I.G.
I.G. Gimbal Tach.	10	Gimbal Rate
I.G. Gimbal Rslvr. Excit.	11,12,13,14	
Sine Rslvr Sig.	15,16	
Cos. Rslvr Sig.	17,18	I.G. and O.G.
O.G. Gimbal Rslvr. Excit.	19,20,21,22	Gimbal Angle
Sine Rslvr Sig.	23,24	
Cos. Rslvr Sig.	25,26	
I.G. Torquer 0 Deg. ϕI (Test)	27	I.G.
I.G. Torquer 90 Deg. ϕI (Test)	28	Torquer
IGRA Vacuum Gauge Output (1,000)	29,30	I.G.R.A.
IGRA Vacuum Gauge Output (20,000)	31,32	Cavity Vacuum
O.G. Gimbal Tach.	33	O.G.
O. G. Gimbal Tach.	34	Gimbal Rate
O.G. Sensor Pivot Thermistor	35,36	Ext. CMG Temp.
Spares	37-52	
CMG Chassis Ground	53	

O.G. Sensor Pivot Connector
JT 02 RE-18-53P

Electrical Interface

FIGURE 1.2-4

```
                                          Pin Nos.

+28V. DC O.G. Actuator          ----⊗----  A,C,E,G      O.G.
        OV. DC                  ----⊗----  B,D,F,H      Rate Servo
Pwr. Shield                     ---------  P            Pwr.


O.G. Torquer 0 Deg. ∅I (Test)----------   J            O.G.
O.G. Torquer 90 Deg. ∅I (Test)----------  K            Torquer
Spares                          ---------  L,M,N,R
```

<div align="center">

O.G. Actuator Pwr. Electronics
PV7C14B15SNC

</div>

```
                                          Pin Nos.

O.G. Rate Comm. (Diff.)         ----⊗----  A
O.G. Rate Comm. (Diff.)         ----⊗----  B
O.G. Motor Tach (Test)          ---------  C
O.G. Error Rate                 ---------  D
O.G. Motor Tach (Monitor)       ---------  E            O.G. Rate
     Spare                      ---------  F            Servo Sig's.
O.G. Servo Sig. Gnd.            ---------  G
            Sig. Shield         ---------  K
Spares                          ---------  H,J
```

<div align="center">

O.G. Actuator Sig. Electronics
PV7C12B10SNC

</div>

<div align="center">

Electrical Interface

FIGURE 1.2-5

</div>

1.3   Sub-Assembly Descriptions

1.3.1   2000 FPS Inner Gimbal And Rotor Assembly (IGRA)

1.3.1.1   General

The inner gimbal and rotor assembly supplied in the advanced 2000 FPS DGCMG consists of the same proven components that have performed so well in the ATM CMG engineering and production units. These units have performed in extensive ground tests, were qualified for flight and flew as part of the Skylab Orbital Mission. To date, inner gimbal and rotor assemblies have logged a total operating time in excess of 400,000 hours. Three units accumulated in excess of 30,000 hours each in the 3 CMGs on the 3 axis motion similator at MSFC. The three flight units accumulated more than 17,000 hours during the Skylab 270 day orbital mission. The rest of the operating time was accrued during other engineering, qualification and ATM system integration testing.

The inner gimbal and rotor assembly supplied is a reworked version of the ATM E-1 Engineering Unit (GFE) and is characterized by a momentum storage capability of 2000 ft-lb-sec, effected by a 22 inch diameter rotor operating at a speed of 8000 rpm. The reworks included:

1) Replacing the A-C spin motors with BDC spin motors.

2) Incorporating replaceable spin bearings.

3) Provisions to mount the electronics, for BDC spin motor control, on the gimbal of the IGRA.

4) Internal IGRA harness and connector redesign to allow bearing replacement without soldering operations.

The rotor is supported at each end by a single size 107 replaceable bearing, and is restrained such that correct bearing preload is maintained, regardless of orientation and within a wide environment range, during its operation. Lubricant is supplied to each bearing by means of an open loop type system in which the same nut which locks the bearing inner race to the shaft is made hollow and filled with lubricant. An orifice permits the desired quantity of lubricant, which is adjusted for the particular unit duty cycle, to be metered by means of centrifugal force to the retainer of the bearing. This lubricating method is in current use on all current Bendix production and engineering CMGs and on all life test fixtures.

The mechanism of oil transport is entirely insensitive to and independent of gravity and operates through centrifugal force only.

The inner gimbal assembly is so configured that optimum rotor performance is maintained throughout ambient and internal temperature and pressure changes. A principal contributor to this capability is the stiffening strut which connects the two sides of the gimbal and runs through the center of the wheel. This strut increases the apparent stiffness of the gimbal as well as matches the wheel thermal expansion characteristics to that of the gimbal. The efficiency of this configuration has been demonstrated by thermal vacuum testing of the existing ATM CMG design. The entire assembly is fitted with gasket sealed covers in order to provide the lowest possible operating pressure within the inner gimbal cavity. The rotor and inner gimbal assembly is suitably instrumented so that bearing vibration, temperature, rotor speed and cavity pressure may be monitored.

The materials of construction of the rotor and inner gimbal assembly were carefully selected and matched for high stiffness to weight ratios, high strength, correct thermal expansion coefficient balance, and vacuum stability.

Wheel rotation is effected by two highly efficient brushless DC spin motors, the rotors of which are located on the flywheel hub. These motors are direct replacements

of the ATM AC Motors without shaft modification. The
safety factors and natural frequencies of the unit are
the same as for the ATM design.

Factor of Safety (Centrifugal)	5.02
Factor of Safety (Fatigue)	65
Natural Frequency (Fan Mode) CPS	177
Natural Frequency (Umbrella Mode) CPS	445

The IGRA performance goals were as shown in Table 1.3.1-1.
Key detail IGRA design data is listed in Table 1.3.1-2.

1.3.1.2 Wheel Design

No modifications were made to the GFE wheel supplied.
The wheel used in the inner gimbal and rotor assembly
is of one piece construction utilizing type 300 Maraging
steel. This design has been proven to more than satisfy
the necessary system performance requirements including
fatigue loading, centrifugal stress and any possible
rapid shutdown stress (i.e. the ATM CMG has a centrifugal
stress safety factor of 5.0 and can tolerate being decel-
erated from full speed to stop in 0.4 seconds). In addi-
tion to the above, the one piece integral web wheel de-
sign has improved heat transfer which results in lower
bearing and lubricant operating temperatures and a lower

IGRA PERFORMANCE GOALS

		2000 FT-LB-SEC UNIT
1.	ANGULAR MOMENTUM (NOMINAL)	2000 FT-LB-SEC ± 5%
2.	RUN UP TIME TO RATED ANGULAR MOMENTUM USING 2 SPIN MOTORS	NOMINALLY 2 HOURS
3.	ANGULAR VELOCITY AT NOMINAL MOMENTUM.	8000 ± 160 RPM
4.	BEARING AND MAGNETIC DRAG (AT RUN)	LESS THAN 4 OZ-IN.
5.	THE UNIT SHALL NOT REQUIRE DYNAMIC BALANCING AFTER IN-STALLATION OF NEW BEARINGS	
6.	MAXIMUM ANGULAR MOMENTUM CAPABILITY DEMONSTRATED BY A 15,000 RPM OVERSPEED TEST	3000 FT-LB-SEC.

TABLE 1.3.1-1

INNER GIMBAL AND ROTOR ASSEMBLY DESIGN DATA

ITEM	2000 IGRA
NOMINAL ANGULAR MOMENTUM (FT-LB-SEC)	2000
NOMINAL SPEED (RPM)	8000
RUN UP TIME TO NOMINAL SPEED (HRS.) MAX.	2
MAXIMUM ANGULAR MOMENTUM (FT-LB-SEC)	3000
MAXIMUM OPERATING SPEED (RPM)	12,000
IGRA WEIGHT (LBS.)	230
MAXIMUM GIMBAL DIMENSION (IN.)	24.126
MAXIMUM MECHANICAL POWER 8000 RPM (WATTS)	24
WINDAGE POWER – ONE MICRON 8000 RPM (WATTS)	2.87
MAXIMUM MECHANICAL POWER – 12,000 RPM (WATTS)	36
IGRA TORSIONAL STIFFNESS – FT-LB/RAD	425,000
BEARING SPACING (IN)	9.5
DYNAMIC UNBALANCE (MICROINCHES)	50
LUBRICANT FLOW RATE (mg/hr)	0.05
CALCULATED CRITICAL SPEED (RPM)	14,500
ACTUAL CRITICAL SPEED (RPM)	10,000
SPIN AXIS INERTIA (IN-LB-SEC^2)	37.15
TORQUER AXIS INERTIA (IN-LB-SEC^2)	25.35
CROSS AXIS INERTIA (IN-LB-SEC^2)	22.85

TABLE 1.3.1-2

more uniform thermal gradient across the Inner Gimbal and Rotor Assembly. The pertinent wheel design data is listed in Table 1.3.1-3.

1.3.1.3   Gimbal Design

The elliptical gimbal used in the ATM CMG and in the Advanced DGCMG program is of an integral type which allows for extreme accuracy in alignment of the spin axis ball bearings. By surrounding the bearings with an extremely rigid integral gimbal structure, the entire Inner Gimbal Assembly assumes a high torsional and transverse stiffness as well as a high natural frequency. Both the high stiffness and natural frequency are required for improved system performance (i.e. allow for as large a system band width as possible). In addition to the above, the elliptical gimbal provides for relatively thick sections at the bearing and gimbal interface allowing for improved heat transfer in the region of the ball bearings. This type of gimbal also facilitates more rigid mounting of actuators and sensors since they are attached to the major axis of the ellipse. Only slight modifications were made to the gimbal supplied in order to accommodate the Brushless DC Spin Motors. This included an additional connector inlet and some minor

WHEEL DESIGN DATA

ITEM	2000 IGRA
MATERIAL	300 MARAGING
MATERIAL ULTIMATE TENSIL STRENGTH (PSI)	275,000
MATERIAL ENDURANCE LIMIT (PSI)	110,000
WHEEL DIAMETER (IN)	22
WHEEL WEIGHT (LBS)	145
INERTIA SPIN AXIS (IN-LB-SEC^2)	29.4
INERTIAL CROSS AXIS (IN-LB-SEC^2)	16.2
TORSIONAL STIFFNESS (FT-LB/RAD)	1.03×10^6
NOMINAL OPERATING SPEED (RPM)	8,000
CENTRIFUGAL STRESS NOMINAL SPEED (PSI)	57,000
CENTRIFUGAL STRESS SAFETY FACTOR	4.8
FATIGUE STRESS AT 200 FT-LB (PSI)	1,700
FATIGUE STRESS SAFETY FACTOR	65
MAXIMUM PRECESSION TORQUE FT-LB	10,400
MAXIMUM OPERATING SPEED	12,000
CENTRIFUGAL STRESS - MAXIMUM SPEED (PSI)	128,000
CENTRIFUGAL STRESS SAFETY FACTOR	2.2
DESIGN PROOF SPEED (RPM)	15,000
DESIGN BURST SPEED (RPM)	17,500

TABLE 1.3.1-3

INNER GIMBAL DESIGN DATA

ITEM	2000 IGRA
MATERIAL	6061 T-6 ALUMINUM
MATERIAL TENSIL STRENGTH (PSI)	42,000
GIMBAL WEIGHT (LBS)	33
GIMBAL DEPTH (IN)	8.312
GIMBAL WIDTH-SPIN AXIS (IN)	13.250
GIMBAL LENGTH (IN)	24.126
OUT OF PLANE TORSIONAL STIFFNESS (INCLUDING COVERS) FT-LB-/RAD	$.756 \times 10^6$
IN PLANE TORSIONAL STIFFNESS (INCLUDING COVERS) FT-LB-/RAD	$.585 \times 10^6$
GIMBAL WALL THICKNESS (IN)	0.25
GIMBAL CONSTRUCTION	HOLLOW RECTANGLE

TABLE 1.3.1-4

screw holes for attaching some new terminal boards. Key
inner gimbal design data is listed in Table 1.3.1-4.

1.3.1.4   Support System Design

The wheel support system design embodies the proven
bearing support system in use on all current Bendix
CMGs and life test fixtures. In this design, the spin
axis bearings are housed within slider assemblies.
These sliders serve to widen the bearing outer race
and thereby to improve the width to diameter ratio for
stability in sliding. The bearing and slider assembly
is free to move within the beryllium support housings.
These housings located within the elliptical gimbal,
allows the slider assemblies to move axially, as lim-
ited by the belleville preload springs. The housing
contains a steel liner to minimize sliding friction
and a Labyrinth seal which maintains a slightly higher
pressure in the vicinity of the bearings thus minimizing
lubricant vaporization. Attached to the support housings
are beryllium end caps. These caps support the steel
thru-strut which runs through the wheel shaft and ties
together both sides of the gimbal. This strut greatly
increases system rigidity and results in preload insen-
sitivity to temperature and pressure change by virtue

of gimbal, strut and wheel thermal coefficient match.
Affixed to each end of the flywheel is the bearing lubricating nut which serves to lock the bearing to the shaft
and acts as a lubricant supply system, metering centrifugally forced oil to the bearing from its hollow center.
The ball bearing design data is provided in Table 1.3.1-5.

BALL BEARING DESIGN DATA

ITEM	2000 IGRA
BEARING TYPE	MODIFIED 107H
NUMBER OF BALLS	15
BALL DIAMETER	0.3125
BORE (IN)	1.3780
OUTER DIAMETER (IN)	3.000
QUALITY	ABEC 9
BASIC DYNAMIC LOAD RATING (LBS)	3510
LIMITING SPEED (RPM)	25823
NOMINAL CONTACT ANGLE (DEGREES)	15
STATIC THRUST CAPACITY (LBS)	2908
STATIC RADIAL CAPACITY (LBS)	2509
NOMINAL RADIAL LOAD (LBS)	75
NOMINAL PRELOAD (LBS)	40
DYNAMIC CAPACITY OF 8,000 RPM (LBS)	564
DYNAMIC CAPACITY AT 12,000 RPM (LBS)	493
NOMINAL BEARING TORQUE (OZ-IN)	2
MAXIMUM TRANSIENT RADIAL LOAD (LBS)	275
CALCULATED B-10 LIFE (HRS) ATM DUTY CYCLE	122,000
RELIABILITY ATM DUTY CYCLE	.998
CUMULATIVE LIFE HISTORY (HRS)	400,000
MAXIMUM SINGLE UNIT RUN TIME (HRS)	30,000

TABLE 1.3.1-5

ITEM	2000 IGRA
SUPPLIERS	BARDEN CORP.
	SPLIT BALL BEARING CO.
METAL PARTS – MATERIAL	CEVM 52100 STEEL
RETAINER – MATERIAL	COTTON PHENOLIC SYNTHANE WITH POST CURE
SPECIAL PROCEDURES	TCP SOAK SMOOTH RACTOR TEST
LUBRICANT	KG–80 SUPER REFINED MINERAL OIL
LUBRICATION METHOD	DYNAMIC LUBRI- CATION SYSTEM
NOMINAL OPERATING TEMPERATURE	$90^{\circ} \pm 30^{\circ}$ F.
PRELOAD METHOD	BELLEVILLE SPRING

TABLE 1.3.1-5 (CONT'D)

In order to accommodate the replaceable spin bearings, the cartridge housings were reworked to accommodate snaprings rather than screw holes. In addition to this, a ball spring device was inserted into the cartridge in order to radially preload the spin bearings thus eliminating radial play while still allowing for axial motion. This was provided for greater bandwidth response by eliminating the bearing dead zone. Steps were machined .010" into the cartridge housing in order to eliminate rocking.

Additional modifications required included the stator support housing. These were modified to accommodate the new wheel performance monitor locations.

1.3.2   Actuator Pivot Assemblies

The CMG actuators provide the rotational torque to the gimbal assemblies and, with the sensors, serve as the gimbal pivots.

For the 2000H Advanced CMG, the inner and outer actuators were to be identical and were required to have the same mechanical interface with the gimbals and frame as the ATM CMG units.

The output requirements for the 2000H actuators were somewhat higher than for the ATM CMG units. The maximum output torque was 200 ft-lb instead of 122 ft-lb and the maximum output speed was 5 degrees per second instead of 3.5 degrees per second. System requirements established the gear ratio at approximately 28:1 where the ATM actuator had a ratio of 56.55:1. The required minimum lifetime was 2 years instead of 300 days.

The design of the new actuator was to utilize the experience gained in the ATM CMG program and to incorporate design approaches recommended by Battelle Memorial Institute in their review of the ATM CMG actuator. Battelle's studies of that unit are documented in their

"Design Review of a CMG Actuator", dated July 31, 1970, copies of which have been delivered to MSFC.

As part of their review, Battelle had taken a broad look at the two stage, parallel path, preloaded gear train which had been used in the ATM unit, and compared it to possible alternative systems and types of gearing that could provide the required performance with high torsional stiffness and zero backlash. Alternate systems that were considered included traction drives, harmonic drives, epicyclic gear systems and the use of helical or herringbone gears. Their study confirmed that the basic configuration of the ATM actuator and its gear train provided the best means of meeting the specified requirements.

Battelle's review suggested several design approaches that would have improved the unit performance, but could not be incorporated into the ATM actuator because of the advanced status of that hardware and that program schedule. These suggestions were aimed at optimizing the gearing against the predominant wear mode of failure by using techniques that improved the load sharing between the two gear paths. The improvement in load sharing would minimize the loading on the gear teeth and shaft bearings

and could be achieved by reducing the clearances that existed in the unpreloaded gear train and by keeping to a minimum the preloading torque required to "wind up" the gear train sufficiently to maintain a zero backlash under all operating conditions.

At the inception of the 2000H Advanced CMG program, an actuator was designed at Bendix that incorporated the Battelle recommendations from their ATM study in addition to providing for the increased output requirements. Wherever possible, features were selected that optimized the design for maximum wear life and maximum actuator spring rate.

At MSFC direction, Bendix had contracted with Battelle to perform a limited review of the Advanced 2000H Bendix design and generate gear tooth geometry optimized to resist the predominant gear tooth wear mode of failure. Layouts and design calculations were transmitted to Battelle, who satisfactorily completed their task before fabrication and procurement of the actuator hardware had started. The engineering data for the gearing, resulting from their study, was used for the Advanced 2000H actuator parts. Copies of Battelle's report, entitled, "Research

Report on MA-2000H Actuator Development", dated Dec. 22, 1970, were delivered to MSFC.

The actuator, shown in Figure 1.3.2-1, and described in detail in the following paragraphs, consists basically of a housing assembly, gear train, torque motor and tachometer.

This actuator employs, as did the ATM unit, a two stage, parallel path, reverted spur gear system. The required zero backlash feature is provided by winding up the gear train so that one path is preloaded against the other.

The basic gearing data for the actuator is tabulated in Figure 1.3.2-2 and the detailed gear engineering data in Figure 1.3.2-3. Gear ratios, diametral pitches, modified gear tooth profiles and face widths were selected so that the resulting sliding velocities and Hertzian contact stresses were conducive to maximum wear life. Gears and shafts utilized to the greatest possible extent, short, large diameter configurations, to minimize torsional deflections, tooth binding and shaft bending, the major contributors to actuator compliance.
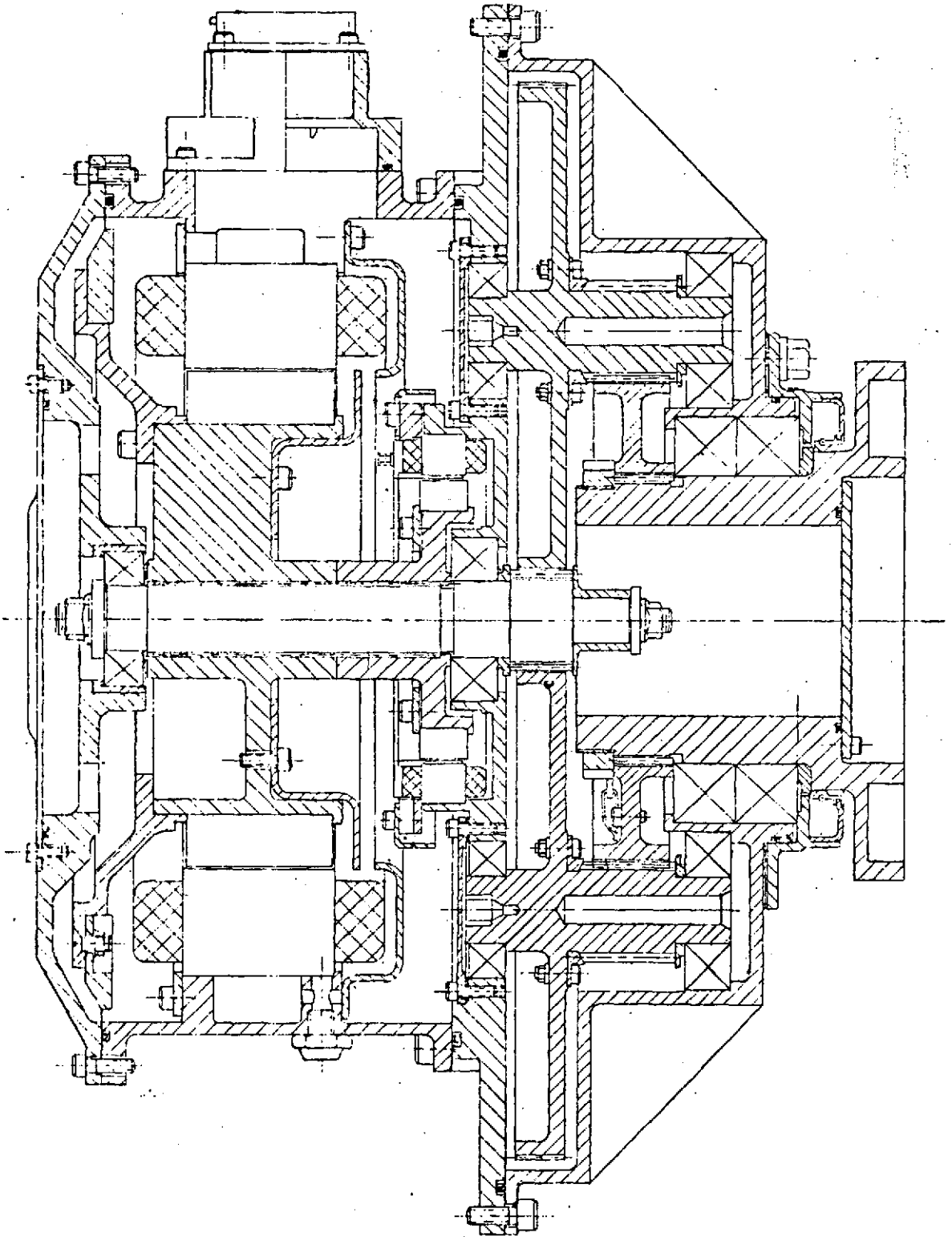
ACTUATOR PIVOT

FIGURE 1.3.2-1

1-37

ACTUATOR GEAR TRAIN

Overall Gear Ratio   28.0419:1

Center Distance   2.9375 In.

Basic Tooth Profile 20° Full Depth Involute

Gear Material   Nitralloy

	1ST STAGE (INPUT)	2ND STAGE (OUTPUT)
Gear Ratio	5.1842	5.4091
Diametral Pitch	40	24
Pinion – No. of Teeth	38	22
Pinion – Pitch Dia.	.950 In.	.9167 In.
Gear – No. of Teeth	197	119
Gear – Pitch Dia.	4.925 In	4.9583 In.
Gear – Face Width	.500 In.	.750 In.

FIGURE 1.3.2-2

SPUR GEAR DATA

	Input Drive		Output Drive	
	Pinion	Gear	Pinion	Gear
Number of Teeth, N	38	197	22	119
Diametral Pitch, P	40	40	24	24
Pressure Angle	20°	20°	20°	20°
Standard Pitch Diameter (N/P)	.950	4.925	.91667	4.95833
Base Circle Diameter (REF)	.89271	4.62799	.86138	4.65931
Tooth Form	Long Add.	Short Add.	Long Add.	Short Add.
Addendum Modification (REF)	+.004	-.004	+.010	-.010
Maximum Addendum (REF)	.0290	.0210	.0517	.0317
Minimum Whole Depth (REF)	.0570	.0570	.0937	.0937
Maximum Calculated Circular Tooth Thickness on Standard Pitch Circle (REF)	.04218	.03552	.07273	.05733
Measuring Pin Diameter	.0432	.0432	.072	.072
Measurement Over Two Pins	1.0174-.0007	4.9761-.0010	1.0325-.0007	5.0382-.0010
Max. Total Composite Error (TCE)	.0004	.0004	.0004	.0004
Max. Tooth-to-Tooth Composite Error (TTCE)	.0003	.0003	.0003	.0003
Outside Diameter	1.0080-.0010	4.9670-.0010	1.0200-.0015	5.0217-.0015
Outside Diameter Runout MAX TIR	.0010	.0010	.0010	.0010
Root Diameter	.8940-.0070	4.8530-.0070	.8326-.0176	4.8343-.0100
Minimum Root Fillet Radius	.0070	.0070	.0110	.0110
Form Diameter, MAX.	.9120	4.8720	.8670	4.8760

FIGURE 1.3.2-3

All gears were fabricated of nitralloy, core hardened to R_c 34/38 and nitrided to a case hardness of R_c 65/67. After nitriding, all gears were finished ground and lapped, insuring that optimum concentricities and tooth accuracies were obtained.

The following refinements that were included in the Advanced 2000H gear train design provided improvements over the ATM unit.

a. The number of teeth in the gear train were selected to provide the smallest preloading increment (the angle that the input pinion must rotate to achieve a wind-up of one tooth mesh). In the ATM actuator this increment was 0.9 degrees. In the advanced 2000H actuator it is 0.431 degrees. Keeping this increment small is an important factor in reducing the preload torque and improving load sharing between the two gear paths, which in turn, minimizes the loading on the gear teeth and shaft bearings.

b. The input pinion of the Advanced 2000H unit is supported by ball bearings in an "overhung" or canti-levered configuration. In the ATM actuator, the

pinion was supported between two bearings, one of which was mounted within the rotating output shaft. While an overhung pinion is usually an undesirable feature because of higher bending moments and higher misalignments due to deflections under load as compared to a "straddle" mounted pinion, in this case, it has an overall advantage. The more load sharing that can be achieved, the lower will be the bending moments and deflections of the pinion shaft. Ideally, if the load were shared equally between the two load paths, the pinion would be subjected to pure torsional loads with no bending moments.

In the ATM configuration manufacturing tolerances of the various elements of the output stage, rotating eccentricities of critical output shaft diameters and structural deflections of the output shaft and housings were all factors that could affect the radial position of the bearing within the output shaft. This changing position of the bearing could introduce misalignments of the input pinion that could drastically reduce the pinion wear life. Use of an overhung pinion avoids these problems.

c. ABEC-7 ball bearings, axially preloaded, are used
    throughout the gear train. Use of these high precision
    components provides better control of tolerances,
    which keep the unpreloaded clearances of the gear
    train to a minimum and result in improved load sharing.

The actuator housing assembly is made of four individual
housings. The two housings that support the gear train
of the Advanced 2000H unit are fabricated of stainless
steel rather than magnesium as in the ATM unit. Elimina-
tion of the thermal expansion differential between the
housings and the steel gears and bearings reduces the
gear train preload torque necessary to maintain zero
backlash at elevated temperatures. As described above,
this improves load sharing and reduces gear tooth loads.

The motor housing and rear bearing support were machined
from 6061 aluminum alloy. All housings were stress
relieved and stabilized during the machining process and
were inspected with both radiographic and fluorescent
penetrant methods.

After the four individual housings were dowelled together,
the bearing bores for all gear centers and the torquer and

tachometer mounting diameters were finish machined to close dimensional and concentricity tolerances.

The output shaft, which also serves as the gimbal pivot shaft, was machined from maraging steel. The higher modulus of elasticity (12,500,000 psi as compared to 6,100,000 psi for the titanium used for the ATM actuator shaft) increased the torsional stiffness of the unit.

The pivot bearings are a preloaded duplex pair, mounted "back to back" for maximum shaft rigidity under moment loads. Operating loads on the pivot bearings are negligible, but the requirement that they be sized to withstand launch vibration loads was the basis for determining the load capacity.

The gear train bearings are all angular contact bearings, purchased to ABEC-7 quality and, at assembly, are shimmed to remove axial clearance. A tabulation of bearing sizes, loads and capacities is given in Figure 1.3.2-4.

As a result of an investigation of lubricant distribution techniques, conducted by Battelle in their review of the ATM actuator, grease retainers were mounted on each side of both the first and second stage pinions. These

ACTUATOR BEARINGS

BEARING LOCATION	BEARING SIZE	BRG. LOAD AT 200 FT-LB OUTPUT	NON-BRINELL CAPACITY
Intermed. Shaft - Output End	20203 (N.D.)	465 lb.	2400 lb.
Intermed. Shaft - Motor End	Q0L03 (N.D.)	210 lb.	1615 lb.
Motor Shaft - Gear End	Q0L04 (N.D.)	112 lb.	2640 lb.
Motor Shaft - Back End	Q0L03 (N.D.)	22 lb.	1615 lb.
Output Shaft (Pivot Bearing)	1915 RD (M.R.C.)	*	26,200 lb. Thrust
			24,900 lb. Radial

*Operating loads are negligible
 Highly loaded during launch vibration only
 Same bearings have passed Qual Vibration

FIGURE 1.3.2-4

retainers trapped the grease that was axially extruded from the meshing gear teeth and effectively kept it where normal action of the gears would carry it into the mesh.

Had the Advanced 2000H CMG been intended for actual space flight, the lubricant used would have been the same perfluorinated ether oil and grease used in the ATM units. As the Advanced 2000H was, however, designated for laboratory use only, it was considered more appropriate to use synthetic diester lubricants. Ball bearings and gears were lubricated with Aeroshell No. 17 grease and the ball bearing phenolic retainers were vacuum impregnated with MIL-L-6085A oil.

Parting surfaces of the housings were provided with "O" ring seals fabricated of Viton A. A lip seal between the stationary housing and the rotating shaft accomplished sealing at the output end.

Where the ATM actuators had used Inland brush type torquers and tachometers, the Advanced 2000H units use brushless dc components for both applications. This eliminates the concern for the ability of sliding contacts

to meet a long life requirement as well as avoiding problems associated with brush noise and wear debris. The brushless dc components are described elsewhere in this report.

For engineering investigations of servo performance, it was desirable to have motor rotor inertias of various values available for test. This was achieved by supplying motor rotor retainers of varying configurations to obtain the selection of desired inertias.

A tabulation of the Advanced 2000H actuator performance characteristics is given in Figure 1.3.2-5.

1.3.3   Sensor Pivot Assemblies

The sensor pivots provide for the transmission of electrical power and signals across the gimbals and, with the actuator, serve as the gimbal pivots.

For the Advanced 2000H CMG, the sensor pivots were to have the same mechanical interface with the gimbals and frame as the ATM CMG units.

As both the inner and outer gimbals of the ATM CMG operated

ACTUATOR PERFORMANCE CHARACTERISTICS

Output Torque – Rated Max.	200 ft-lb
Output Speed – Rated Max.	5°/sec
Gear Ratio	28.04:1
Torque Sensitivity – Motor	1 ft-lb/amp
Torque Sensitivity – Actuator	28 ft-lb/amp
Tachometer Scale Factor	1 volt/rad/sec
Backlash	0
Actuator Spring Rate (Avg.)	150,000 ft-lb/rad
Motor Shaft Inertias Provided	.004 ft-lb-sec^2
	.009 ft-lb-sec^2
	.014 ft-lb-sec^2
Actuator Weight	46.6 lbs.

FIGURE 1.3.2-5

with only limited rotation, it was possible for both ATM sensors to utilize flex lead assemblies for the transfer of power and signal circuits. The requirement of the Advanced 2000H CMG to perform with complete gimbal freedom resulted in both sensors using slip ring assemblies.

The sensor pivot, shown in Figure 1.3.3-1 consists of a housing, a ball bearing mounted pivot shaft, a slip ring assembly, a resolver assembly and a tachometer. The resolver and tachometer are included to provide gimbal position and rate information for engineering test purposes.

In the Advanced 2000H units, the cable assemblies that exit from the pivot shafts and cross the gimbals are integral with the slip ring assemblies. In the ATM configuration, separate cable assemblies were mated to the sensor shafts through center connectors.

With the exception of the sensor housings and the wiring, the two sensor assemblies are essentially the same. To achieve outer gimbal balance, it was necessary to add weight to the inner sensor to counter the much heavier inner actuator assembly. This was accomplished by adding
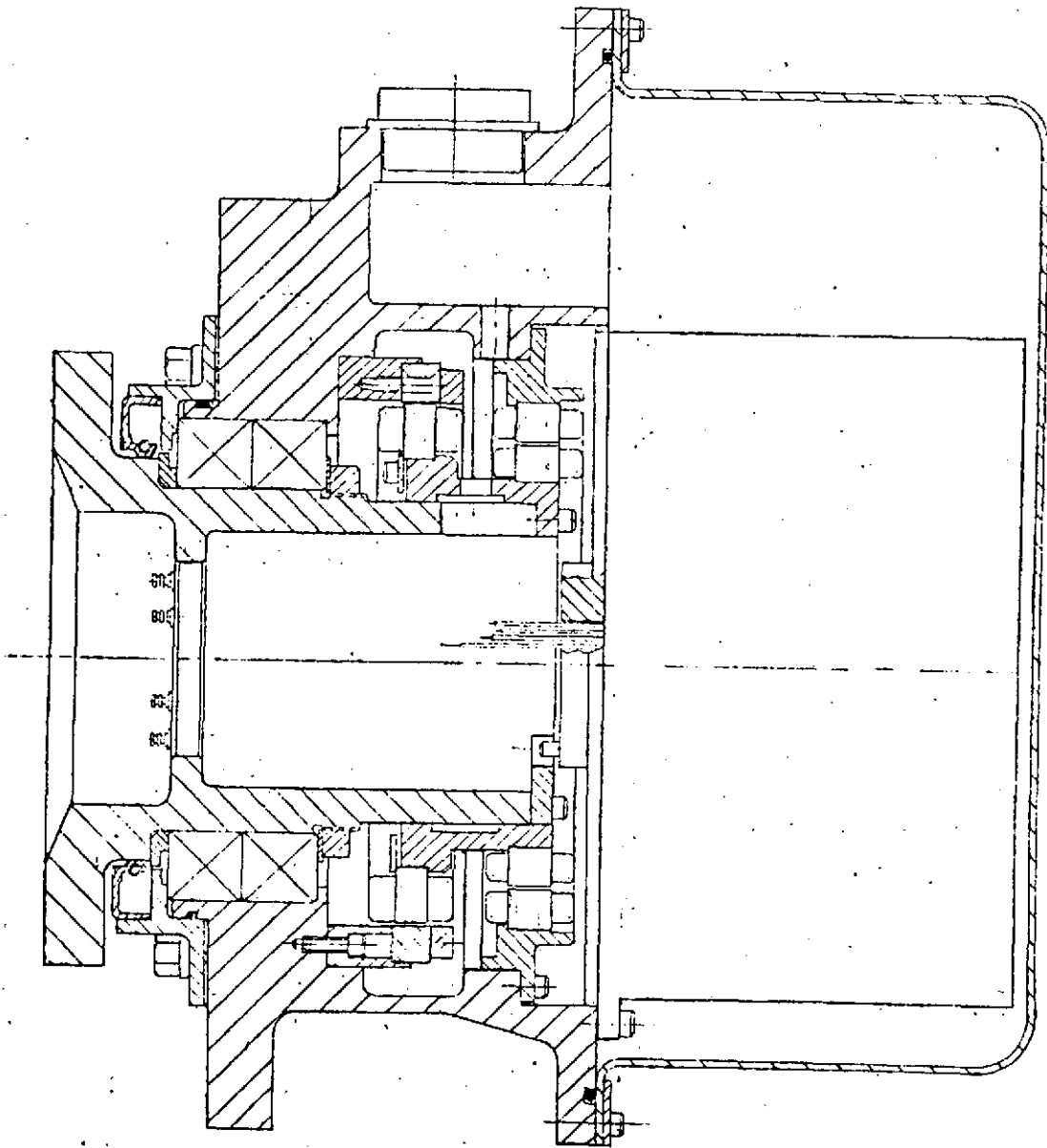
SENSOR PIVOT

FIGURE 1.3.3-1

some non-functional volume to the housing and fabricating it of stainless steel. For the outer sensor assembly, where no balance requirement existed, the housing was machined from 6061 aluminum.

The stainless steel pivot shaft is supported in the sensor housing by the same stainless steel, preloaded, duplex ball bearing pin used in the actuator. The pivot bearings and the slip ring bearings use the same lubricants described in the actuator section (Section 1.3.2).

The slip ring assembly circuits are packaged in a multiple pancake configuration. This assembly uses gold wire brushes, gold plated contact rings and wet lubricated bearings. Five pancakes are used, each providing 10 power and 20 signal circuits. Each power circuit has four brushes per ring and each signal circuit, two brushes per ring. The 50 power circuits are each rated at 3.5 amps in a vacuum environment and the 100 signal circuits at 1.0 amp. The slip ring assembly was procured from Poly-Scientific Division of Litton Industries and is shown in Figure 1.3.3-2.
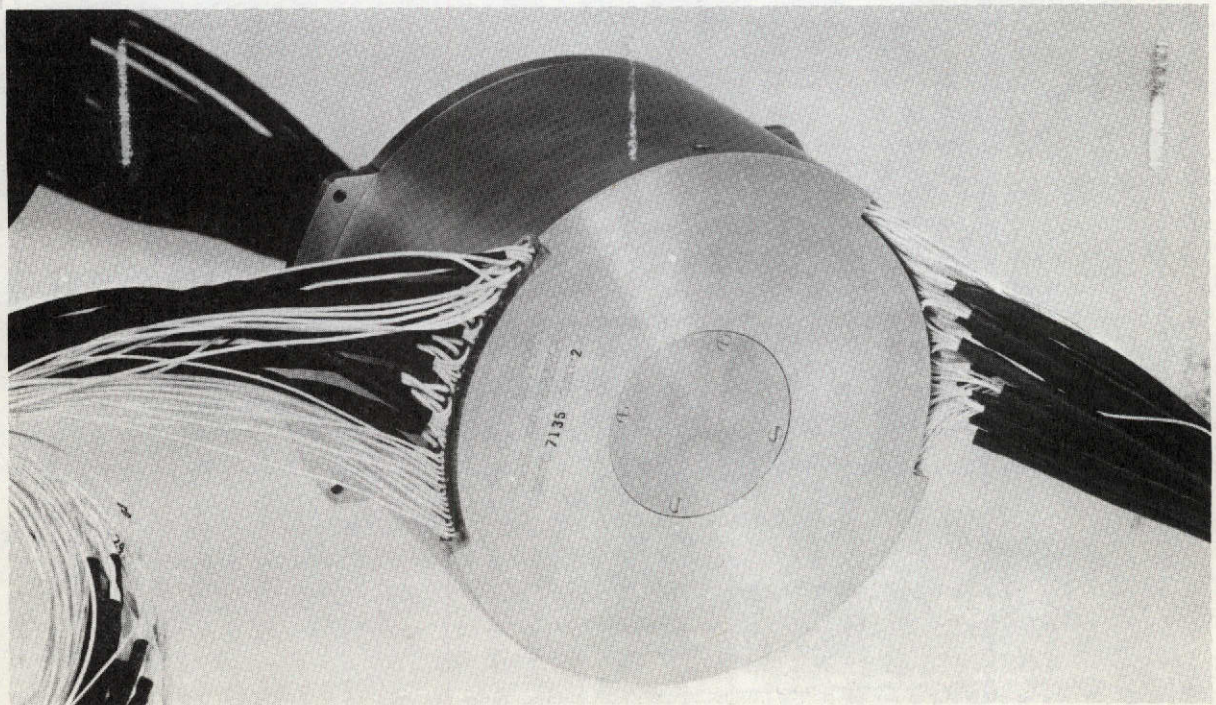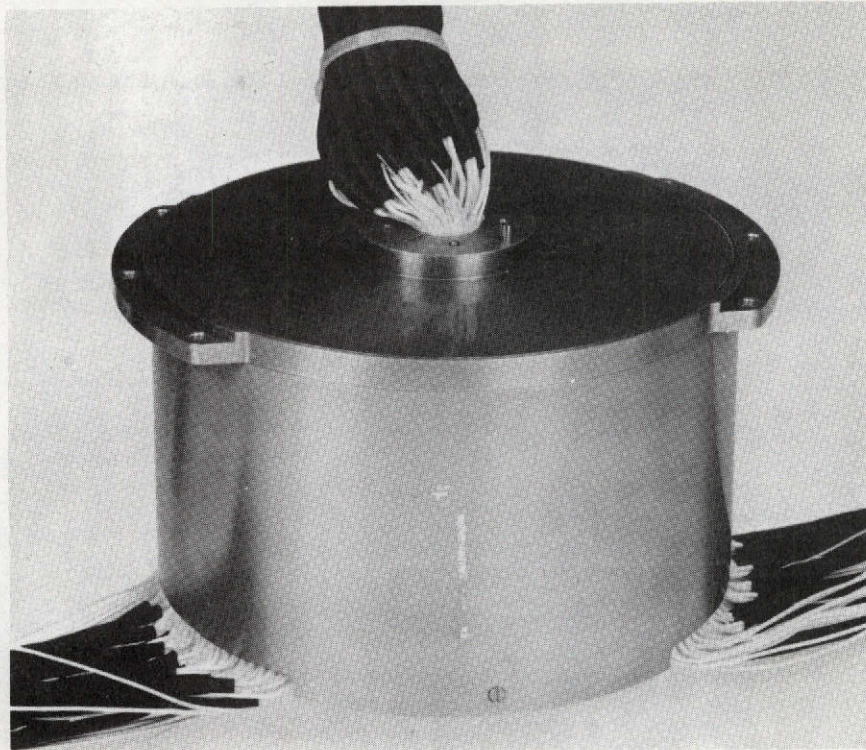
SLIP RING ASSEMBLY

FIGURE 1.3.3-2

1-51

The tachometer is an Inland brush type component (TG4401B). The brush material used is Boeing 046-45, selected for its low wear characteristics in vacuum operation. The tachometer operates at gimbal speed and has a voltage sensitivity of 3.9 volts/rad/sec.

Gimbal position information, for engineering test purposes, is provided by a single speed resolver designed and manufactured at Bendix. The electrical characteristics of this component are tabulated in Figure 1.3.3-3.

1.3.4   Outer Gimbal

The outer gimbal of the Advanced 2000H CMG was similar to that used with the ATM CMG except for the addition of mounting brackets to accommodate the actuator drive electronics.

An ATM gimbal, procured as a contingency part for that program, was available in the unfinished stage. This basic part consisted of a thin walled magnesium sand casting to which magnesium stiffening plates were welded as an outer skin. A photograph of the ATM gimbal is shown in Figure 1.3.4-1.

GIMBAL RESOLVER TRANSMITTER

ELECTRICAL CHARACTERISTICS

	Stator
Primary Winding	
Excitation, Volts	26
Freq. Hz	400
Input Power, Watts (Max.)	0.2
Output Voltage, Volts (Max.)	13
Phase Shift, Degrees	15
Sensitivity (MV/Deg)(Nom.)	225
Output Impedance (Ohms)(Nom.)	1000
Null Voltage (mv)(Max.)	30
Accuracy (Minutes, Max.)	± 6

FIGURE 1.3.3-3
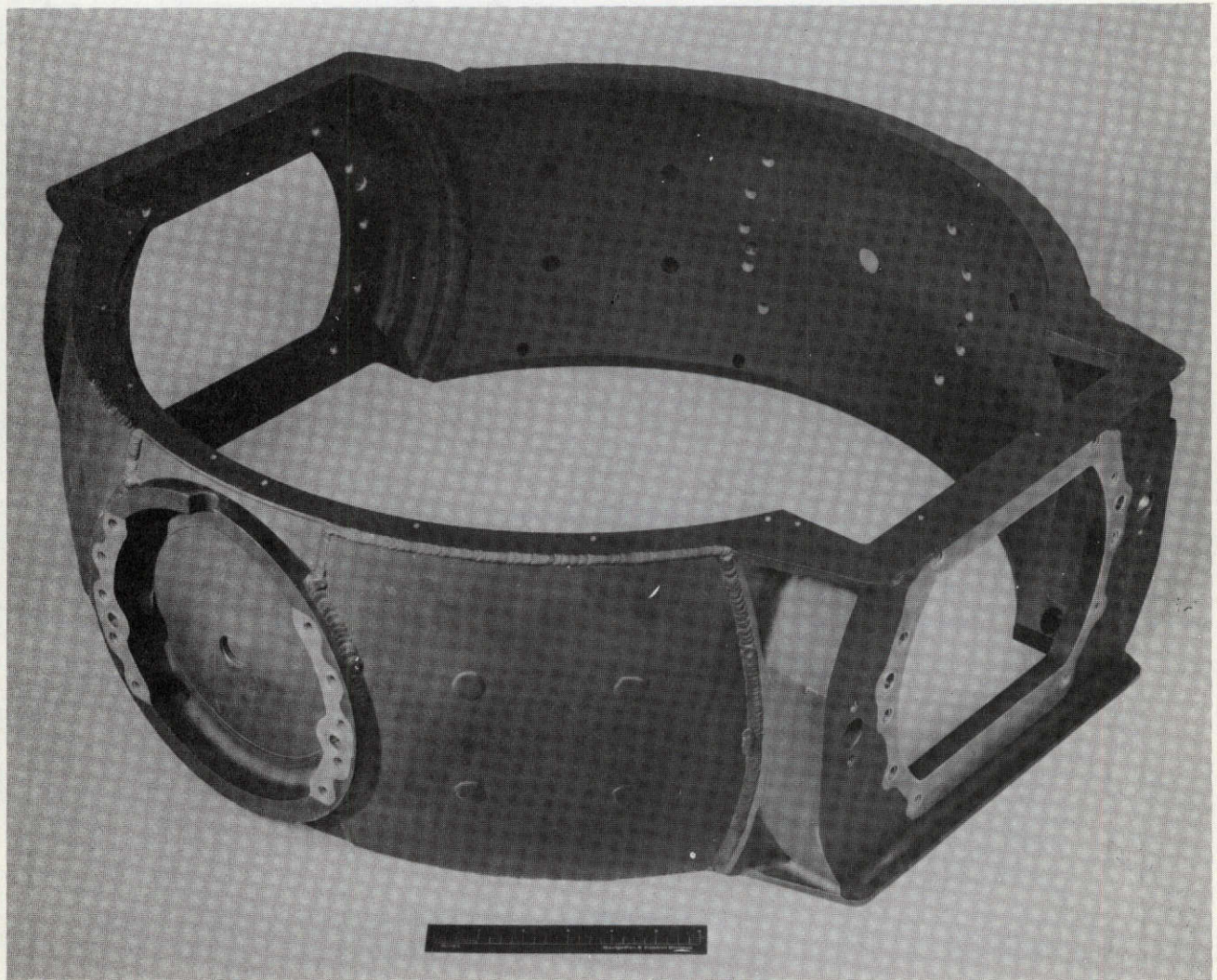
BOX SECTION GIMBAL

FIGURE 1.3.4-1

The gimbal was finish machined as P/N 2123983-1 which included modifications required for the electronics mounting brackets. The same inspection and finishing processes were performed as were done on the ATM parts. This included stress relieving and stabilizing operations, X-ray and fluorescent penetrant inspection, coating with Iridite 15 and application of flat black epoxy paint.

1.3.5   Frame

It was necessary to design and build a new frame for the Advanced 2000H CMG, as the ATM frame did not provide the clearance required to rotate the outer gimbal assembly with its larger actuator and gimbal mounted electronics.

The guidelines for the new frame design were to accommodate the larger outer gimbal assembly envelope while still permitting the complete CMG to be tested in the existing Torque Measuring Fixture. Mechanical interfaces with the pivot assemblies were to be identical to the ATM frame. No frame covers were to be supplied.

The frame was constructed as a welded assembly, using 6061 aluminum throughout. The individual parts - an inner wall plate, top and bottom plates, cross ribbing

plates, two hogged out pivot mounting bosses and an outer stiffening skin, were TIG welded using appropriate holding fixtures. Figure 1.3.5-1 is a photograph taken before the outer skin was assembled and shows the type of construction used.

After welding, the frame was solution heat treated and age hardened to T6 condition. The part was then rough machined, stress relieved and stabilized. Fluorescent penetrant inspections were performed several times during the fabrication process. After finish machining the frame was treated with Iridite and the appropriate surfaces were coated with a flat black epoxy paint.

The finished frame is shown in Figure 1.3.5-2.
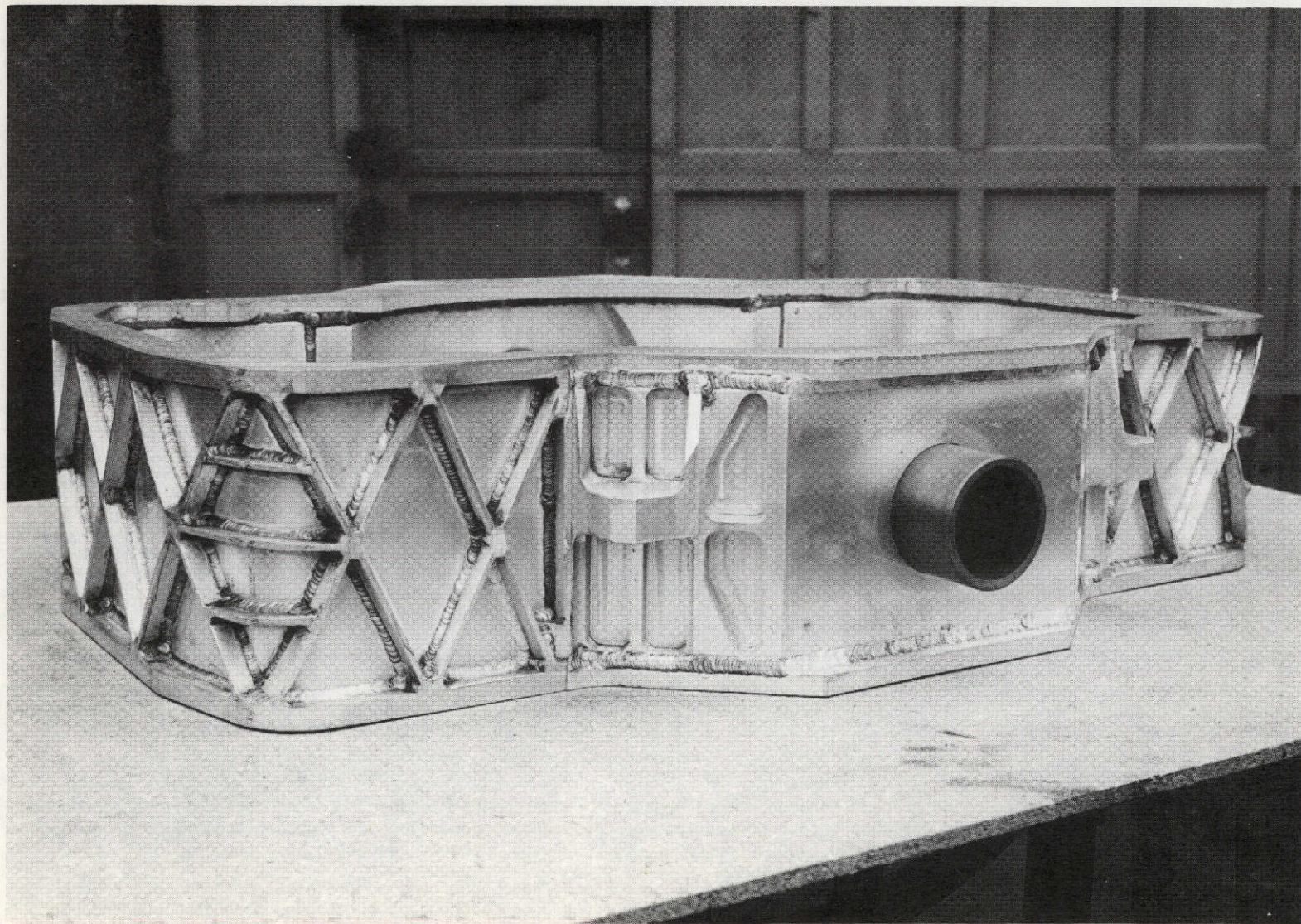
FRAME - UNFINISHED

FIGURE 1.3.5-1
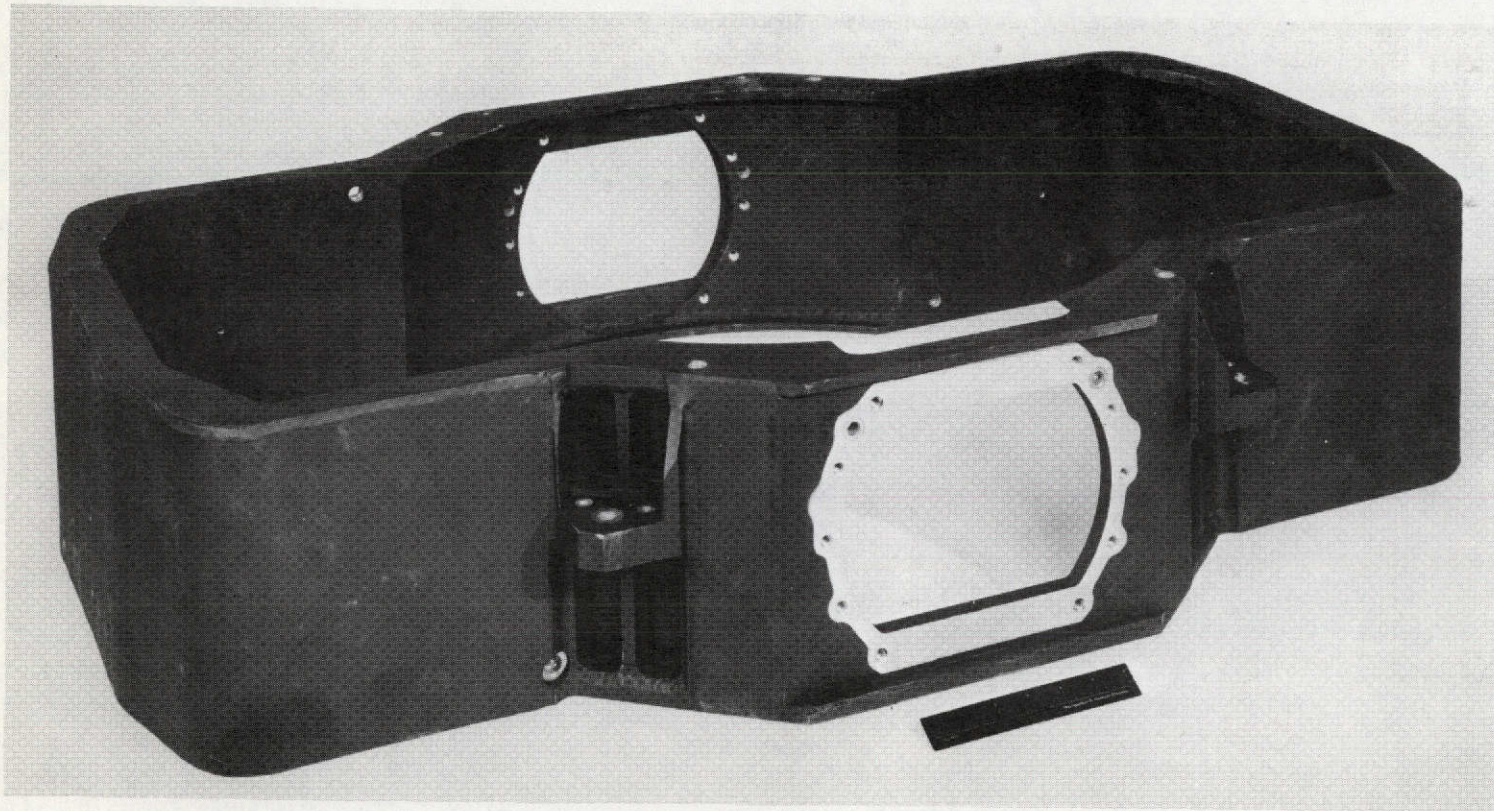
FRAME

FIGURE 1.3.5-2

1.3.6   Wheel Control Electronics

1.3.6.1   Spin Motor Electronic System

The spin motor electronic system consists basically of
four drive channels: one each per phase for two two-
phase DC Brushless motors on the same rotor shaft. The
goals of high performance with long life and high re-
liability are achieved by highly efficient switching
mode electronics, employing quadruple electronic re-
dundancy in the run mode. Two motor run-up permits
run-up times of less than two hours and permits run-up
power to be shared by two systems. One motor electron-
ics drive system is employed in the run-mode and
operation can be maintained with one phase removed.
While the discussion below is applicable to the
electronics for one motor, two sets of electronics are
required (one for each motor) and are identical. Tables
1.3.6-1 and 1.3.6-2 indicate the required design goals.
The indicated performance was provided by the hardware.

1.3.6.2   Spin Motor Electronics Design

A block diagram of the DC Brushless Spin Motor Electron-
ics is shown in Figure 1.3.6-1. This shows the electron-
ic scheme for one motor. Both motors employ completely

separate electronics (speed controls, power drives and control loops).

Hall-device position sensors are employed and are monitored on the stator in the air-gap of the motor structure and have, under constant motor speed conditions, a constant DC excitation. As the motor shaft rotates, the Hall sensors become pulse generators with a frequency proportional to motor speed. A reference frequency is generated by an oscillator and a direct digital comparison is made. The Hall generator output is squared-up with a Schmitt circuit for this purpose, with the comparison circuit giving an output DC level proportional to the frequency difference, or also to the speed error.

WHEEL CONTROL SYSTEM

DESIGN GOALS

- $H = 2000 \pm 5\%$ FT-LB-SEC

- $\omega = 8000 \pm 2\%$ RPM

- RUN-UP-TIME $\leq$ 2 HRS

- RUN-DOWN-TIME $\approx$ 4 - 5 HRS

    (NO ENERGY RECOVERY REQ'D)

- $\eta \approx$ 75% at 175 W. MECH. POWER OUTPUT

- MOTOR TORQUE OUTPUT $\geq$ 30 OZ.-IN./MOTOR

TABLE 1.3.6-1

SPIN MOTOR SYSTEM REDUNDANCY

WITH:

- ALL FOUR CHANNELS EXTERNALLY CONTROLLED AT BASE

- MONITORING PROVIDED AT BASE TO ASSESS EACH CHANNEL'S OPERATIONAL STATUS

- EACH MOTOR'S STATORS ALIGNED AND ROTORS SKEWED 45°

THEN:

- RUN-UP GUARANTEED WITH ANY TWO CHANNELS (TIME $\gg$ 4 HRS.)

- SYNCHRONOUS SPEED GUARANTEED WITH ANY ONE CHANNEL

TABLE 1.3.6-2

$e_o = Bi$
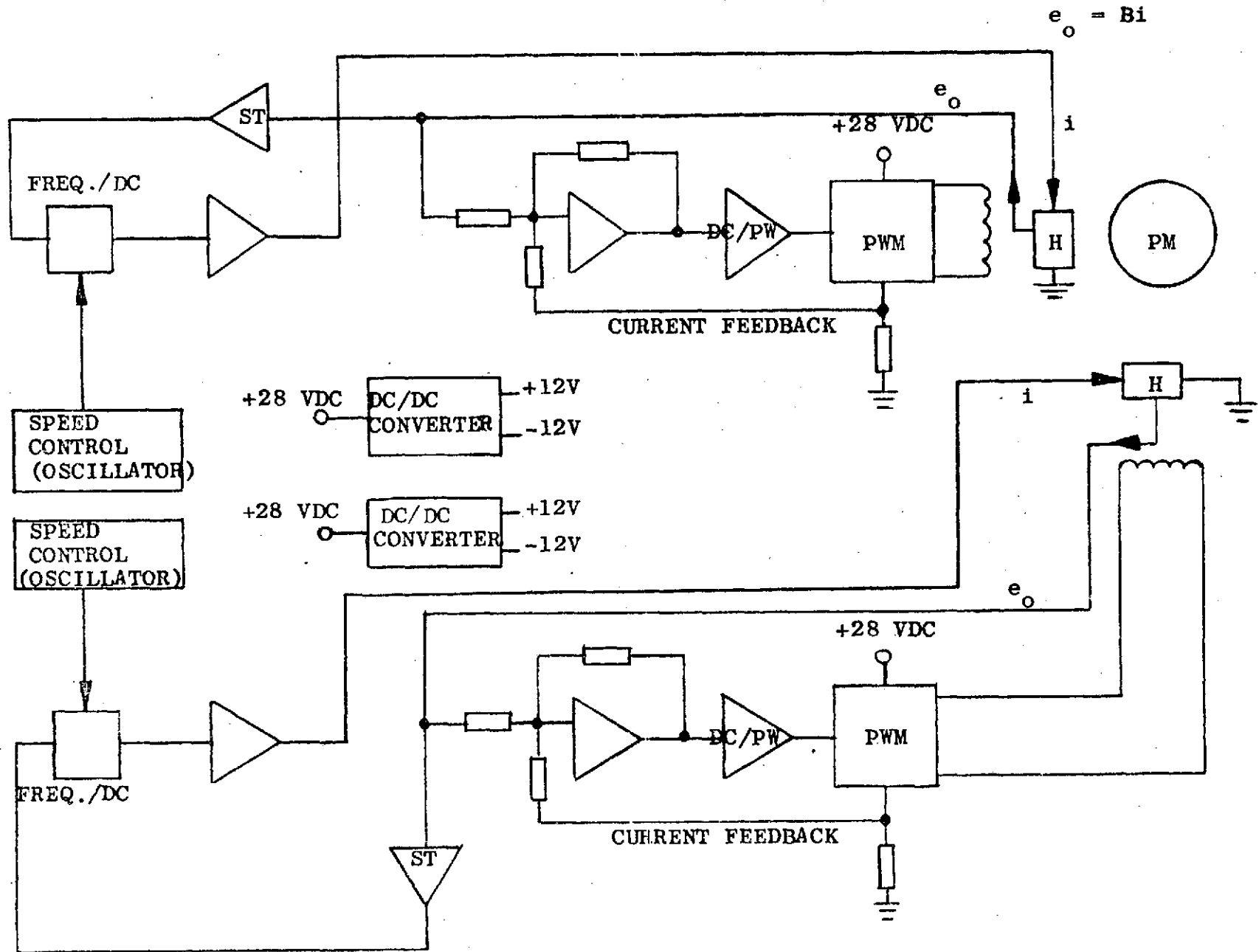
BLOCK DIAGRAM
DC BRUSHLESS SPIN MOTORS ELECTRONICS – (2 MOTORS WITH INTEGRAL HALL RESOLVERS)
FIGURE 1.3.6-1

Each motor's electronics employs a separate PWM switching bridge for each motor winding. Each produces a close approximation to sinusoidal output current as the motor turns at constant speed. It does this by controlling the duty cycle application of the 28V supply to the winding. The net effect is proportional control but with the losses associated with saturated switch operation. At the input, a DC torque command drives a proportional current through the Hall generators. At constant speed, the two Hall output voltages are sine θ and cos θ and are amplified by the Hall voltage differential amplifiers. Each signal is then compared with the current feedback signal from its respective motor winding and then amplified to drive the DC to pulse-width converter. Both channels are identical and drive their respective windings. A DC to DC converter supplies excitation for the integrated circuit electronics.

1.3.6.3   Spin Motor Electronic Circuits

A functional block diagram of the spin motor electronics is shown in Figure 1.3.6-2. The electrical schematic diagrams for the major functional blocks,

which are incorporated in each of the four spin motor
electronic packages, are included herein for reference
as follows:

a)   Isolated and Regulated DC-DC Converter -
        Drawing 2127089 (Spin Motor Power Supply)

b)   Pulse Width Modulator and Power Bridge -
        Drawing 2127069 (Schematic Diagram - PWM Spin
        Motor Assembly)

c)   Speed Control -
        Drawing 2127079 (Schematic Diagram Wheel Speed
        Control - Bang-Bang System)

        Drawing 2127131 (Schematic Diagram - Linear
        Speed Control - Spin Motor)

Two different speed control techniques were investi-
gated i.e., a "Bang-Bang" control circuit and a Linear
Control circuit as indicated in the referenced drawings.
The "Bang-Bang" control technique was the most success-
ful and was therefore provided in the consignment
hardware delivery.
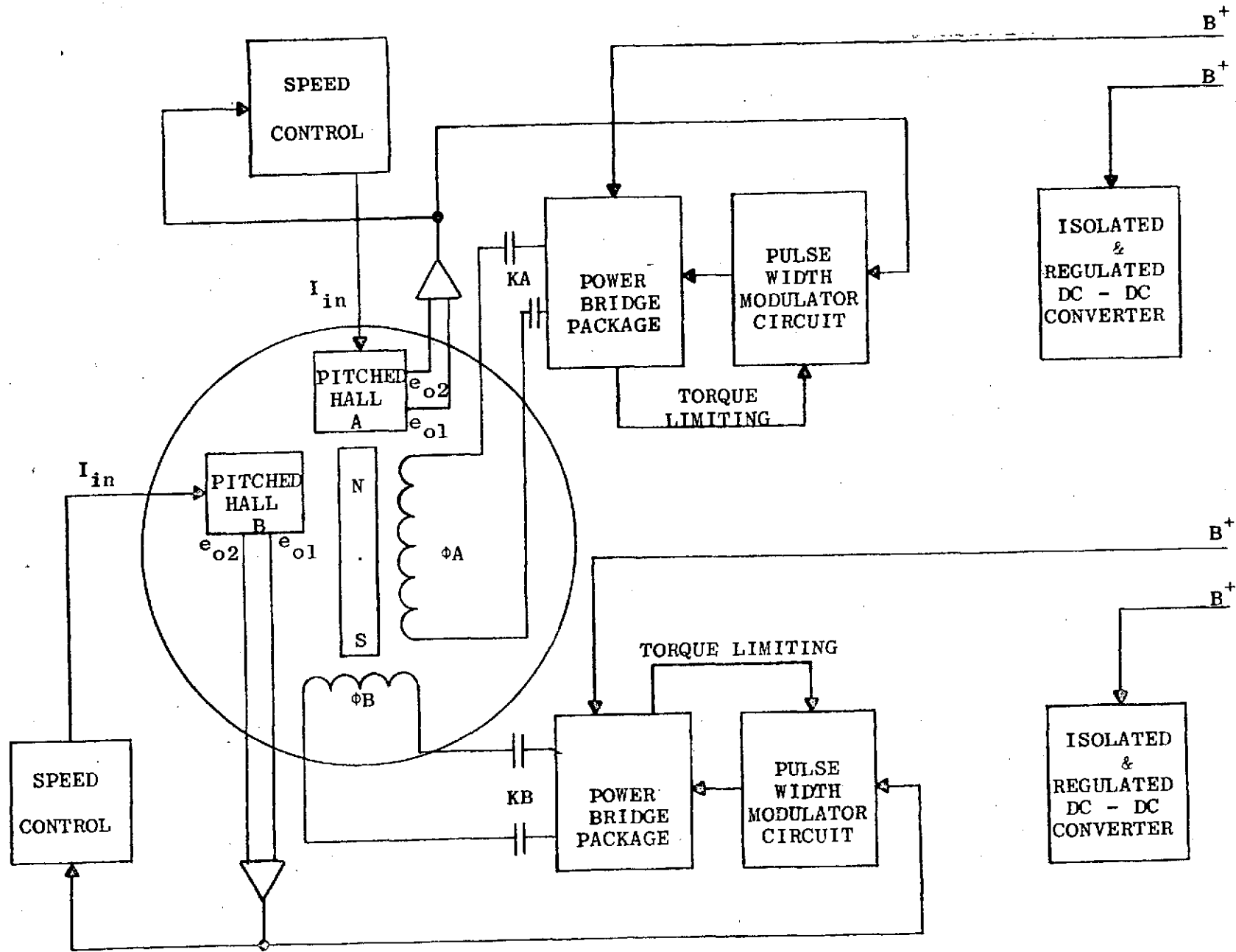
SPIN MOTOR ELECTRONICS FUNCTIONAL BLOCK DIAGRAM

FIGURE 1.3.6-2

Figures 1.3.6-3, 1.3.6-4 and 1.3.6-5 are block dia-
gram representations of the two spin control electronic
system circuits. For the final selected non-linear
system the nominal design point operating speed was
set at 8085 RPM established by an internal reference
frequency of 269.5 HZ. Conditions for operation at
the three selected speeds are as follows:

Nominal H FPS	Nominal Speed RPM	Selected Set Speed RPM	Internal HZ	External KHZ
1000	4000	4044	134.8	153.6
2000	8000	8085	269.5	307.2
3000	12000	12129	404.3	460.8

BLOCK DIAGRAM

LINEAR SPEED CONTROL SYSTEM
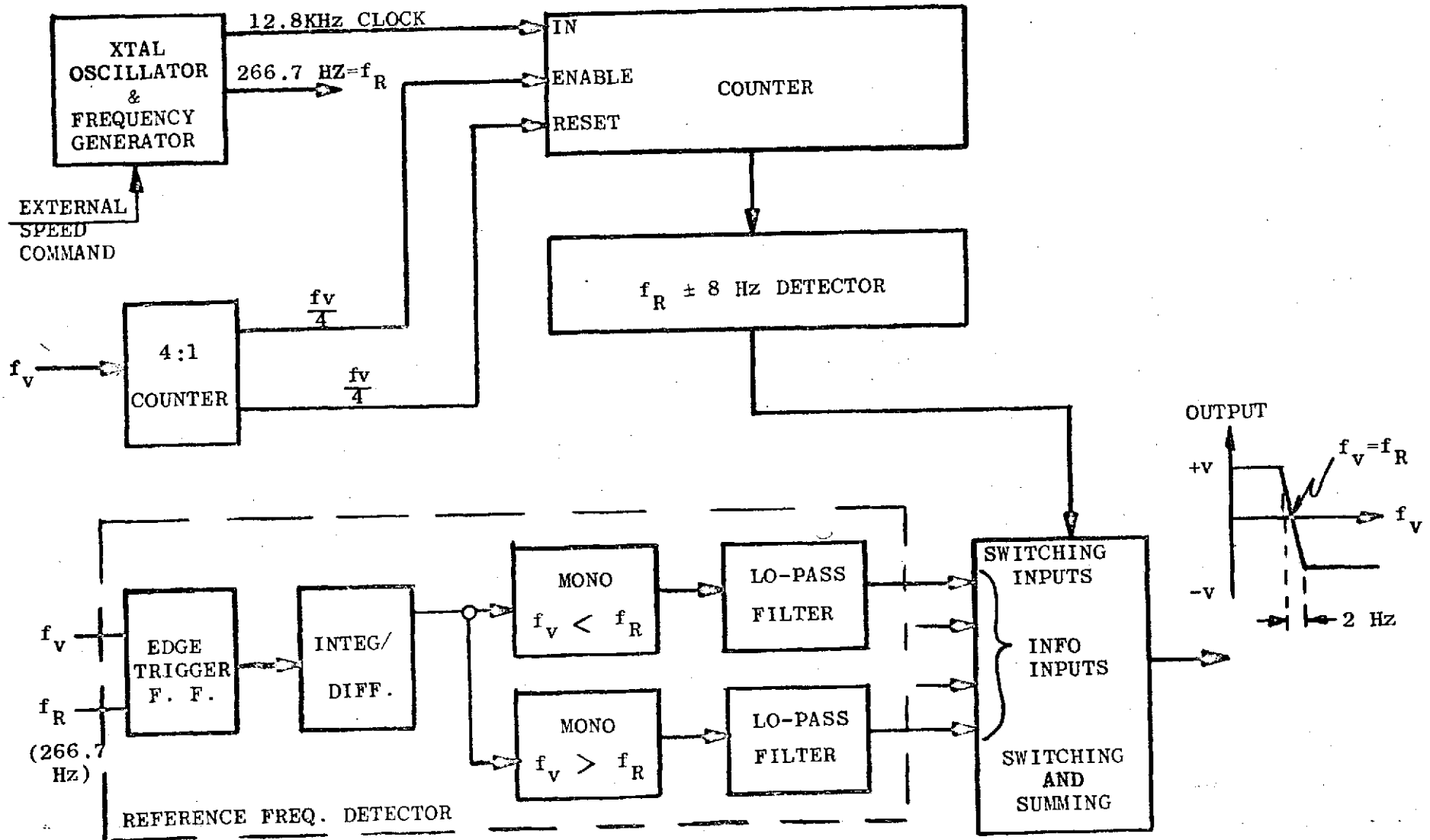
FIGURE 1.3.6-3
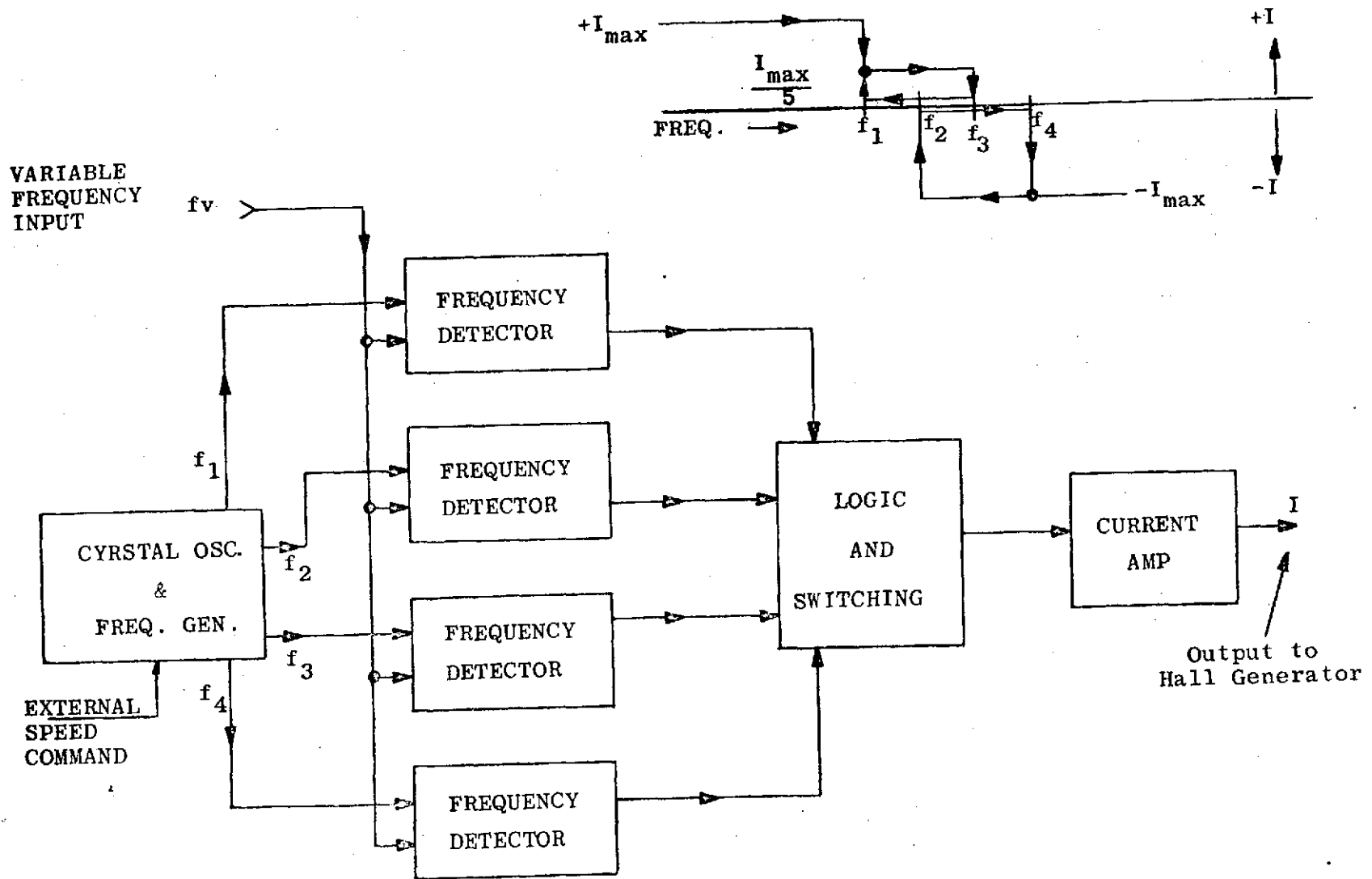
NON-LINEAR SPEED CONTROL SYSTEM
BLOCK DIAGRAM

FIGURE 1.3.6-4

FREQUENCY DETECTOR
NON-LINEAR SPEED CONTROL SYSTEM
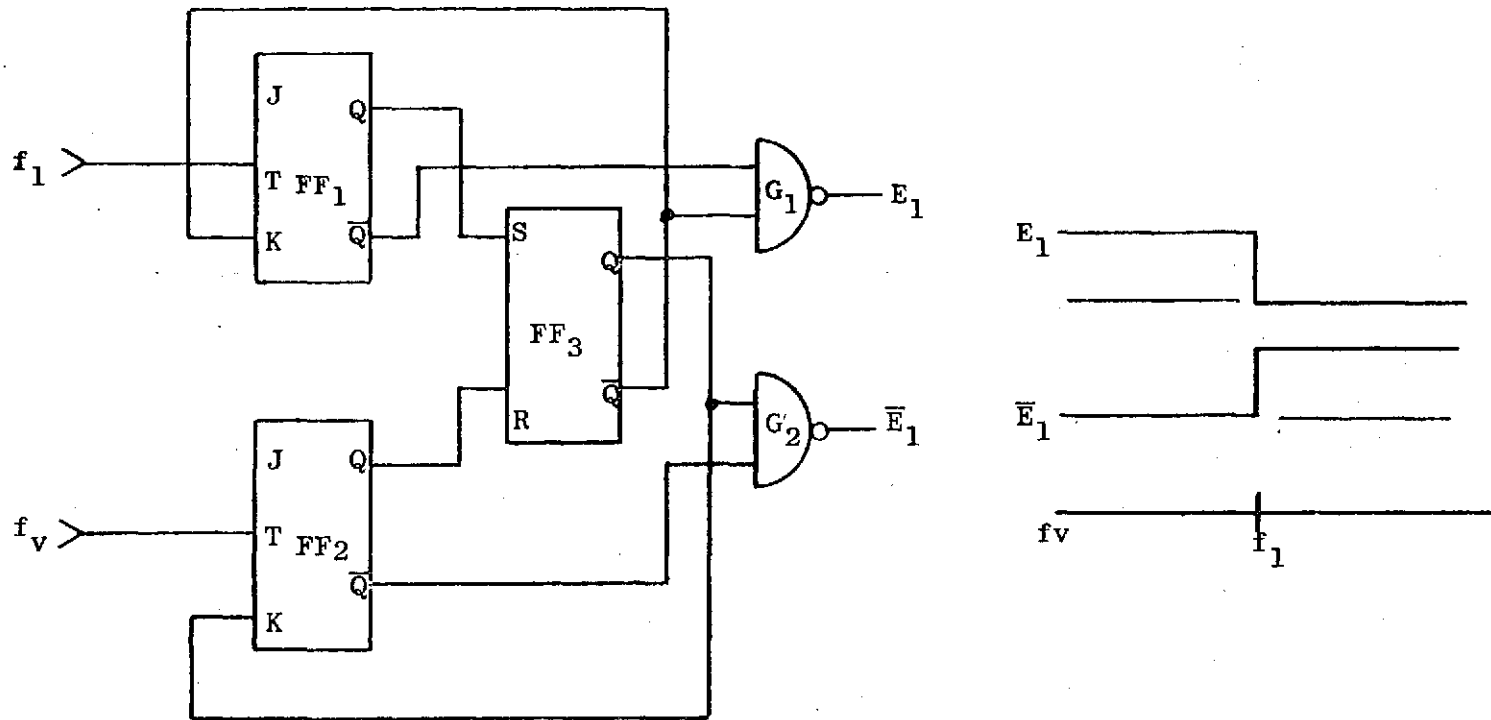
FF_1, FF_2	J-K Flip Flop SN54L73
FF_3	AC Coupled R-S Flip Flop DTμL 9950
G_1, G_2	Gates SN54L00

FIGURE 1.3.6-5

REPRODUCIBILITY OF THE
ORIGINAL PAGE IS POOR

SPIN MOTOR
POWER SUPPLY

PREPARED BY NAVIGATION AND CONTROL
DIVISION OF THE BENDIX CORPORATION
FOR
GEORGE C. MARSHALL SPACE FLIGHT CENTER
NASA, HUNTSVILLE, ALABAMA

THE BENDIX CORPORATION — NAVIGATION & CONTROL DIVISION
TETERBORO, NEW JERSEY, U.S.A.

SIZE D | CODE IDENT NO. 19315 | DRAWING NO. 2127089

1-71

Schematic Diagram — Pulse Width Modulator (Spin Motor Assy)

THE BENDIX CORPORATION — NAVIGATION & CONTROL DIVISION, TETERBORO, NEW JERSEY, U.S.A.

SIZE F | CODE IDENT NO 19315 | DRAWING NO. 2127069

NOTE: UNLESS OTHERWISE SPECIFIED
1. ALL RESISTOR VALUES IN OHMS ±5% AND 1/4 WATT.

SCHEMATIC DIAGRAM, WHEEL SPEED CONTROL (BANG-BANG SYSTEM)

THE BENDIX CORPORATION — NAVIGATION & CONTROL DIVISION, TETERBORO, NEW JERSEY, U.S.A.

SIZE F · CODE IDENT NO. 19315 · 2127079

THE BENDIX CORPORATION — NAVIGATION & CONTROL DIVISION, TETERBORO, NEW JERSEY, U.S.A.

SCHEMATIC DIAGRAM
LINEAR SPEED CONTROL
(SPIN MOTOR)

SIZE F   CODE IDENT NO. 19315   DRAWING NO. 2127131

OLDOUT FRAME

FOLDOUT FRAME

1.3.7   Gimbal Control Electronics

1.3.7.1   Actuator Electronics System

The actuator electronics for each actuator consists of
a DC Brushless Tachometer and a two-phase DC Brushless
Torquer drive. The goals of high performance and reli-
ability are achieved in part, by the DC Brushless design
approach which eliminates brushes and, therefore, brush
wear as well as other associated reliability and main-
tainability problems. With a permanent magnet rotor,
all heat losses are developed in the stator where heat
removal can be effected more efficiently. In addition,
the motor drives employ highly efficient switching mode
electronics, which in conjunction with the DC Brushless
design, results in a high efficiency and an increased
peak torque capability. This latter advantage permits
a lower gear ratio and less friction.

1.3.7.2   Actuator Electronics Design

A block diagram of the Actuator Electronics, consisting
of a brushless DC torquer and brushless DC tachometer is
shown in Figure 1.3.7-1. The shaft has the motor section
and position sensor side by side. The Hall type of pos-
ition sensor is employed and is inherently brushless; its
simplicity lends itself to this application. A seperate
magnetic structure is used for position sensing, which
assures low ripple torque since commutation is unaffected
by the motor stator current. It is also convenient to use
the same structure to obtain a DC tachometer signal.

CC

+28 VDC

PWM

PM

H

H

H

PM

H

+28 VDC

PWM

H

+28 V — DC/DC CONVERT. — +12 V
— -12 V
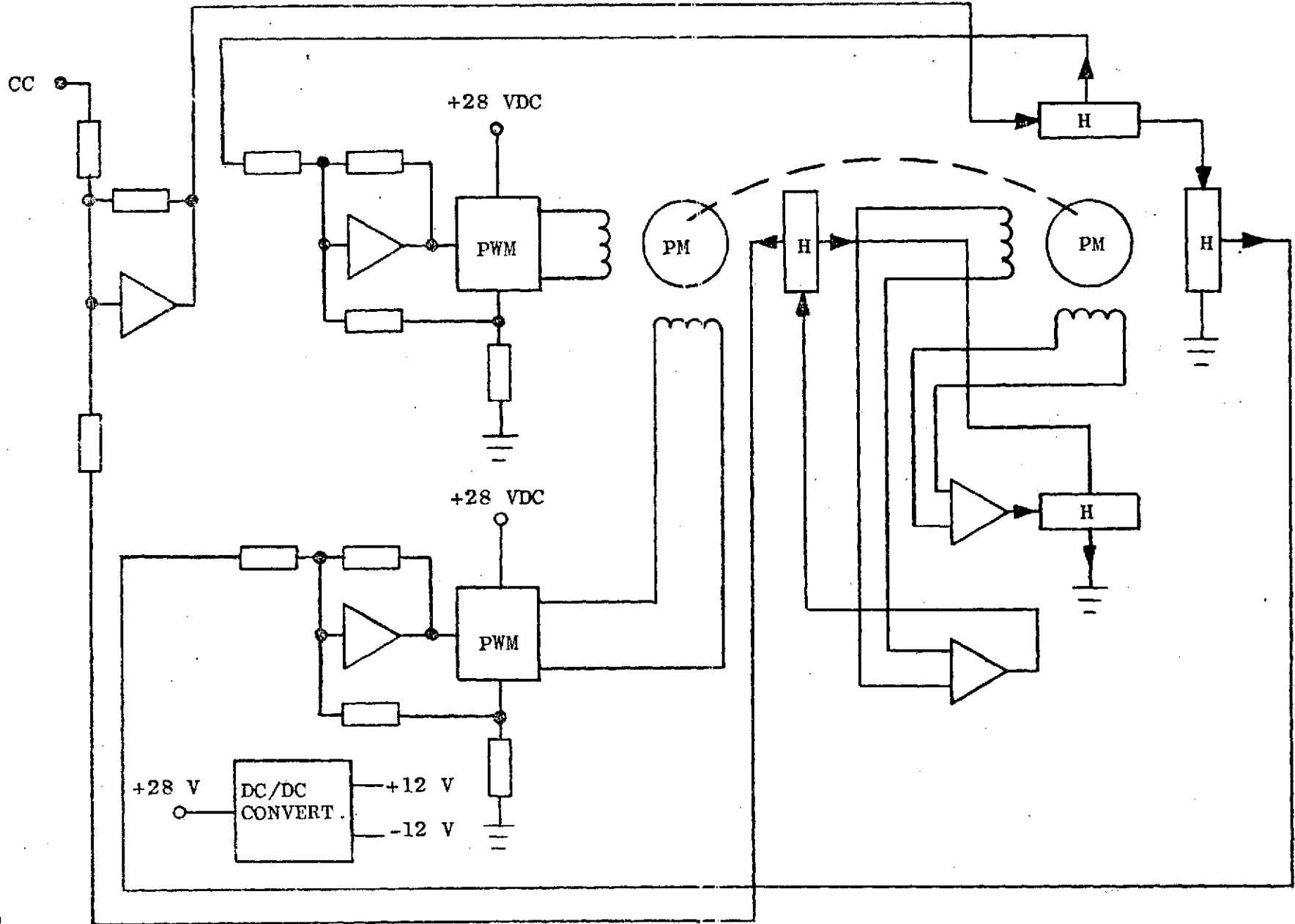
TACH FEEDBACK SIGNAL

BLOCK DIAGRAM
ACTUATOR ELECTRONICS
(BRUSHLESS TORQUE AND TACHOMETER)
FIGURE 1.3.7-1

This is done by adding two stator windings and two additional Hall generators. Two amplifiers are incorporated in the circuit comprising the brushless tachometer.

1.3.7.3   Brushless DC Torquer Electronics

The Torquer Drive electronics are similar to the Spin Motor Electronics described previously. There is a seperate PWM switching bridge for each motor winding. A close approximation to sinusoidal output current is produced as the motor turns at constant speed. This is accomplished by controlling the duty cycle application of the 28V supply to the winding. The net effect is proportional control, but with the losses associated with saturated switch operation. A DC torque command at the input drives a proportional current through the Hall generators. At constant speed, the two Hall output voltages are sine θ and cos θ and are amplified by the Hall voltage differential amplifiers. Each signal is then compared with the current feedback signal from its respective motor winding and this error signal is amplified to drive the DC to pulse-width converter. Both channels are identical and drive their respective motor windings. A DC to DC converter supplies the necessary integrated circuit excitation.

1.3.7.4   Brushless DC Tachometer Electronics

Low ripple voltage is the most important consideration in the design of a brushless DC tachometer; next of importance is null stability. In this application, ripple voltage may be caused by deviations from ideal conditions. The main source of ripple voltage is distortion in the flux density distribution versus rotation. This is controlled in manufacture by appropriate attention to the magnetization process. A second source is error in the location of both Hall generators. This error source is minimized by accurate positioning of these devices. A third contributor is gain unbalance variation, over a temperature range, between the two Hall generators. Under this condition, the large AC components out of both Hall generators are unequal in amplitude but 180° out of phase so incomplete cancellation takes place. Hall generators were purchased in matched pairs to alleviate this effect.

The null voltage, or output at various shaft positions while standing still, is due to the amplifiers which are used to drive current through the Hall generators. This effect depends on the ratio:

$$\frac{\text{peak AC tach winding output voltage}}{\text{Equivalent amplifier input offset}}$$

For a given amplifier offset, the peak AC output should be as large as possible. The high winding resistance, as a result, is not detrimental since the amplifier acts as a high input resistance buffer.

1.3.7.5   Actuator Electronic Circuits

A functional block diagram of the actuator electronics and brushless tachometer electronics (for gimbal control) is shown in Figures 1.3.7-2 and 1.3.7.-3. The electrical schematic diagrams for the major functional blocks, which are provided for each gimbal control subsystem, are included herein for reference as follows:

a)   Schematic Diagram Actuator Electronics - Dwg. 2127124

b)   Electrical Schematic, Power Supply, Actuator - Dwg. 2127099

c)   Electrical Schematic, Current Monitor, Actuator - Dwg. 2140010

d)   Schematic Diagram Servo Compensation,Hall Drivers, and PWM Current Limit (Signal Conditioning Assy). - Dwg. 1999499

e)   Electrical Schematic, PWM, Actuator - Dwg. 1999479

f)   Electrical Schematic, DC Tachometer, Actuator - Dwg. 2127129

1.3.7.6   Gimbal Control

The advanced CMG actuator design has a lower gear ratio than the ATM CMG and a brushless torquer and tachometer. Since the gear ratio and torque and tach scale factor are basic parameters in the gimbal rate loops, it became essential to rescale the rate loop. Furthermore, it is apparent that the reduced gear ratio will cause a change in the gyro nutation frequency, which can have a profound effect on loop coupling and subsequent bandwidth. The gimbal control performance goals that were attempted are shown in table 1.3.7-1.

GIMBAL CONTROL
PERFORMANCE GOALS

SERVO LOOP 3 DB BANDWIDTH:

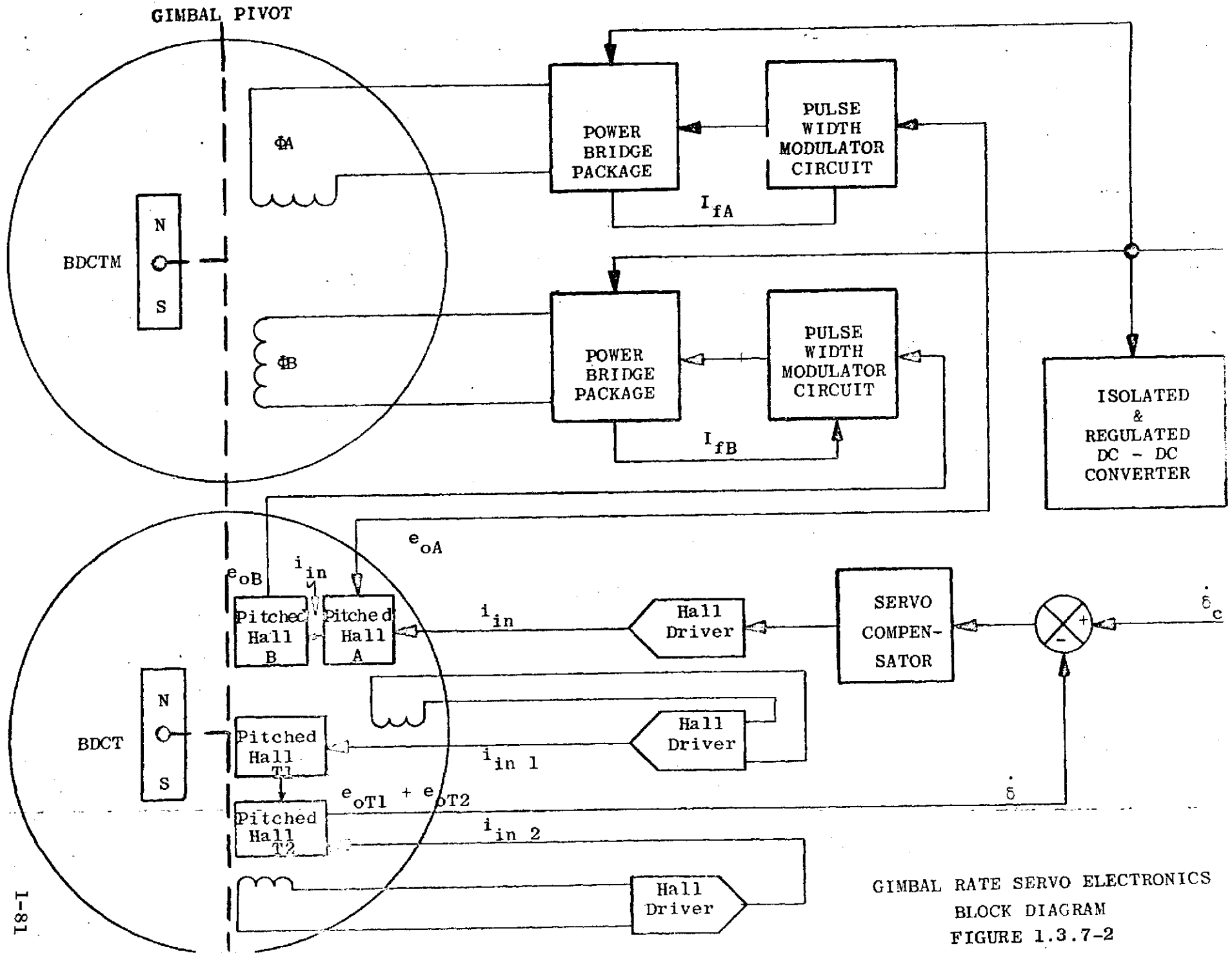62.8 RAD/SEC (10 CPS)

TORQUE OUTPUT:

200 FT-LB (PEAK);   175 FT-LB (SIMULTANEOUS PEAK)
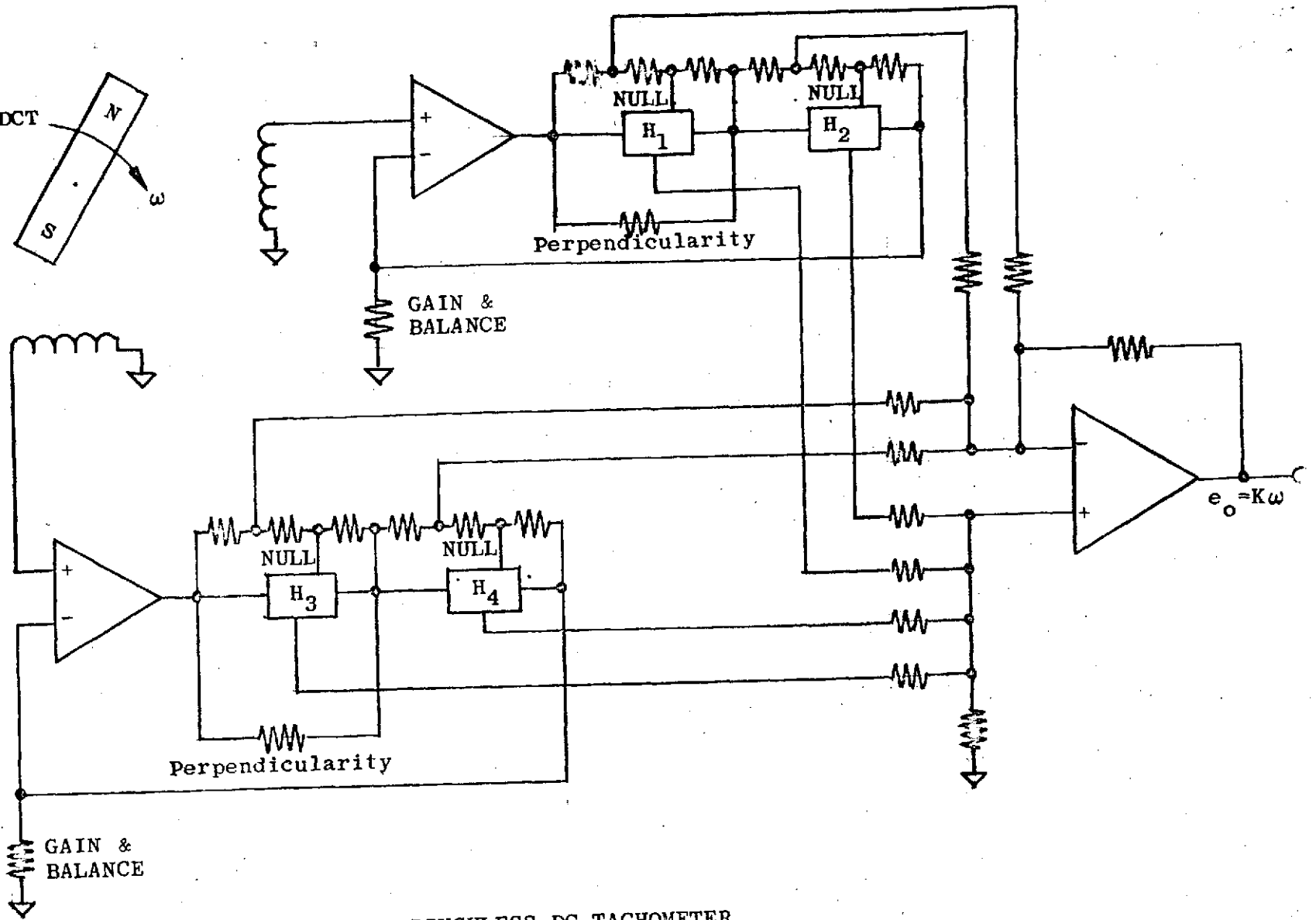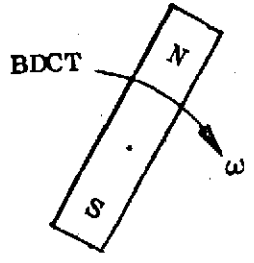

CROSS COUPLING:

LESS THAN .1 OF DIRECT AXIS RESPONSE AT

OPERATIONAL FREQUENCIES

LINEARITY:

MAINTAIN BANDWIDTH WITH INPUT RATE OF .1°/SEC - 5°/SEC

TABLE 1.3.7-1

GIMBAL RATE SERVO ELECTRONICS
BLOCK DIAGRAM
FIGURE 1.3.7-2

BRUSHLESS DC TACHOMETER
ELECTRONICS

FIGURE 1.3.7-3

1.3.7.6.1   Loop Coupling

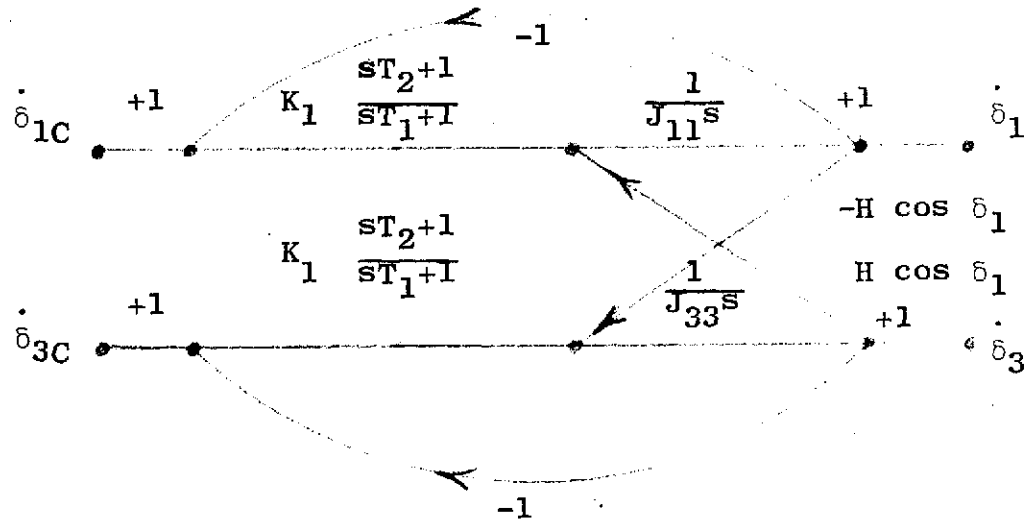A signal flow diagram of the inner and outer CMG loops is shown in Figure 1.3.7-4.

FIGURE 1.3.7-4

The gyro nutation frequency is defined as:

$$(1)\quad \omega_g = \frac{H}{\sqrt{J_{11} \quad J_{33}}}$$

and using ATM/CMG values, and correcting for the new gear ratio

$$(2)\quad J_{33} = (6.8 - .5 \cos 2\delta_1) \text{ ft-lb-sec}^2$$

Solving for ω_g

(3) $\omega_g = 455$ rad/sec

This increase over the 100 rad/sec nutation frequency of
the ATM/CMG is a clue to a reduced bandwidth at zero
inner gimbal angle where loop coupling is most severe.

The characteristic equation can be written from Figure
1.3.7-4 as:

(4)

$$\Delta = \left[s^2 \frac{T_1}{\omega_u} + s \frac{(1+\omega_u T_2)}{\omega_u} + 1 \right]^2 + (s T_1 + 1)^2 \frac{\omega_g^2}{\omega_u^2} \cos^2 \delta_1$$

The uncoupled loop poles will be used as a normalizing
frequency u

(5) $\omega_b = \sqrt{\dfrac{\omega_u}{T_1}}$

$u = \dfrac{s}{\omega_b}$

Substituting into eq. (4) with (5) equals

(6)

$$\Delta = \left[u^2 + u \omega_b T_2 \left(1 + \frac{1}{\omega_u T_2} \right) + 1 \right]^2 + (u \omega_b T_1 + 1)^2 \frac{\omega_g^2}{\omega_u^2} \cos^2 \delta_1$$

The following approximations are valued

$1 \gg \dfrac{1}{\omega_u T_2}$

$u \omega_b T_1 \gg 1$ around $u = 1$

and reduce (6) to

$$(8) \quad \Delta = \left[u^2 + u\omega_b T_2 + 1 \right]^2 + u^2 \, \frac{\omega_g^2}{\omega_b^2} \, \cos^2 \delta_1$$

Figure 1.3.7-5 compares the coefficients of (8) for the advanced CMG and the ATM/CMG.

	u^4	u^3	u^2	u^1	u^0
	1	$2\omega_b T_2$	$2 + \omega_b^2 T_2^2 + \dfrac{\omega_g^2}{\omega_b^2}\cos^2 \delta_1$	$2\omega_b T_2$	1
ATM	1	6.32	$12 + 2.5\cos^2 \delta_1$	6.32	1
Advanced	1	6.32	$12 + 51.8\cos^2 \delta_1$	6.32	1

FIGURE 1.3.7-5

The characteristic equation uncoupled poles of both CMG's appear at 63.2 rad/sec. However, in the advanced CMG, the influence of the $\cos^2 \delta$ coefficient will yield poles at approximately 505 rad/sec and 7.9 rad/sec at zero inner gimbal angle.

1.3.7.6.2   Loop Coupling Investigations

Extensive investigations were conducted to reduce the loop coupling experienced with the ATM CMG. All techniques investigated failed to provide significant improvement on the loop coupling and hence the bandwidth of the gimbal rate control loops. These investigations were conducted using six mass CMG servo models developed during the course of the ATM CMG program. Four techniques were investigated without success. There were:

1. Motor rate cross feed, Figure 1.3.7-6

2. Gimbal rate crossfeed; same as Figure 1.3.7-6 but with the crossfeed rate picked off the gimbal rate tachometer output.

3. Cross Axis gimbal rate control, Figure 1.3.7-7

4. Direct Axis control using motor rate and no cross-feed; same as Figure 1.3.7-6 but without crossfeed.

As a result, the simplest implementation was chosen for the prototype hardware to be technique 4.

Insight to the optimization of the selected configuration is derived by study of equation (8). It is apparent that the ratio of ω_g / ω_b controls the severity of loop coupling. This ratio is reduced by:

1. Increasing the brushless torquer rotor inertia: The actuator was designed to provide three torquer inertias for Engineering evaluation as follows: 0.004 Ft-Lb sec^2 is the basic torquer inertia; 0.009 or 0.014 Ft-Lb sec^2 by the addition of tungsten parts supplied to be attached to the torquer rotor inside of the actuator assembly.

2. Increasing the zero db crossover frequency: This frequency is usually held to a minimum to avoid complicating the loop models with the structural dynamics and the gear compliances. The 28 to 1 gear train produces a higher inertia to stiffness ratio; and ATM experience indicates that the structural dynamics are not as limiting as originally thought to be.
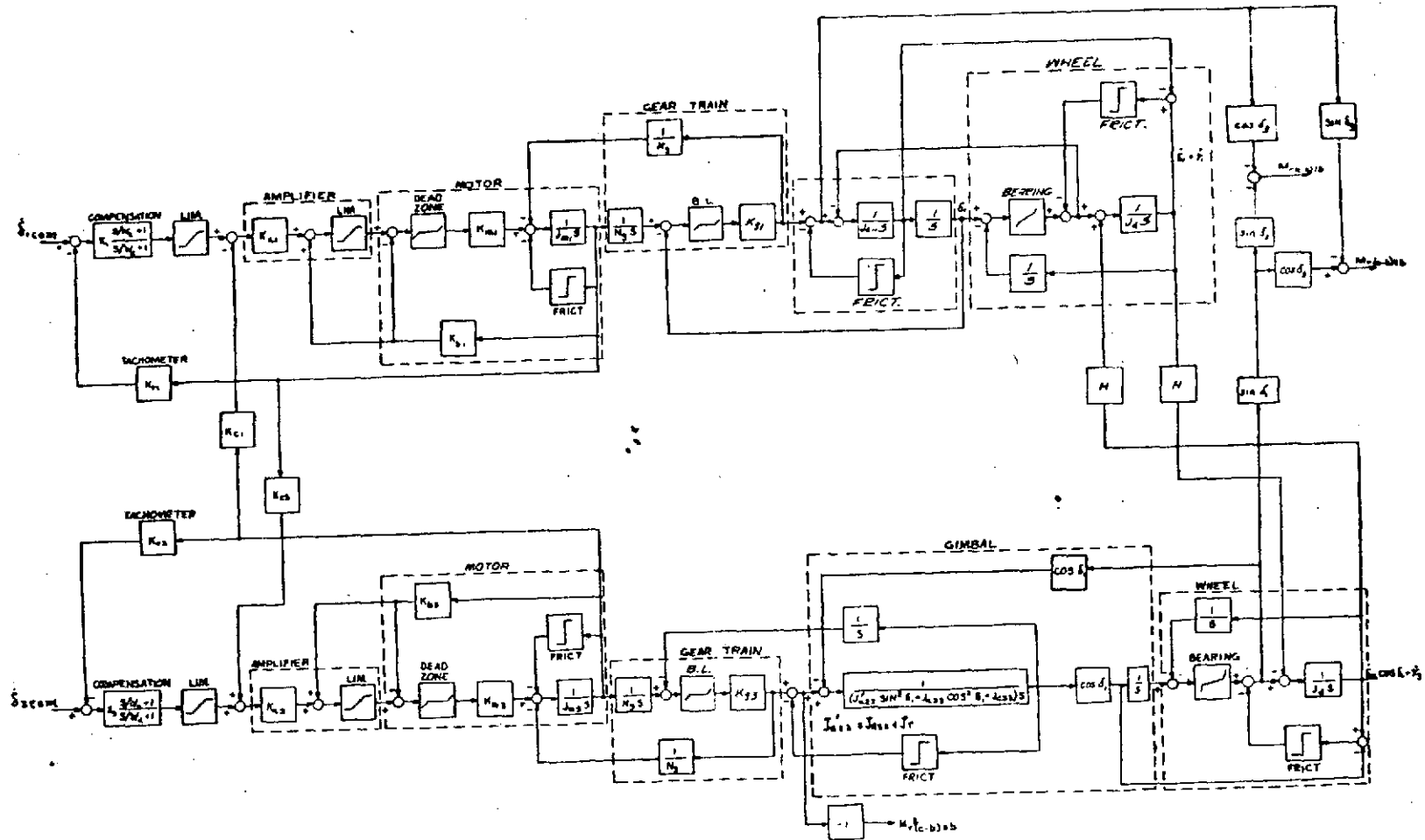
SIX-MASS CMG SERVO MODEL

WITH MOTOR RATE CROSSFEED
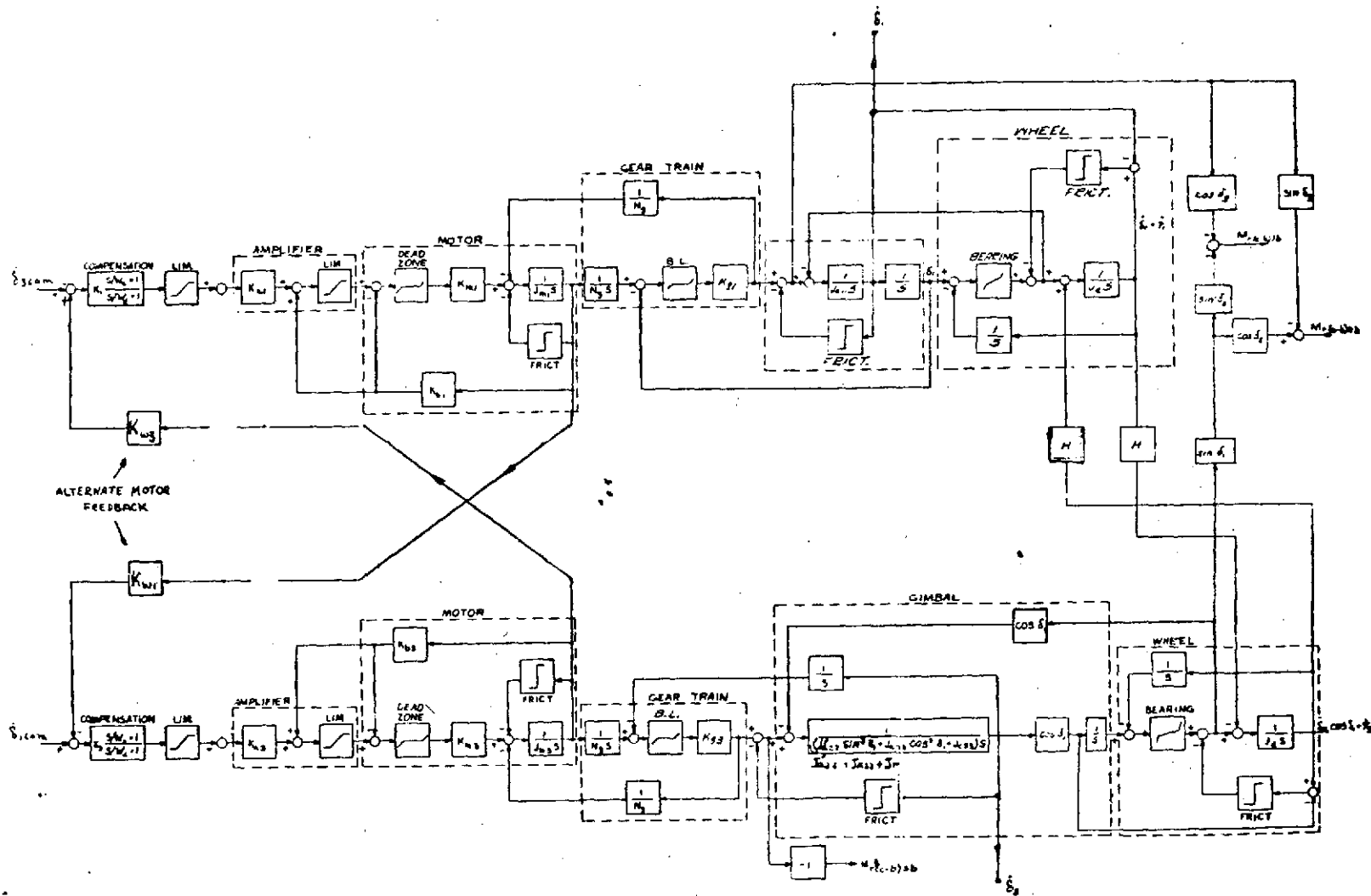
FIGURE 1.3.7-6

ALTERNATE

SIX-MASS CMG SERVO MODEL

(CROSS AXIS GIMBAL RATE CONTROL)

FIGURE 1.3.7-7

1.3.7.6.3   Gimbal Rate Servo Implementation

The selected gimbal rate servo implementation is shown
in Figure 1.3.7-8 "Gimbal Rate Servo Scaling Block
Diagram" and Figure 1.3.7-9 "Gimbal Rate Servo Open
Loop Gain". Sizing requirements for the gimbal torquers
is shown in Figure 1.3.7-10.

Tests were conducted varying the torquer inertia, open
loop gain and G(s) in order to optimize performance for
the selected servo loop implementation. Based on these
tests, the final servo loop implementation delivered was
as follows:

Torquer Inertia = 0.014 FT LB SEC^2

Open Loop Gain = 40,000 rad/sec

$$G(s) = \frac{\left(\frac{S}{20} + 1 \right)}{\left(\frac{S}{0.2} + 1 \right)}$$

GIMBAL RATE SERVO SCALING BLOCK DIAGRAM

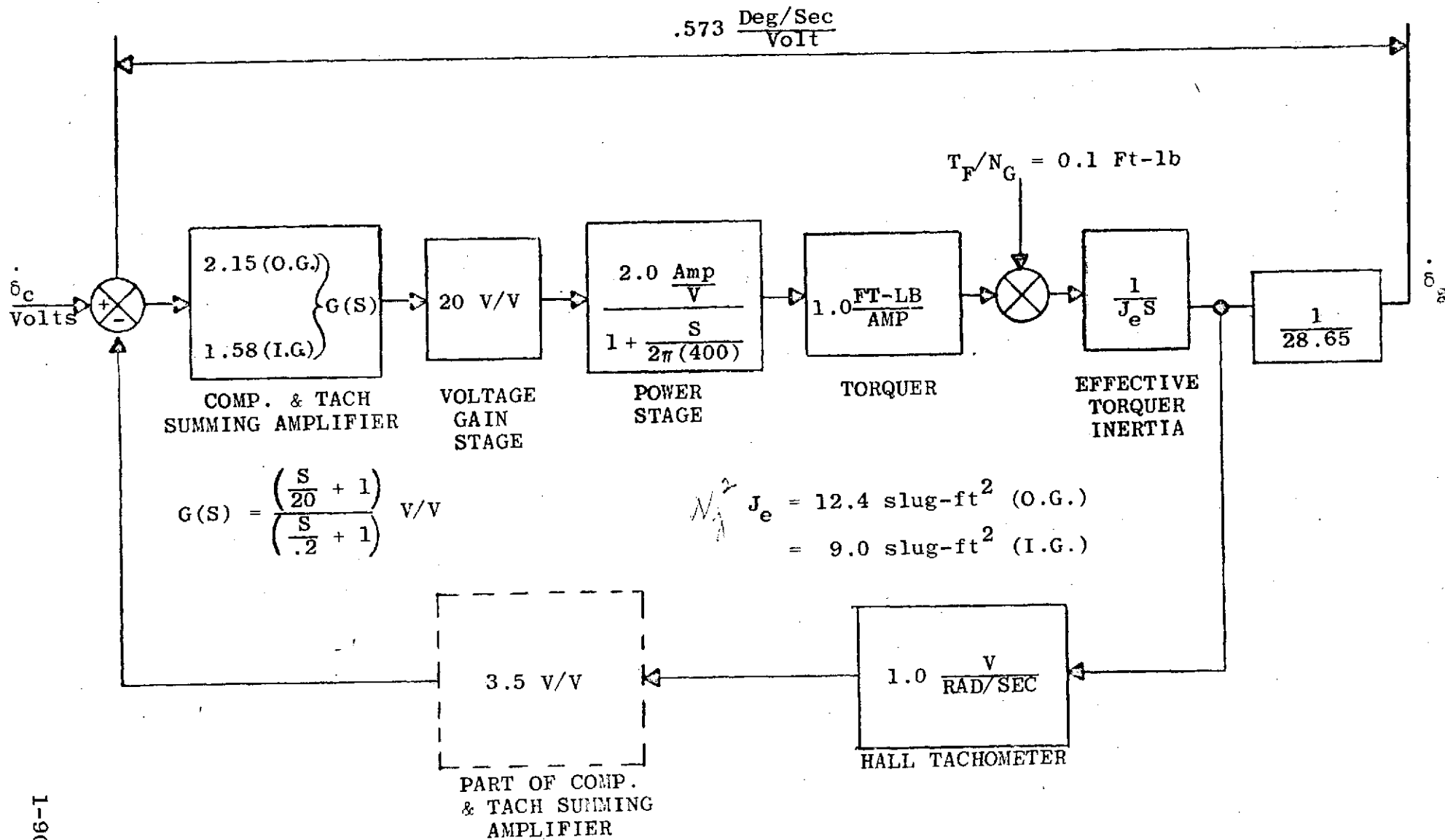
$$.573 \ \frac{\text{Deg/Sec}}{\text{Volt}}$$

$$T_F/N_G = 0.1 \ \text{Ft-lb}$$

$$\frac{\delta_c}{\text{Volts}}$$

Blocks:

- **COMP. & TACH SUMMING AMPLIFIER**: $\left. \begin{array}{c} 2.15 \ (\text{O.G.}) \\ 1.58 \ (\text{I.G.}) \end{array} \right\} G(S)$
- **VOLTAGE GAIN STAGE**: 20 V/V
- **POWER STAGE**: $\dfrac{2.0 \ \frac{\text{Amp}}{\text{V}}}{1 + \frac{S}{2\pi(400)}}$
- **TORQUER**: $1.0 \dfrac{\text{FT-LB}}{\text{AMP}}$
- **EFFECTIVE TORQUER INERTIA**: $\dfrac{1}{J_e S}$
- $\dfrac{1}{28.65}$ → $\dot{\delta}_g$

$$G(S) = \frac{\left(\frac{S}{20} + 1\right)}{\left(\frac{S}{.2} + 1\right)} \ \text{V/V}$$

$$N_A^2 \ J_e = 12.4 \ \text{slug-ft}^2 \ (\text{O.G.})$$
$$= 9.0 \ \text{slug-ft}^2 \ (\text{I.G.})$$

PART OF COMP. & TACH SUMMING AMPLIFIER: 3.5 V/V

HALL TACHOMETER: $1.0 \ \dfrac{\text{V}}{\text{RAD/SEC}}$
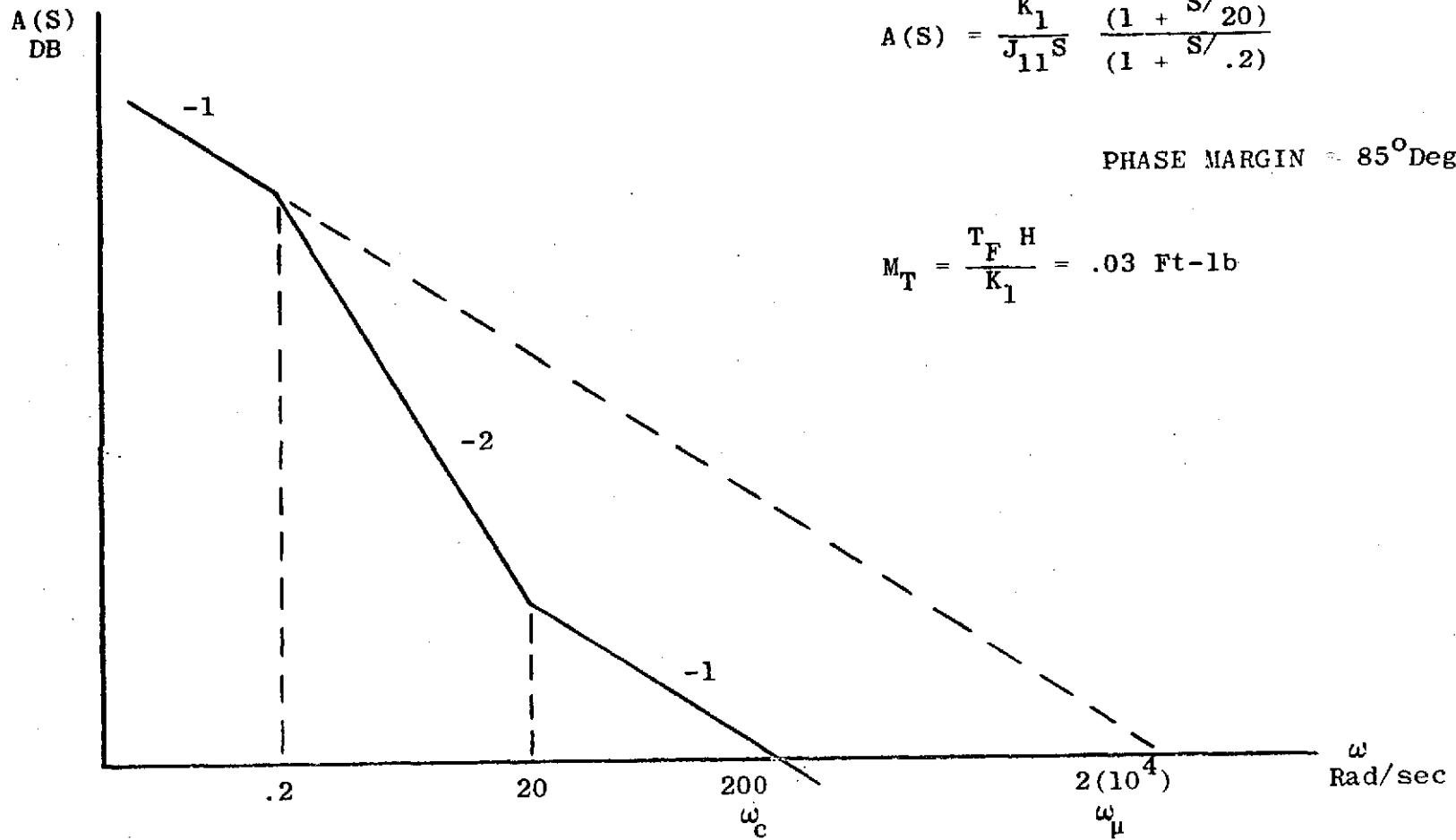
FIGURE 1.3.7-8

GIMBAL RATE SERVO OPEN LOOP GAIN

$$A(S) = \frac{K_1}{J_{11}S} \frac{(1 + S/20)}{(1 + S/.2)}$$

PHASE MARGIN = 85^ODegrees

$$M_T = \frac{T_F H}{K_1} = .03 \text{ Ft-lb}$$

$K_1 = 1.80 (10^5)$ Ft-lb-sec

$K_3 = 2.48 (10^5)$ Ft-lb-sec

$J_{11} = 9.0$ Ft-lb-sec^2

$J_{33} = 12.4$ Ft-lb-sec^2 (at $\zeta_1 = 0^O$)

FIGURE 1.3.7-9

GIMBAL TORQUER REQUIREMENTS

1. 200 Ft-lb at Stall
2. 175 Ft-lb at Max. Gimbal Rate of 5°/Sec
3. DO NOT LIMIT DGCMG BANDWIDTH BY TORQUER ACCELERATING CAPABILITY

$$T_{ACC} = J_{M+G} \, \alpha_M = J_{M+G} \, \dot{\omega}_M \qquad \text{where:} \quad \omega_M = \omega_{Max} \sin \omega_c t$$

$$T_{ACC} = J_{M+G} \, \omega_{Max} \, \omega_c \cos \omega_c t \qquad \omega_{Max} = 23.9 \text{ RPM} = 2.5 \, \frac{Rad}{Sec}$$

$$T_{ACC \, Max} = .02(2.5)70(1) = 3.5 \text{ Ft-lb} \qquad \omega_c = 70 \, \frac{Rad}{Sec} \quad \text{(Chosen Beyond DGCMG BW)}$$

$$J_{M+G} = .02 \text{ slug ft}^2$$
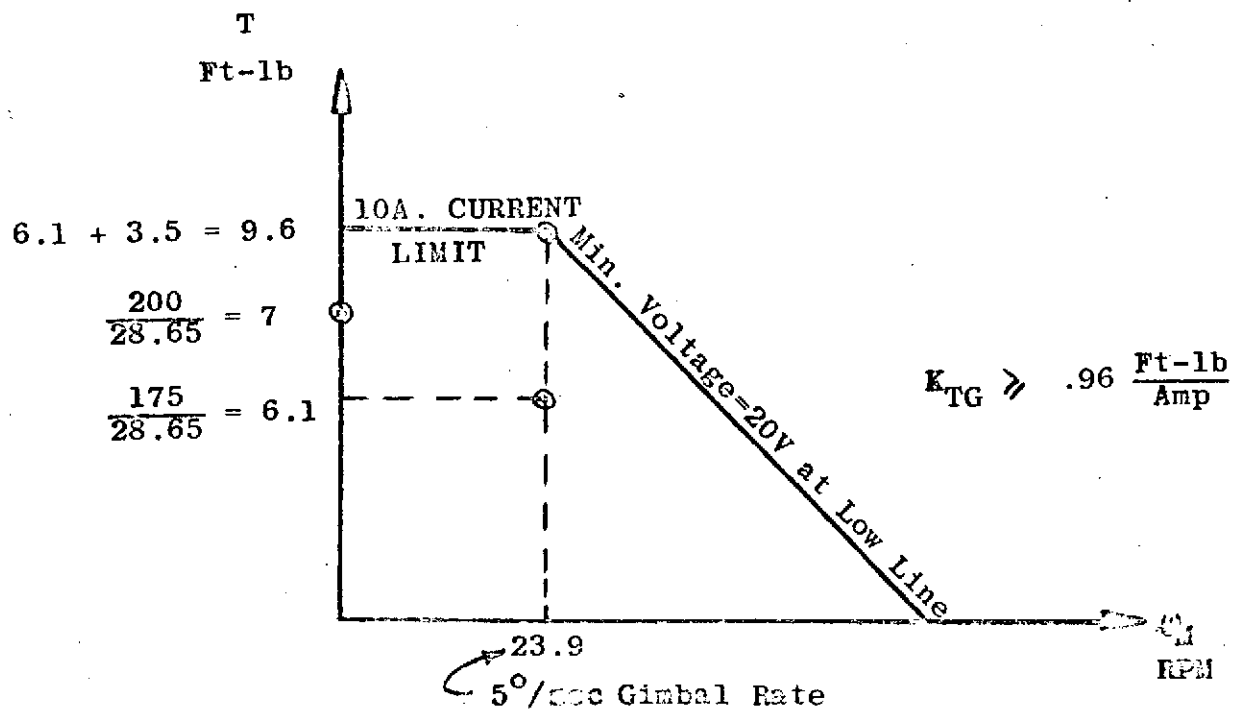
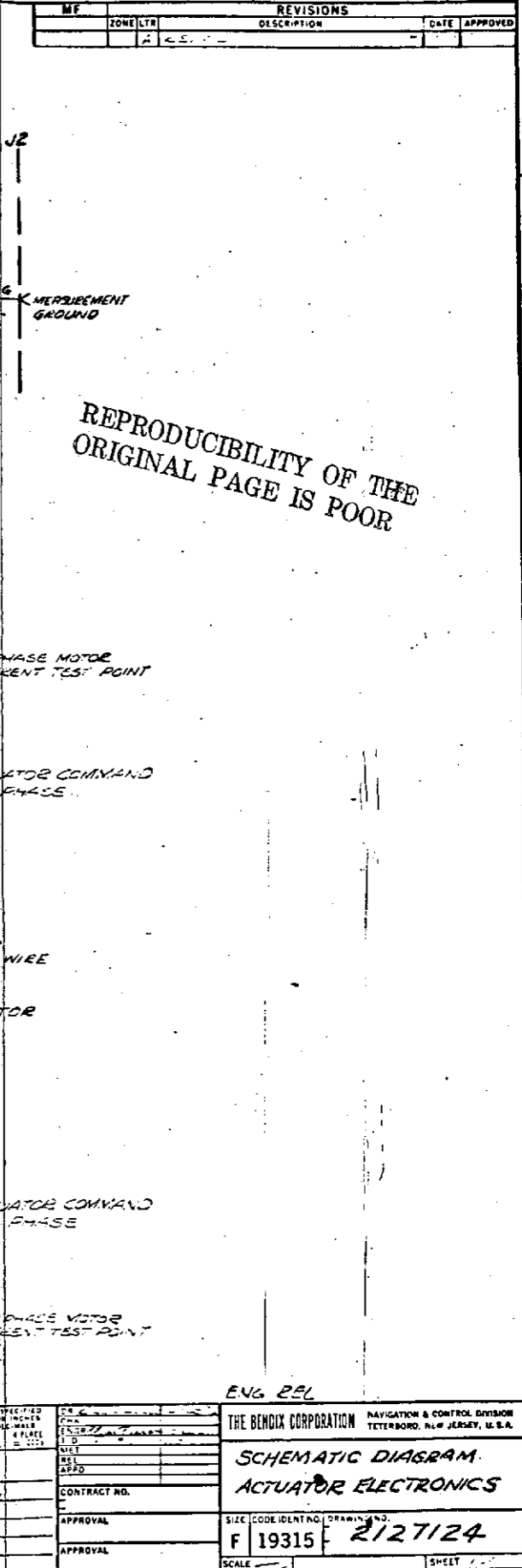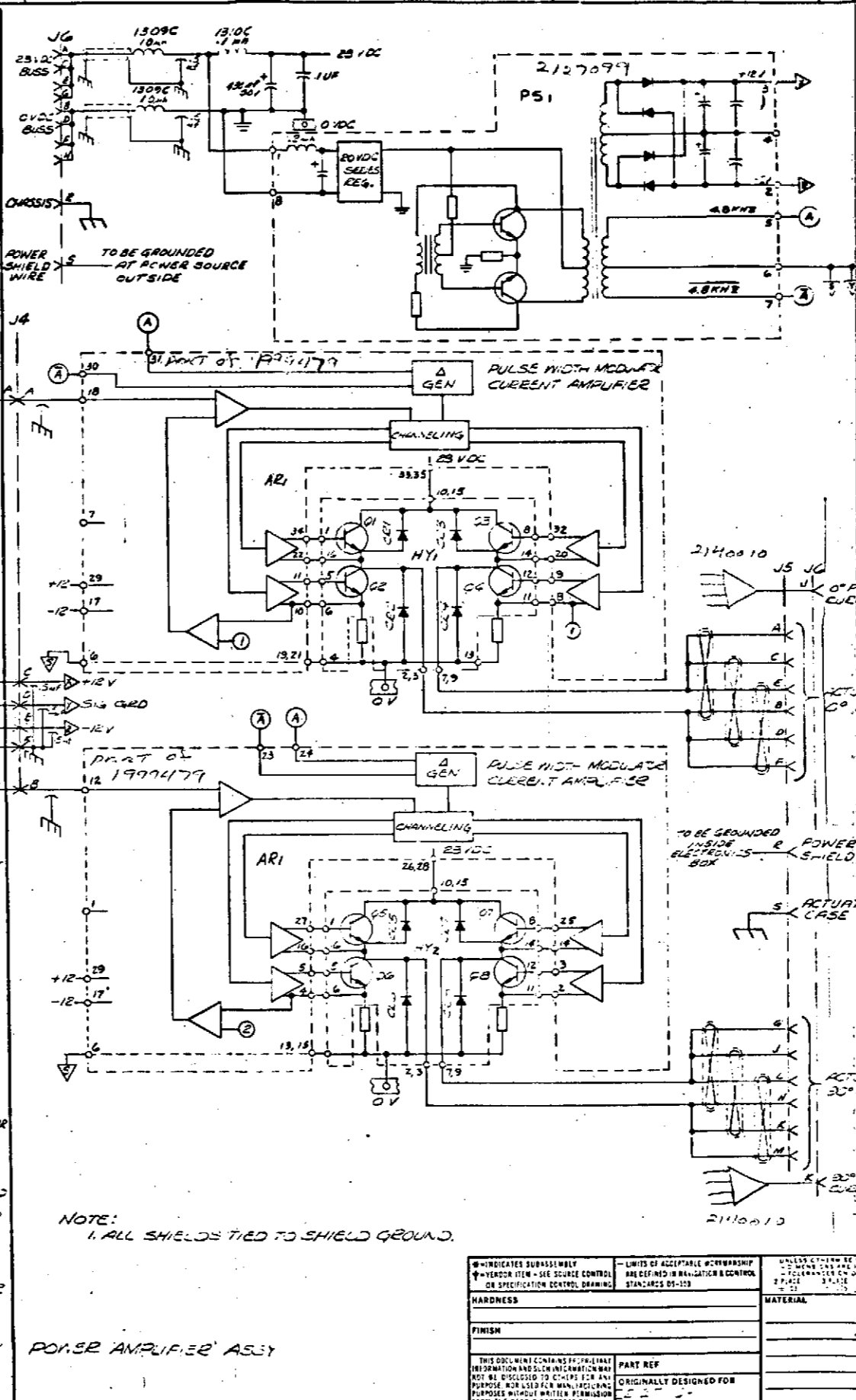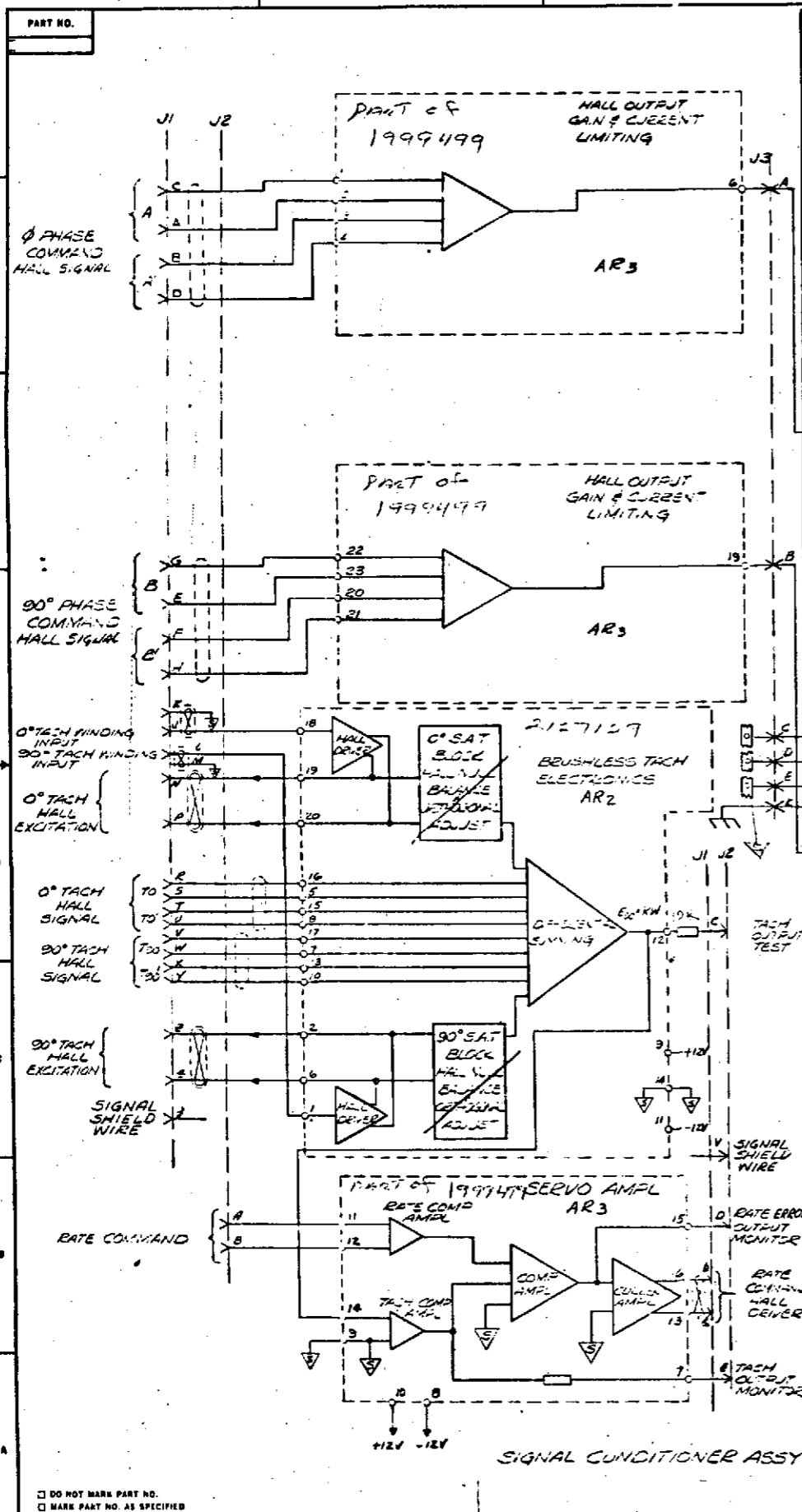$$K_{TG} \geqslant .96 \, \frac{Ft\text{-}lb}{Amp}$$

FIGURE 1.3.7-10

Schematic Diagram — Actuator Electronics (Bendix Corporation, Drawing No. 2127124)

NOTE:
1. ALL SHIELDS TIED TO SHIELD GROUND.

THE BENDIX CORPORATION — NAVIGATION & CONTROL DIVISION, TETERBORO, NEW JERSEY, U.S.A.

SCHEMATIC DIAGRAM
ACTUATOR ELECTRONICS

SIZE F   CODE IDENT NO. 19315   DRAWING NO. 2127124

SIGNAL CONDITIONER ASSY   POWER AMPLIFIER ASSY

ELECTRICAL SCHEMATIC, POWER SUPPLY, ACTUATOR

NOTES:
1. UNLESS OTHERWISE SPECIFIED RESISTOR VALUES ARE GIVEN IN OHMS ±5% TOLERANCE AND ARE 1/4 WATT RATING.
2. ALL CAPACITOR VALUES ARE GIVEN IN MICROFARADS, SECOND FIGURE IS VOLTAGE RATING.

ENG REL

SIZE D | CODE IDENT NO. 19315 | DRAWING NO. 2127099

PART NO. 2127099

FOLDOUT FRAME

CMG609

225

1-94

NOTES:

1. ALL RESISTERS ARE RNR55 UNLESS OTHERWISE NOTED.

☐ DO NOT MARK PART NO.
☐ MARK PART NO. AS SPECIFIED

NOTES:
1. ALL RESISTORS ARE RNR55 UNLESS NOTED.
2. ALL NON POLAR CAPACITORS CK12,13 OR CKR05 ±.06 UNLESS NOTED
3. ALL POLAR CAPACITORS CSR13,14
4. AR1 THRU AR9: PIN 7 IS +12V, PIN 4 IS −12V

THE BENDIX CORPORATION — NAVIGATION & CONTROL DIVISION, TETERBORO, NEW JERSEY, U.S.A.

SCHEMATIC DIAGRAM
SERVO COMPENSATION,
HALL DRIVERS & PWM CURRENT LIMIT
(SIGNAL CONDITIONING ASSY)

SIZE F   CODE IDENT NO 19315   DRAWING NO. 1999499

CMG 609

258   1-96

FOLDOUT FRAME

PART NO.

28VDC COM
+28VDC

A1 (REF)

4.8 KHz
SQUARE
WAVE

MONITOR

COMMAND

CURRENT
FD BK

+12
GRD
-12

A30 SAME AS A1
(REF)   (REF)

4.8 KHz
SQUARE
WAVE

MONITOR

COMMAND

CURRENT
FD BK

PULSE WIDTH MODULATOR

POWER
STAGE

POWER
STAGE

E OUT

HY 1
HKG 101

HY 2
HKG 101

HIGHEST DESIGNATION USED

AR6	C26	CR8	HY2	G12	R56

NOTES:
1. UNLESS OTHERWISE SPECIFIED RESISTOR VALUES ARE GIVEN IN OHMS
   ±5% TOLERANCE AND ARE 1/4 WATT RATING.
2. UNLESS OTHERWISE SPECIFIED CAPACITOR VALUES ARE GIVEN IN MICROFARADS
   SECOND FIGURE IS VOLTAGE RATING.
3. ▽ ALL LIKE DESIGNATED POINTS ARE CONNECTED.

ENG. REL.

THE BENDIX CORPORATION
NAVIGATION & CONTROL DIVISION
T. TERBORO, NEW JERSEY, U.S.A.

ELECTRICAL SCHEMATIC
PULSE WIDTH MODULATOR
(ACTUATOR)

SIZE F | CODE IDENT NO. 19315 | DRAWING NO. 1999479

FOLDOUT FRAME

CMG609

REPRODUCIBILITY OF THE
ORIGINAL PAGE IS POOR

FOLDOUT FRAME

240   1-97

HIGH TACH WINDING 1 COMM 3,4,14

HIGH DC TACH OUTPUT 12

COMM 3,4,14

+12VDC 9

−12VDC 11

HIGH TACH WINDING 2 COMM

REVISIONS

ZONE	LTR	DESCRIPTION	DATE	APPROVED

HIGHEST REFERENCE DESIGNATIONS USED

AR3	C13	R36	CR8	Q4	

REFERENCE DESIGNATIONS REMOVED

CR1 THRU CR4	R7 THRU R12	
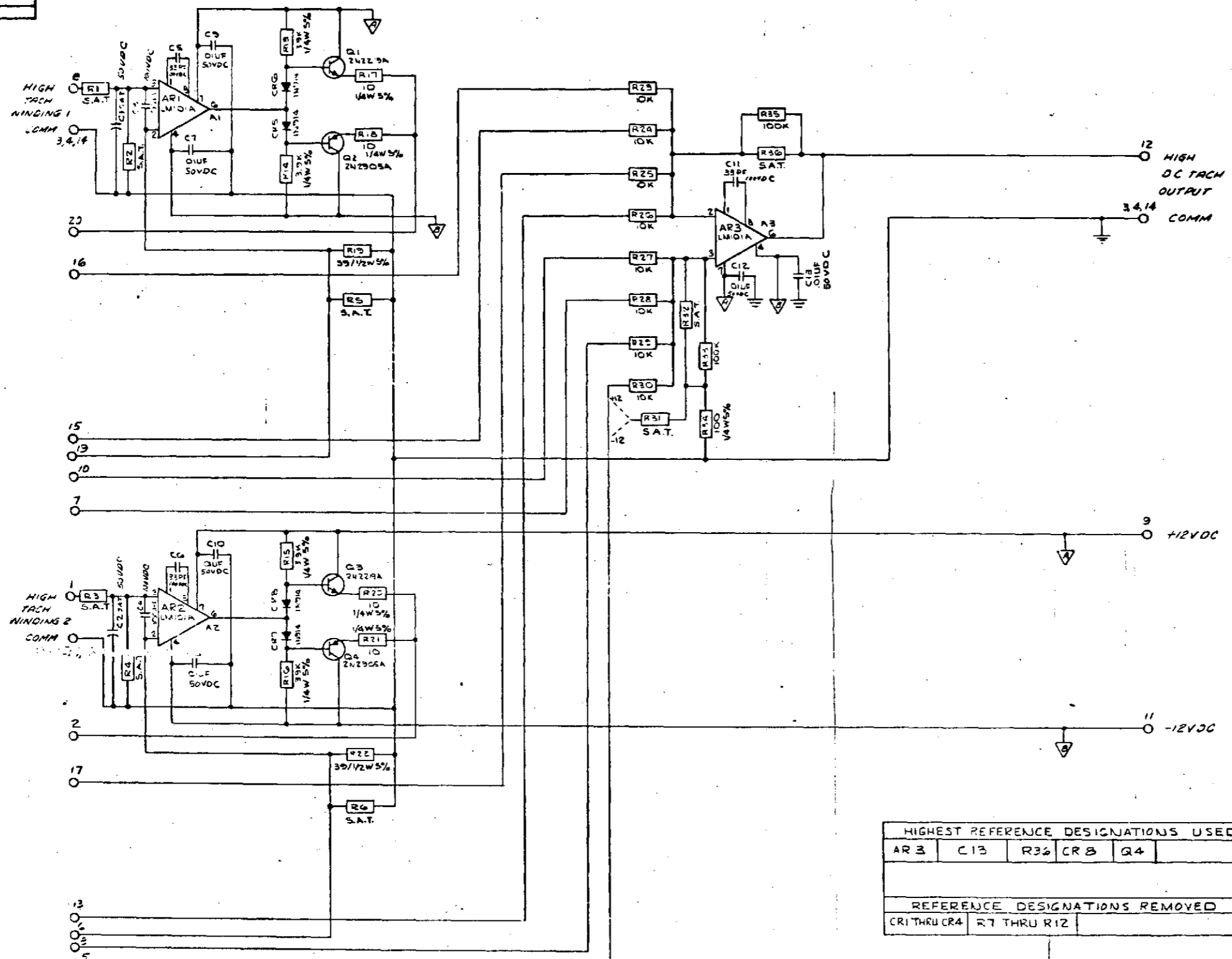
NOTES:
1. UNLESS OTHERWISE SPECIFIED:
ALL RESISTORS ARE SPECIFIED IN OHMS 1/10WATT ±1% (RNR55H)
UNLESS OTHERWISE SPECIFIED.
2. ALL CAPACITORS EXPRESSED IN MICROFARADS (M39014)
AND THE SECOND FIGURE IS THE VOLTAGE RATING.

PREPARED BY NAVIGATION AND CONTROL
DIVISION OF THE BENDIX CORPORATION
FOR
GEORGE C. MARSHALL SPACE FLIGHT CENTER
NASA, HUNTSVILLE, ALABAMA

THE BENDIX CORPORATION — NAVIGATION & CONTROL DIVISION
TETERBORO, NEW JERSEY, U.S.A.

ELECTRICAL SCHEMATIC
DC TACHOMETER
ELECTRONICS (ACT)

SIZE	CODE IDENT NO.	DRAWING NO.
F	19315	2127129

1.3.8   Brushless DC Spin Motor

1.3.8.1   Introduction

The CMG's that were used on Skylab were each driven
with two AC dual cage induction motors, one mounted
on each side of the inertia wheel. The motors were
designed to develop constant torque up to the vicinity
near synchronous speed and in that region to have a
very steep torque versus speed slope. This would as-
sure that the wheel momentum could be maintained with-
in close limits as torque loads were applied to the
CMG and as the bearing friction changed in level. The
motors were also designed to run with minimum losses
at the steady state speed. These features were accom-
plished for the motor configuration dictated by the
CMG design.

In order to further reduce the steady-state power it
was decided to design a brushless DC motor to replace
the AC motor. The brushless DC motor was to develop
higher torque and run more efficiently.

1.3.8.2   Description

The brushless DC motor for the Advanced CMG (See Figure
1.3.8-1) is a two phase, four pole, machine. The rotor
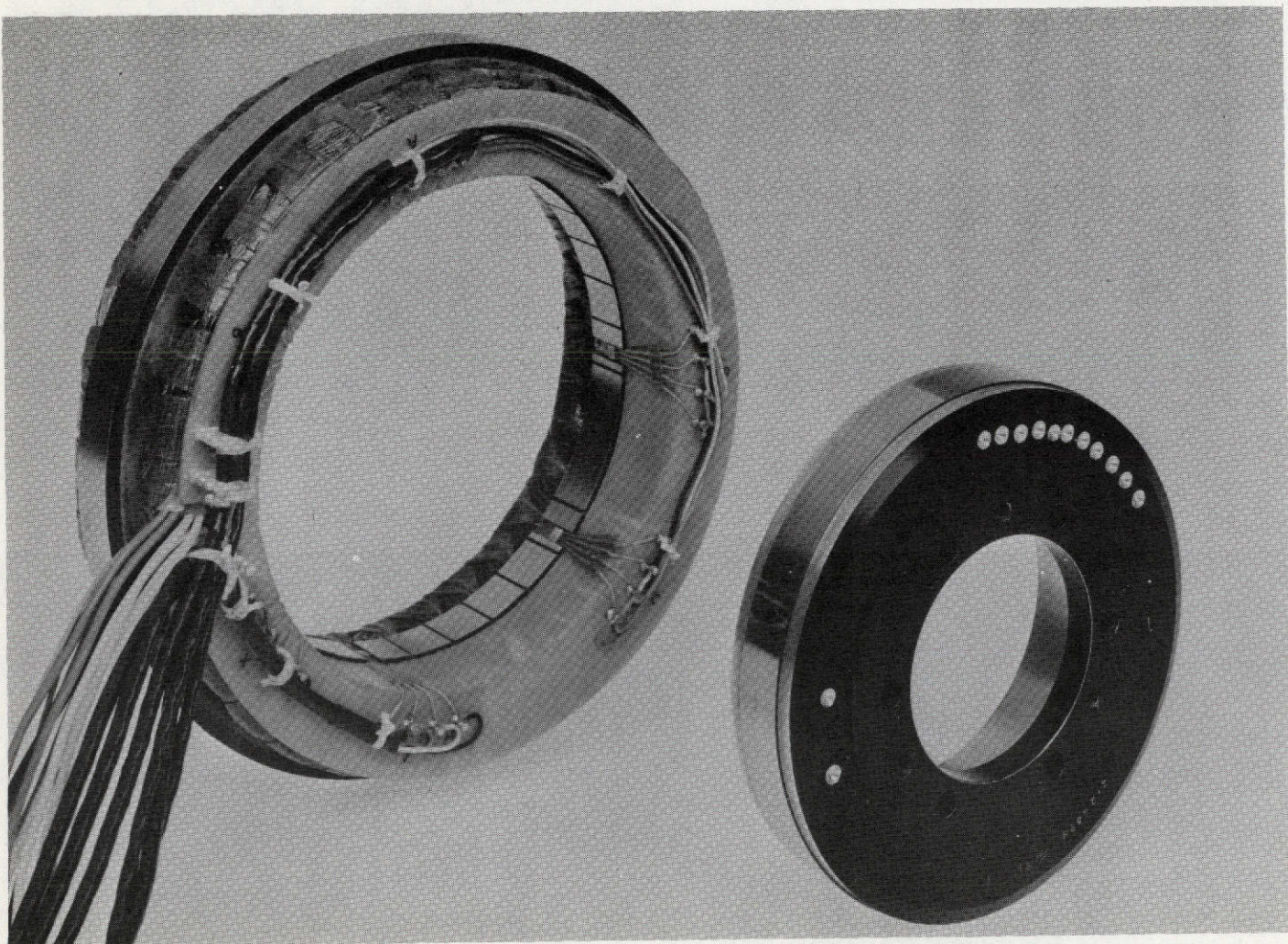
BRUSHLESS DC SPIN MOTOR

FIGURE 1.3.8-1

is the inner member which is mounted on the shaft. It contains a four pole magnetized alnico 6 permanent magnet ring with a protective band of inconel. The band is intended to prevent rupture of the magnet ring under centrifugal loads at high speeds. The two phase wound stator is the outer member of the machine. The windings are excited from electronic circuitry that is controlled by hall generators located in the air gap of the machine. There are two hall generators for each phase located in grooves in the inside surface of the stator. These generators produce signals proportional to the flux density present in the air gap. Two additional hall generators are used for speed sensing. Since the major portion of the magnetic flux in the air gap is from the permanent magnet, the hall signals indicate the actual position of the rotor. The two hall devices in each phase are separated physically by 150 mechanical degrees. When they are summed electrically, they eliminate completely any third harmonic distortion of the air gap flux that may be present. Higher order harmonic distortions are also reduced. The hall devices of the second phase produce signals which are 90 electrical degrees displaced from the pair of the first phase.

The four hall devices are located in positions such that the summed outputs of each pair will excite the circuitry for the stator winding located in electrical quadrature. In this manner true DC machine operation will be realized.

1.3.8.3 Characteristics

The parameters listed below were measured on the motor alone (exclusive of electronic circuitry).

Back Emf constant   = 0.002314 volts peak/rpm

Torque constant   = 3.13 oz-in/amp

Winding Resistance   = 0.17 ohms

Electrical time constant = L/R_{DC} = 4 millisec

Maximum current   = 10 amps peak

Maximum torque   = 31.3 oz-in

Maximum stall power = 17 watts

Magnetic drag Torque at 8000 rpm = 0.5 oz-in.

Outside diameter   = 6.00 inches

Inside diameter   = 2.50 inches

Length   = 2.00 inches

The motor power flow diagrams are given in Figure 1.3.8-2. The values given in the diagrams are based on the parameters given above.

STALL

I = 10a

17 W →

STATOR

31.3oz-in

0 W →

ROTOR

31.1 oz-in

0 W →

↓

COPPER LOSS

17.0 W

↓

MAGNETIC DRAG

.2 oz-in

0 W

8000 RPM FULL TORQUE

I = 10a

202.3 W →

STATOR

31.3oz-in

185.3 W →

ROTOR

30.8 oz-in

182.3 W →

↓

COPPER LOSS

17.0 W

↓

MAGNETIC DRAG

.5 oz-in

3.0 W

8000 RPM STEADY STATE

I = .16a

3.1 W →

STATOR

.5 oz-in

3.0 W →

ROTOR

↓

COPPER LOSS

.1 W

↓

MAGNETIC DRAG

.5 oz-in

3.0 W
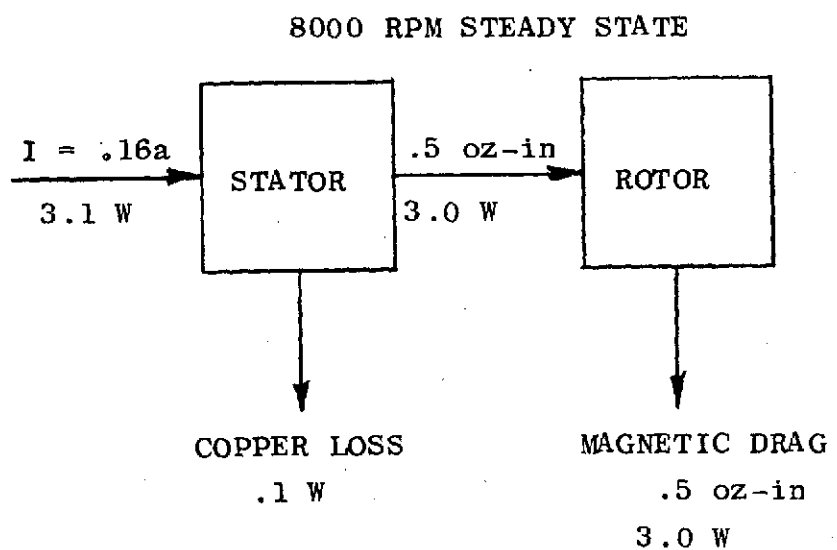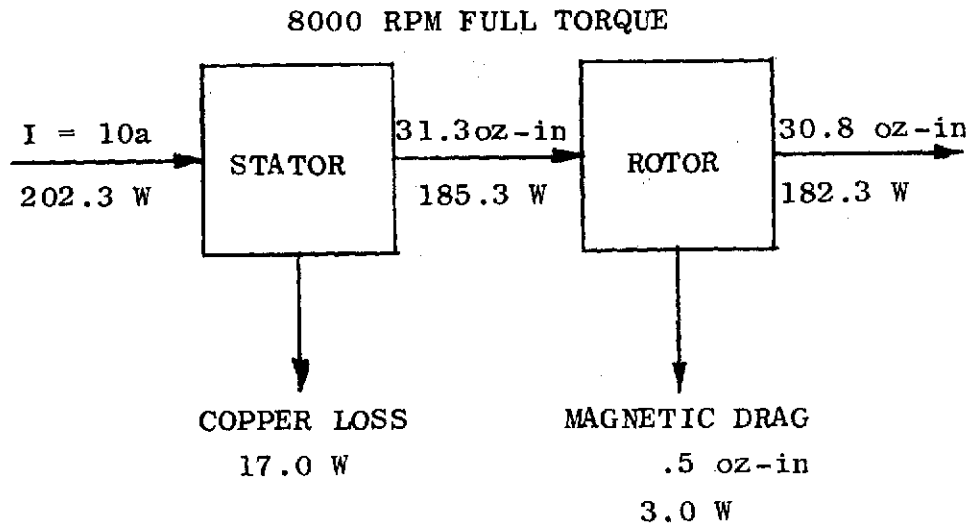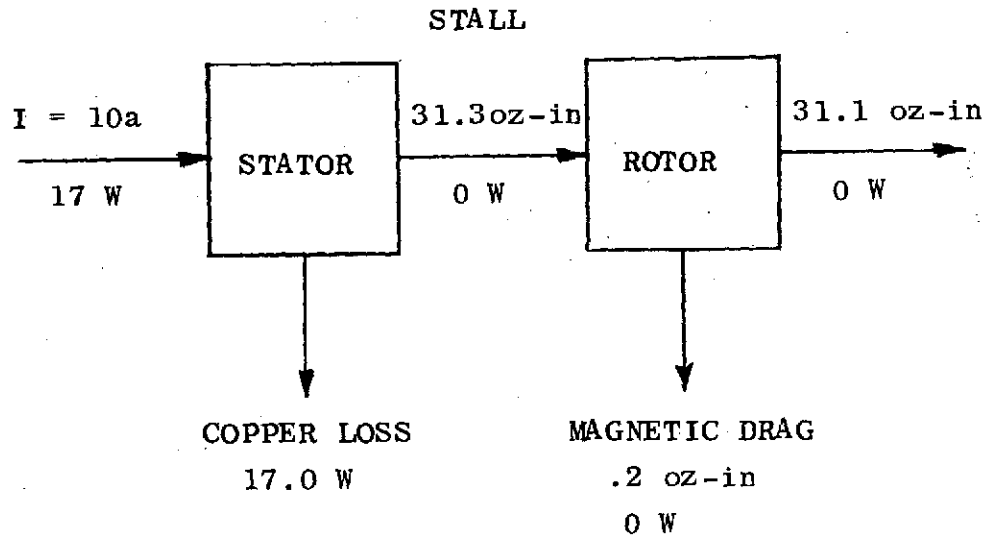
FIGURE 1.3.8-2

1.3.8.4 Improvements

In order for the brushless DC spin motor to replace the AC induction motor from a reliability consideration, there has to be an absolute guarantee that demagnetization cannot occur and that the permanent magnet rotor cannot fail structurally. Another desirable but not mandatory characteristic would be the reduction of magnetic drag losses.

1.3.8.4.1 Magnet Drag Losses

This loss is present when the brushless DC machine rotates regardless if it is excited or not.

If there is relative motion of parts of the magnetic circuit, these hysteresis and eddy current losses will be dissipated. An effective means of reducing drag is to minimize the number of poles; then the frequency of magnetic flux variation and the losses are lowered. If the CMG motor is to be designed for 2 poles using conventional methods, the shaft diameter would have to be drastically reduced and the length of the motor would be increased. This configuration was not permissible for the given application. A practical solution is to design the machine using high energy permanent magnet materials such as samarium cobalt. This

type of magnet has such high covercive force that the air gap of the machine can be made much longer than for conventional style machines. This will allow the use of a stator whose windings are not imbedded in an iron structure but are placed in the air gap. The basic design applicable for the CMG is the concentric style shown in Figure 1.3.8-3. It consists of three concentric aligned cylinders. The inner and outer cylinders form the magnetic circuit and are attached to the shaft. They rotate together and dissipate no drag losses. The middle cylinder is the ironless stator containing the windings and the hall generators. With this type of machine, there is no longer the limitation of minimizing the number of poles.

1.3.8.4.2 Demagnetization

One of the most important characteristics of high energy magnets is that it takes a tremendous amount of energy to magnetize and demagnetize. In fact standard magnetizing equipment cannot supply the energy required. Due to this characteristic it is virtually impossible to demagnetize the magnets in the motor. Alnico magnets, on the other hand, can be demagnetized if high current spikes flow through the motor windings, or if

HIGH ENERGY
PERMANENT MAGNET

MAGNETIC CIRCUIT

SHAFT

STATOR WINDINGS

HALL GENERATOR
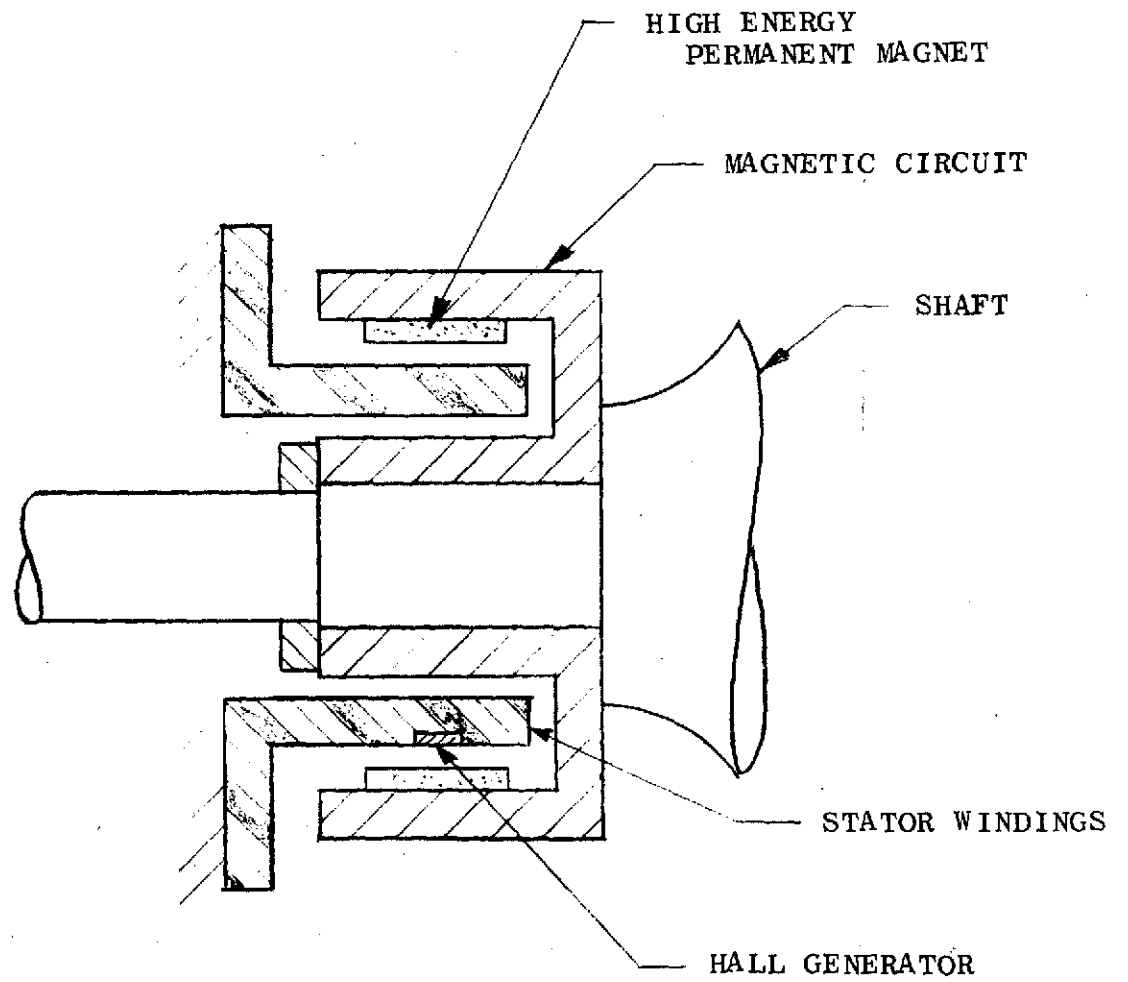
HIGH ENERGY
BRUSHLESS DC SPIN MOTOR
FIGURE 1.3.8-3

the windings are short circuited at high speeds, or
if a high DC voltage is applied to the windings at
low speeds. High energy magnets are impervious to
each of these conditions.

1.3.8.4.3   Structural Integrity

Since permanent magnets are very brittle and poor in
tensile strength, they should be protected from centri-
fugal stresses. The conventional ring magnet designs
have to be heavily banded with non-magnetic (inconel)
material to prevent rupture at high speeds. This band
adds to the magnetic air gap of the machine and sacri-
fices performance. The structural integrity problem
is solved when high energy magnets are used in the
configuration shown in Figure 1.3.8-3. Here the mag-
nets may be in small sections all being protected in
centrifugal stress by the outer magnetic circuit of
the rotor.

1.3.8.5   Recommendation

Brushless DC spin motors can be built reliability and
safely with good performance characteristics if the
high energy concentric design of Figure 1.3.8-3 is
employed. It is recommended that work be done toward
this goal.

1.3.9   Brushless DC Torquer

1.3.9.1   Introduction

The gimbal torquers used on the Skylab CMG's were of
conventional brush DC type. The primary concern in
using this type of machine centered on the reliability
of the brushes. Special compound brushes had to be
used because of the high vacuum environment.

In order to eliminate the need for brushes and commuta-
tor, it was proposed to develop a brushless DC machine.

1.3.9.2   Description

The brushless DC torquer for the Advanced CMG (See
Figure 1.3.9-1) is a two phase, twelve pole machine
that is operated in conjunction with a separate hall
resolver, described in Section 1.3.10. The rotor is
the inner member of the torquer and is mounted on the
shaft. It consists of twelve alnico 9 magnets circum-
ferentially oriented and assembled alternately with
twelve soft iron pole pieces. The rotor is banded
with a thin ring of titanium for mechanical protection.
The two phase wound stator is the outer member. It is
skewed and wound to minimize cogging and ripple torques.
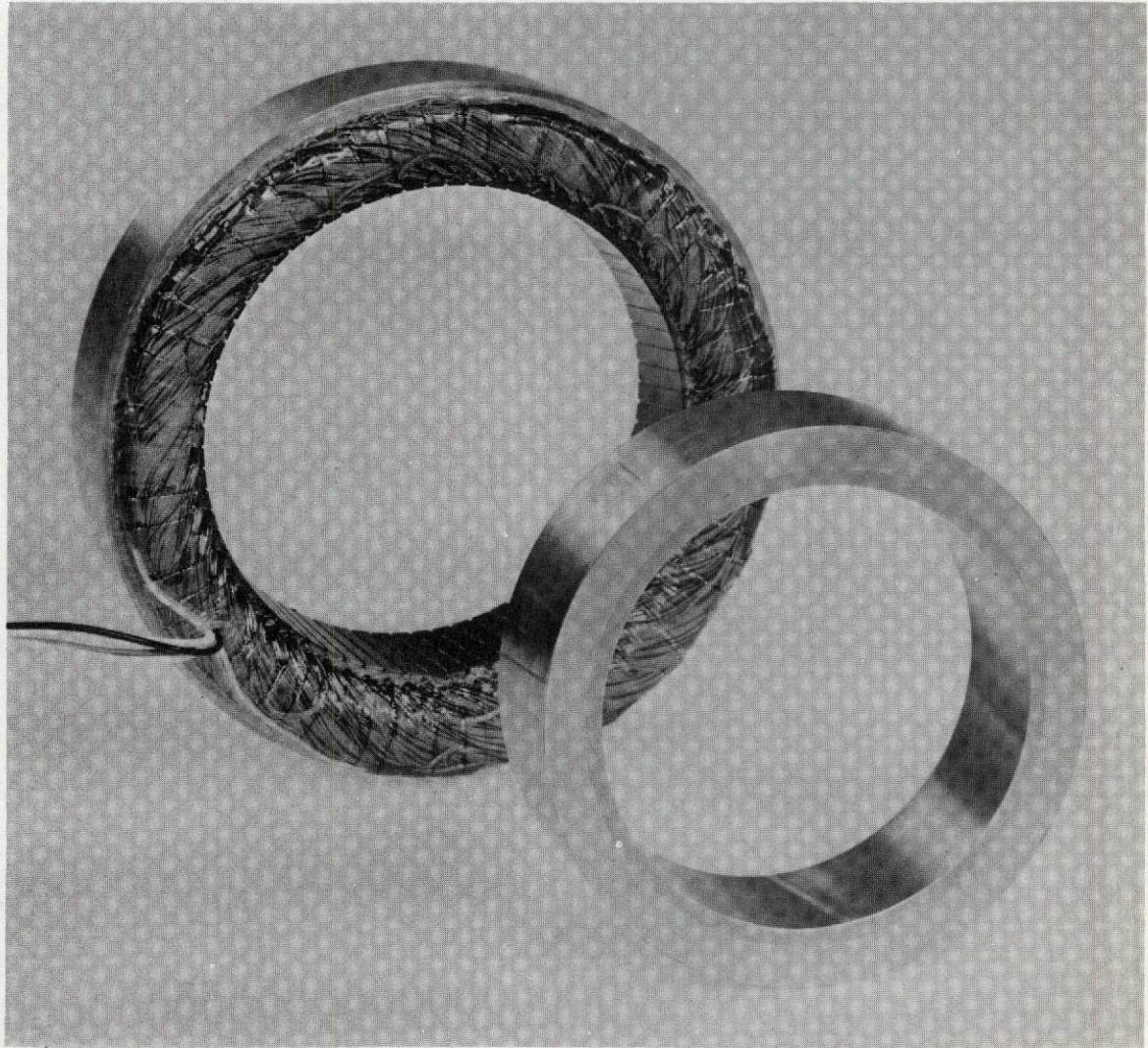
BRUSHLESS DC TORQUER

FIGURE 1.3.9-1

1.3.9.3 Characteristics

The parameters listed below were measured on the torquer alone (exclusive of electronic circuitry).

Machine constant $= 0.810$ ft-lb/$\sqrt{\text{watt}}$

Back emf constant $= 1.20$ volts/rad/sec

Torque constant $= 0.885$ ft-lb/amp

Winding resistance $= 1.19$ ohms

Electrical time constant $= L/R_{DC} = 8.3$ millisec

Rated current $= 10$ amps

Rated torque $= 8.85$ ft-lb

Average cogging torque $= 0.6$ in-lb

Outside diameter $= 7.20$ inches

Inside diameter $= 3.95$ inches

Length $= 2.50$ inches

Weight $= 9.7$ lb.

The system ripple torque was measured as $\pm 6.25\%$

1.3.9.4 Improvements

The brushless DC torquer can replace the brush type torquer to offer improved reliability by eliminating brushes and commutator wear problems. However, there are refinements that will improve performance and reliability even further.

1.3.9.4.1   Demagnetization

When using alnico magnets, the possibility is present
where demagnetization can take place and deteriorate
the performance of the torquer. This will occur if a
high current spike flows through a winding. In order
to overcome this problem the machine can be redesigned
to utilize high energy permanent magnets (samarium
cobalt). This material is virtually impervious to
demagnetization. As an added feature, no keepering
will be necessary when transferring the rotor structure,
making assembly simpler. The air gap of a high energy
permanent magnet machine can have a larger air gap than
conventional; therefore, cogging and ripple torques
can be reduced.

1.3.9.4.2   Brushless AC Resolver

The output wave shape and the overall reliability of
the present hall resolver can be greatly improved if
the device is redesigned to a brushless AC resolver
operating on the varying reluctance principle. The
ripple torque of the brushless DC torquer will be
reduced by the purer sinusoidal outputs of the brush-
less AC resolver.

1.3.9.5   Recommendation

If the brushes and commutator of a DC torquer is to be eliminated then the brushless DC machine is a satisfactory replacement. But, to further the improvement of the machine, it is wise to use high energy magnets instead of the alnicos and a brushless AC resolver instead of the hall resolver. It is recommended that work be done toward these goals.

1.3.10   Brushless Tachometer

1.3.10.1   Introduction

As a result of the requirement for a D.C. tachometer

that does not have the problem of poor contacts, sparks

or excessive friction torque, the brushless tachometer

was developed.   (See Figure 1.3.10-1).

The mechanical commutating mechanism has been replaced by

Hall Generators and a summing amplifier. (See Figure 1.3.10-
A number of units have been built proving that the

design goals can be satisfactorily met.

As a result of the development of the brushless D.C.

tachometer, methods and techniques were developed that

are discussed in the following paragraphs.

1.3.10.2   Design Considerations

The brushless tachometer requires the proper placement

of the Hall generators in the air gap.

The location of Hall generators has to be within 5 min-

of-arc of the theoretical position in order to keep the

perpendicularity errors to a minimum as well as to

derive the maximum benefit from the pitched Hall elements.
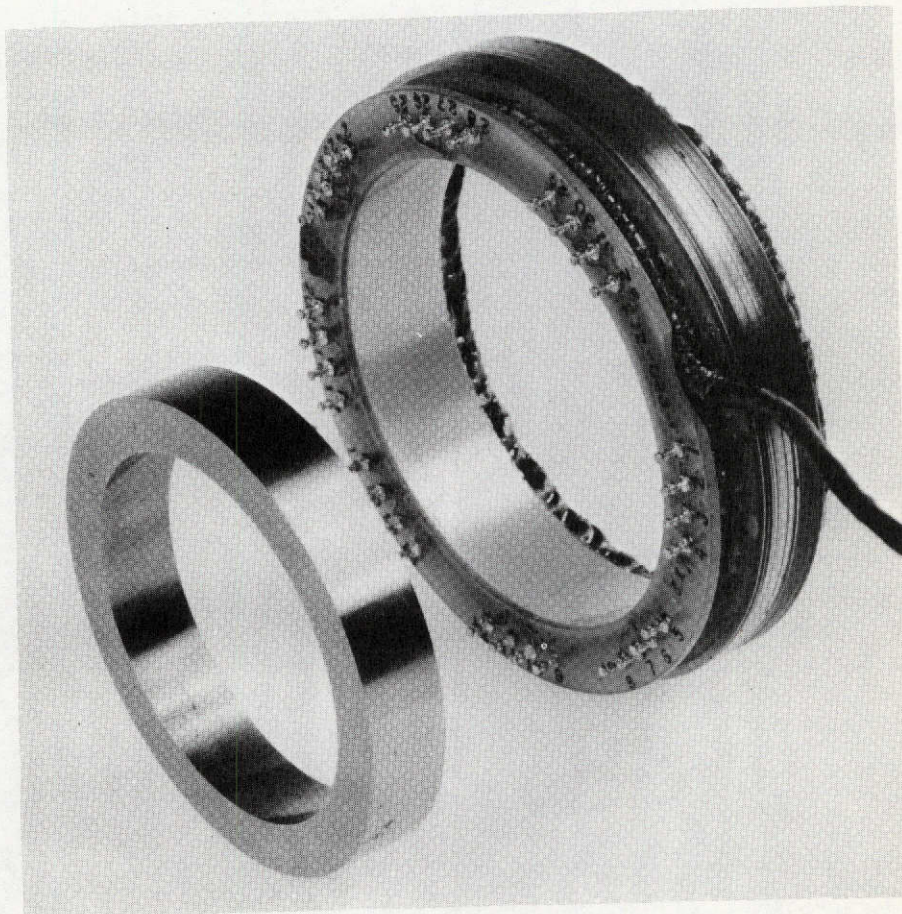
BRUSHLESS DC TACHOMETER

FIGURE 1.3.10-1

BRUSHLESS D.C. TACHOMETER

$$I_A = \frac{K'\phi\omega}{R} \cos \omega t$$

$$e_A = K\phi_m\omega \cos \omega t$$

$$e_B = K\phi_m\omega \sin \omega t$$

12 POLE SINUSOIDAL MAGNET

$$\phi = \phi_m \cos \omega t$$

$$\phi = \phi_m \sin \omega t$$

$$Y_{H_A} = K\phi_m^2\omega \cos^2 \omega t$$

$$E_o = K\phi_m^2\omega$$

$$Y_{H_B} = K\phi_m^2\omega \sin^2 \omega t$$

SUMMING AMPLIFIER
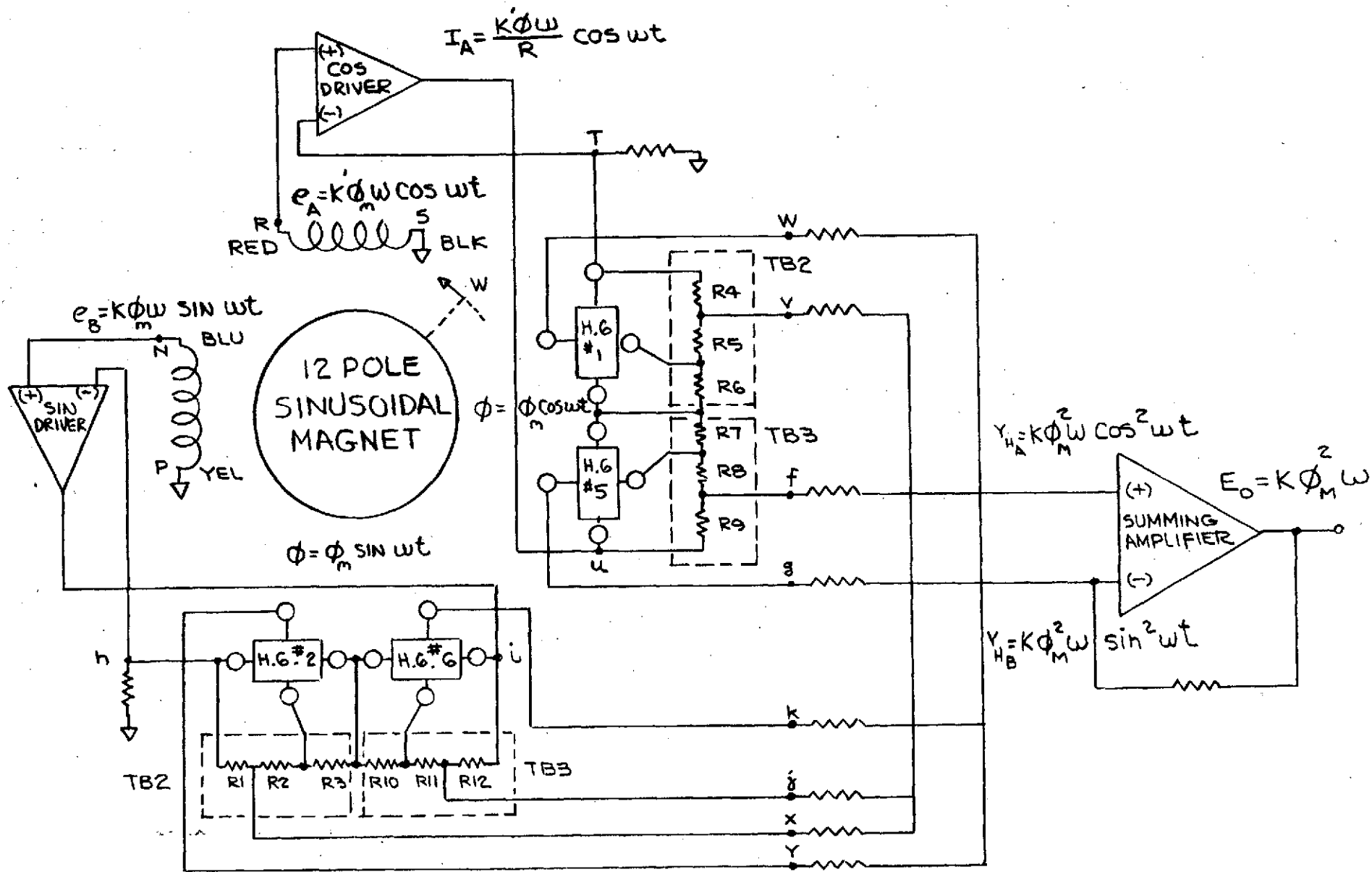
* ω IS CCW FROM LEAD END

FIGURE 1.3.10-2

Any error in the position of the Hall generators will
increase the magnitude of the ripple harmonics.

A method of reducing the 4th harmonic ripple voltage
has been very successful by pitching the Hall generators
which minimizes the predominant 3rd mmf harmonic.

Similarly, care is required to avoid unequal flux
caused by unsymetrical poles on the Hall generators
which otherwise will result in a 2nd harmonic ripple
voltage.

The control of the other ripple harmonics can be accom-
plished by using a magnetization fixture that approxi-
mates an ideal sine-wave.   At the present time, the
fixture design is determined from empirical data.

In order to provide the uniform flux density for the
Hall generators, the winding flux axis should be
located in front of a stator tooth. Thus, the flux
axis will be coincident with the Hall generator and
the winding, which is essential for proper commutation.

1.3.10.3   Magnet Flux Evaluation

The method used to determine the quality of the imprinted sinusoidal function on the magnet is to rotate the magnet past a Hall generator and analyze its output with a wave analyzer. In order to determine the frequency and the magnitude of the harmonics, a 1800 RPM synchronous motor is used to drive the rotor at a constant speed.

The revolving magnet produces a field that can be described by:

$$\phi = \sum_{p=1} \phi_{pm} \cos (p\omega t + \theta_p)$$

Where

ϕ_{pm} = amplitude of the p-th harmonic

p = order of the p-th harmonic

ω = angular rotation

θ_p = phase of the p-th harmonic

Thus, the harmonic content of the magnetic field can be determined by analyzing the Hall generator output in the time domain.

The fundamental frequency is determined from:

$$f_{FND} = \frac{RPM \times P}{120} = \frac{1800 \times 12}{120} = 180 \text{ cps}$$

Where

P = No. of poles (12)

Evaluating the magnitude and the order of the harmonics present in the Hall generator output, the quality of the charged magnet can be determined as indicated in the table below.

HARMONIC	FREQ. (Hz)	ERROR SOURCE	ACCEPTABLE LIMIT
1	30	Rotor Eccentric	1.0%
5	150)	Pole to Pole field	1.5%
7	210)	strength unbalance	1.5%
18	540)	Characteristic of	5.0%
30	900)	magnetizing fix-	1.5%
		ture, air gap, and	
		magnetizing current.	

Similarly a wave analysis of the D.C. output ripple

voltage is performed from which additional sources of error can be detected. Some of these harmonics can be reduced by calibrating the system using the S.A.T. resistors. The following table presents the causes and/or means for correction of the error harmonics as detected by a ripple voltage analysis.

As was indicated previously, the system is initially checked out at a speed of 1800 RPM so that the wave analyzer can be used to detect the problem areas. During this test, the winding output is reduced with a voltage divider to a level that simulates a speed of 10 RPM.

BRUSHLESS TACHOMETER ERROR SOURCES

RIPPLE VOLTAGE HARMONICS		SOURCE	CAUSE (MEANS OF CORRECTION)
PER REVOLU.	PER EL. CYCLE		
1		Mechanical	Eccentricity of Rotor with respect to the stator
		Magnetic	Eccentric Magnetic Pole imprintation on magnet
2		Magnetic (8th mmf Harm.)	Harmonic due to Pole to Pole unbalance
3 thru 5		Magnetic	Non Sinusoidal Magnetic Field
6	1st(Fund)	Electrical	Resistive null offset in Hall generators. D.C. bias in current drivers and/or summing amplifier
7 thru 9		Magnetic	Non Sinusoidal Magnetic Field
10	4th mmf Har.)		Pole to Pole field strenth unbalance resulting in mmf harmonics due to non-homogeneousness of the magnetic material
11	5th mmf Har.)		
13	7th mmf Har)		
14	8th mmf Har.)		

CONT.

RIPPLE VOLTAGE HARMONICS		SOURCE	CAUSE (MEANS OF CORRECTION)
PER REVOLU.	PER EL. CYCLE		
12	2nd	Electrical	Gain unbalance of current drivers, Hall generator outputs, and/or summing amp. inputs.
		Magnetic	Inaccurate location of magnetic poles of magnet. Result of higher order harmonics in magnetic field
		Mechanical	Orthogonality error of Hall generator position and/or winding position
15 thru 23		Magnetic	Non Sinusoidal Magnetic Field
24	4th	Magnetic (18th mmf Harmonic)	The most predominant megnetic field harmonic (3rd/El.Cycle) due to non-sinusoidal imprintation. Higher order harmonics.
			Winding distribution inaffective in eliminating 18th mmf harmonic.
		Mechanical	Inaccurate positioning of "PITCHED" Hall generators.

RIPPLE VOLTAGE HARMONICS		SOURCE	CAUSE (MEANS OF CORRECTION)
PER REVOLU.	PER EL. CYCLE		
25 and Higher		Magnetic	Due to magnetic field harmonics

1.3.10.4   Test Results

TACHOMETER WINDING CHARACTERISTICS

D.C. Resistance	=	1150 Ohms
Output Impedance	=	1200 Ohms
Air Gap Flux	=	5000 maxwells
Sensitivity	=	0.175 V peak/RPM
	=	1.6 V peak/Rad/sec.

Output Voltage Distortion	=	0.21% (RSS)

MAGNET CHARACTERISTICS

Material	–	Alinco VI
		Circumferentially oriented
Poles	–	12
Field Distortion	–	3.0% (RSS)

BRUSHLESS D.C. TACHOMETER OUTPUT CHARACTERISTICS

Sensitivity	=	0.190 V/RPM
	=	1.80 V/Rad/Sec
Ripple Voltage	=	±3.6% (Based on max. output at 20 RPM)

1.3.10.5   Conclusion

This development program indicated that a Brushless
D.C. Tachometer using Hall generators can be built
whose ripple voltage is less than ±4%. To achieve this

tolerance, the error sources that contribute to the ripple voltage have to be minimized or its effects compensated for by calibration and careful magnetization.

This can be attained by careful evaluation and control of each error source during the build stage. The magnet assembly has to be properly magnetized to ensure a sinusoidal magnetic field.

Due to a high winding impedance, the magnet will not be demagnetized with an external short circuit. A possible precaution that could be taken for higher speed application is the banding of the O.D. and the use of side plates on the rotating magnet. The size of the tachometer can be reduced by using the rare earth magnets (Samarium Cobalt or Misch Metal).

To improve the reliability of the Brushless D.C. Tachometer, especially during manufacturing, printed circuit Hall generators should be used. The printed circuit leads, together with the encapsulation of the

Hall generator, produce a reliable mounting arrangement. To simplify the system calibration for the reduction of the ripple voltage, the Hall generators should be matched as closely as possible.

1.4 Conclusions and Recommendations

1.4.1 Maintainability and Life Considerations

Parts replacement, at feasible levels of CMG subassemblies, has been inherently provided for in the packaging design of the ATM CMG as well as this Adv. CMG except for the spin bearings which are readily replaceable only in the Adv. CMG (see Section 3). The CMG subassemblies most readily replaceable are the IGRA, the Actuator Pivot Assemblies, the Sensor Pivot Assemblies, the Outer Gimbal, the Frame, Electronic Boxes, Cables and Spin Bearings.

The Outer Gimbal and Frame are rugged structural members which do not contain electromechanical or electronic parts subject to normal reliability and wearout considerations. Assuming conservative estimates can be made for probable ground handling and test loads and temperatures, launch loads and orbital loads and temperatures, these subassemblies can be designed with adequate margins to maintain integrity, stiffness, parallelism and orthogonality requirements typical of the performance requirements of this CMG. These structural members would not normally require replacement.

The IGRA, Actuator and Sensor Pivot Assemblies, and Electronic Boxes are all removed by unmating electrical connectors and removing mounting screws. Although not provided in this prototype CMG, these subassemblies can be designed with captive mounting screw arrangements or other disconnects so as to minimize loose parts in an orbital replacement. Although the development of detail procedures and holding fixtures for orbital replacement of these subassemblies is beyond the scope of this contract, such replacement is considered feasible. Cables may be replaced since they can be accurately preformed and cable clamps can be designed without resulting in loose parts during replacement. The spin bearings can be replaced by procedures and tools as discussed in Section 3.

The only parts of this CMG subject to wear considerations are as follows;

1. Lip Seal, Output Shaft - Used in each Actuator and Sensor Pivot Assembly - an earthbound humidity environmental consideration which is possibly not required for some applications.

2. Gimbal Pivot Bearings - used in each actuator and Sensor Pivot Assembly.

3. Gears and Gear Bearings - Used in each Actuator Pivot
   Assembly.

4. Slip Rings - Used in each Sensor Pivot Assembly.

5. Spin Bearings - Used in the IGRA.

As previously discussed, these can all be replaced in
scheduled or unscheduled maintenance; i.e. the Actuator
Pivot Assemblies, the Sensor Pivot Assemblies, the IGRA
or the Spin Bearings.

Since this CMG is mechanically very similar in design
to the ATM CMG, it is reasonable to assume a useful life
of 2 years without repairs based on demonstrated ground
test use in excess of 30,000 hours on each of 3 full
ATM CMGs at MSFC (HSL Motion Simulator Units) as well as
the 270 day Skylab ATM orbital mission. The orbital
failure of an ATM CMG spin bearing has been studied and a
retainer fix is working well in demonstration testing
under contract NAS-8-20661. The slip ring life has not
yet been demonstrated in the full Adv. CMG system,
however, component slip ring testing indicates feasibility.
A useful life of 5 to 10 years with minimum parts replace-
ment and with low order skills appears feasible consider-
ing the subassembly packaging design, minimum number of
wearing parts and subassembly replacement discussed pre-
viously.

The following further effort is recommended:

1. The Advanced 2000H DG CMG prototype unit should be retrofitted with the spin bearing fix developed under NAS8-20661. During this retrofit (in light of the explosion accident on the 6000H IGRA – see section 2) the wheel should be put through another series of non-destructive inspections/tests before operation at 12,000 RPM. Upon completion of the above, the unit should be reassembled and put through an extended life test under a typical gimbal rate and environmental duty cycle to demonstrate the life capabilities of the actuator gears, bearings and lip seals, and sensor slip rings, bearings and lip seals and provide additional life test data on the spin bearings.

2. If future NASA missions, requiring CMGs of this type and capacity, require orbital replacement of CMG subassemblies as part of their logistics plan – then more detail design work should be done to develope detail procedures, holding fixtures, tools and CMG subassembly design changes as required.

1.4.2   Wheel Control System

The desired improvements in spin up time, speed control,

brushless DC spin motors, PWM electronics and increased
angular momentum have been provided in this engineering
prototype CMG. Further evaluation of performance is
recommended in an extended life test under a typical
gimbal rate and environmental duty cycle as mentioned
in 1.4.1. Optimization of design should be based on
life testing, more detailed application requirements
and the application of state of the art development
in electronics and spin motors. Specifically, further
development work should be undertaken to provide a
brushless DC spin motor utilizing high energy permanent
magnet materials, such as samarium cobalt, and an ironless
stator (see Section 1.3.8). A design of this type has
the potential of eliminating magnetic drag losses and
susceptibility to demagnetization.

1.4.3   Gimbal Control System

The desired improvements in output torque, brushless dc
torquers and tachometers, PWM electronics and unlimited
gimbal freedom have been provided in this engineering
prototype CMG. Further evaluation of performance is
recommended in an extended life test under a typical
gimbal rate and environmental duty cycle as mentioned in
1.4.1. Optimization of design should be based on life

testing, more detailed application requirements and the application o f state of the art development in electronics and torquers and resolvers. Specifically, further development work should be undertaken using high energy magnets and a brushless AC resolver instead of the Hall resolver (see Section 1.3.9).

Gimbal rate bandwidth for this size DG CMG on the order of 6Hz has been demonstrated for the maximum coupled condition of zero relative gimbal angle with conventional rate servo loop implementations. The achievable stiffness of gears and structural members for reasonable cost, size and weight is a basic constraint. If direct drive gimbal torquers were used, eliminating gears, it is expected that bandwidth improvement can be made but probably at the expense of size and weight considering the output torque objectives. Further development work should be done in this area as well as investigating other cross-axis response compensation techniques than studied during this program (see Section 1.3.7.6).

SECTION 2

ADVANCED IGRA DEVELOPMENT

6000H IGRA

6000 H IGRA (TOP COVER REMOVED)

MOUNTED IN HOLDING FIXTURE

FIGURE 2.1-1

73-2733

2.1 GENERAL

The advanced 6000 Ft Lb Sec Inner Gimbal and Rotor Assembly
(6000H IGRA) developed under this contract is shown in Figure 2.1-1
in the test area at Bendix. This IGRA was designed for nominal
operation at 8000 RPM (6000 FPS) with a non-optimized set of charac-
teristics at operating conditions of 4000 RPM and 12,000 RPM. The
IGRA was to have been consigned to MSFC for evaluation. All per-
formance goals were met under operation at 8000 RPM and 4000 RPM.
Operation at 12000 RPM was not evaluated since the unit was de-
stroyed in an explosion accident on 25 October 1973 when the rotor
experienced a burst failure while being run up to the high speed
condition for performance testing. The rotor burst at a speed of
11,933 RPM.

The basic concept for this IGRA was to use the desirable
features of the Skylab ATM CMG IGRA and to incorporate new features
based on new technology as well as provide for new and changing Pointing
Control System requirements for potential future missions such as
Earth Orbiting Space Station/Base. As a result, the following de-
sign philosophy was adopted;

> a. Inner Gimbal and Rotor Assembly (IGRA)

Use the same design type wheel (rotor), gimbal, strut, covers,
performance monitors and wheel suspension system as that employed
in the Skylab ATM CMG appropriately scaled up for the larger angular
momentum. The wheel suspension system consists of the spin bearings,
their lubrication technique, the lubricant sealing technique and

the bearing preload technique. The desired new technique included replaceable spin bearings and, initially, the same brushless dc spin motors and associated electronics as those provided in the advanced 2000H DGCMG. However, as the design proceeded, MSFC requested that this unit be provided with A-C spin motors with breadboarded variable voltage and frequency spin control electronics. This change was incorporated in the hardware.

b. Outer Gimbal and Frame

An O.G. and Frame was designed and built capable of supporting the 6000H IGRA. This was done in expectation of future added scope to provide additional Actuator Pivot Assemblies, Sensor Pivot Assemblies and all packaged wheel and gimbal control electronics to form a full DGCMG Assembly for future system evaluation. Ultimately, the added scope was never authorized or required.

2.2 IGRA DESCRIPTION

The Inner Gimbal and Rotor Assembly and its external wiring harness, as depicted in Figures 2.2-1 and 2.2-2, was designed by Bendix Guidance Systems Division to have the capability of storing an angular momentum of 6000 Ft-lb-sec while operating at a speed of 8000 RPM. Wheel acceleration to operating speeds of 4000, 8000, or 12,000 RPM was accomplished by using two variable frequency variable voltage A.C. motors with associated electronics. The performance goals for this unit were as follows:

- Angular Momentum   6000 Ft-Lb-Sec $\pm$5%

- Run-up Time to Rated   Less than 8 hours
  Angular Momentum (2 spin
                      motors)

- Angular Velocity at   8000 RPM
  Nominal Momentum

- Bearing Windage and   Less than 8.0 oz-in
  Magnetic Drag at Run

- Dynamic Balance Not
  Required After Installation
  of New Bearings

- Maximum Angular Momentum   9000 Ft-Lb-Sec
  at 12,000 RPM

- Wheel Overspeed Tested at   15,000 RPM

These goals were met with an inner gimbal and rotor assembly with the following design characteristics:

INNNER GIMBAL AND ROTOR ASSEMBLY DESIGN DATA

ITEM	6000 IGRA
NOMINAL ANGULAR MOMENTUM (FT-LB-SEC)	6000
NOMINAL SPEED (RPM)	8000
RUN UP TIME TO NOMINAL SPEED (HRS.) MAX.	8
MAXIMUM ANGULAR MOMENTUM (FT-LB-SEC)	9000
MAXIMUM OPERATING SPEED (RPM)	12,000
IGRA WEIGHT (LBS)	418
MAXIMUM GIMBAL DIMENSION (IN.)	29.250
MAXIMUM MECHANICAL POWER 8000 RPM (WATTS)	48
WINDAGE POWER - ONE MICRON 8000 RPM (WATTS)	6.1
MAXIMUM MECHANICAL POWER-12,000 RPM (WATTS)	72
IGRA TORSIONAL STIFFNESS - FT-LB/RAD	1,000,000
BEARING SPACING (IN)	12
DYNAMIC UNBALANCE (MICROINCHES)	50
LUBRICANT FLOW RATE (mg/hr)	0.30
CALCULATED CRITICAL SPEED (RPM)	11,000
ACTUAL CRITICAL SPEED (RPM)	NOT DETERMINED
SPIN AXIS INERTIA (IN-LB-SEC^2)	86
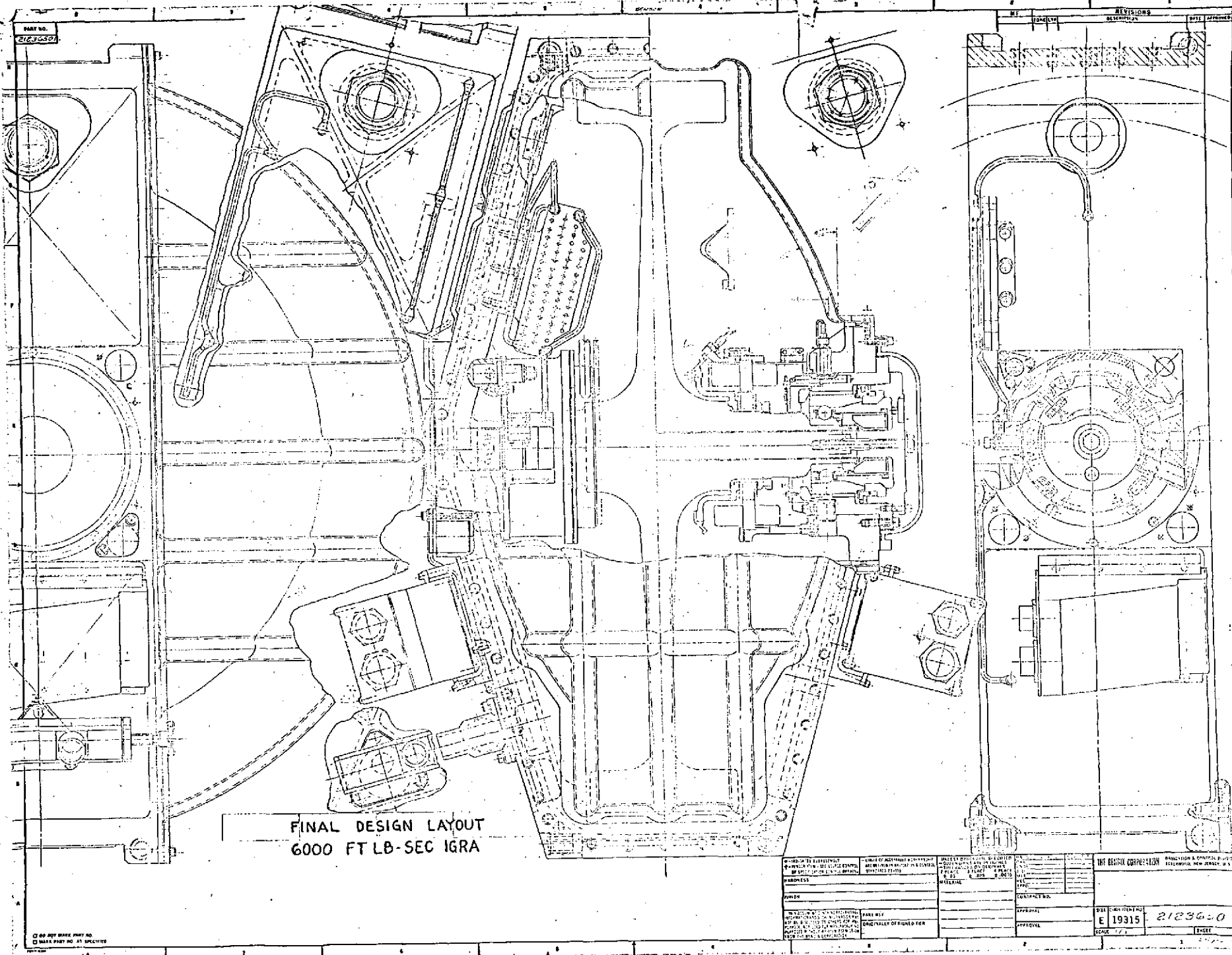
FINAL DESIGN LAYOUT
6000 FT LB-SEC IGRA

FIGURE 2.2-1

FIGURE 2.2-2

2-8

J2 JT07H-24-6P(150)   TB-2   6000 HCM6 I4RA AC WIRING
                                                    SIDE 2
                                                VALVE SIDE

φC { cc 20   1 18 BLU
     kk 20   2 18 BLK
     pp 20   3

φB { BB 20   4 18 RED
     EE 20   5 18 WHT
     MM 20   6   φB   φA   → 3φ A.C.
                                                             MOTOR
                  10 1/11 18
                  11 WHT 18
                  12 RED 18
                  13 BLK 18
                  14 BLU 18
                  15 BRN 18

φA { AA 20   7   φC
     DD 20   8 18 YEL
     LL 20   9 18 BRN
     f   20   30 20
     C   20   3
SPO2 { A 26   28 28 BLU   SPO2
       B 26   29 28 VIOLET

THERM { b 26   16 28 NAT/YEL
        c 26   17 28 NAT/GRN   (M) RT2
        d 26   18 28 NAT/YEL
        e 26   19 28 NAT/GRN   (M) RT4

+28   f 26   20 30 NAT   A VIBRATION
RETURN   g 26   21 30 NAT   B
ST2   h 26   22 30 NAT   H MONITOR
OUTPUT   i 26   23 30 NAT   E
                              20   D
                                       J4 (2120709)

20, cu   X 26 WHT   4 26 WHT   B VACUUM
MICRON   z 26 WHT   25 26 WHT   A
VACUUM   m 26 WHT   26 26 WHT   C SENSOR
SENS   n 26 WHT   27 26 WHT   D
                                       J6 (PCY 06A-8-4S(409))

                              J8 J10 TB4
                                            22   HT 60 WATT
+28   P 22 WHT   41 22   A   A 22   22
+28   s 22 WHT   42 22   B   B 22   22   HT 60 WATT
                                            22
LOW   r 22 WHT   43 22   C   C 22   22   HT 12 WATT
                                            22
+28   u 22 WHT   57 22   D   D 22   22
                                            22   HT 12 WATT
LOW   FF 22 WHT 58 22   E   E 22
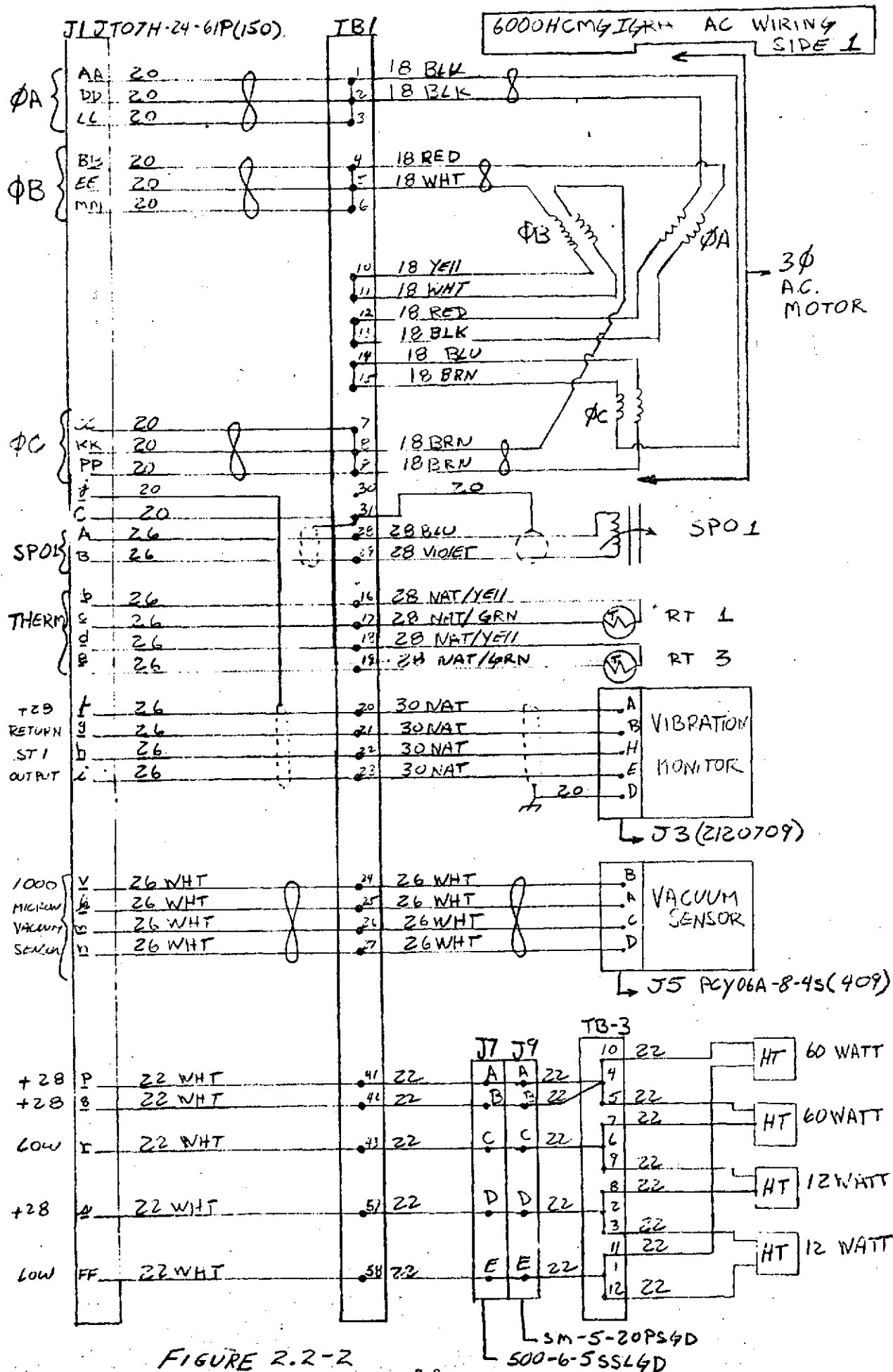   SM-5-20PSGD
FIGURE 2.2-2 (CONT.) 500-6-5SSLGD
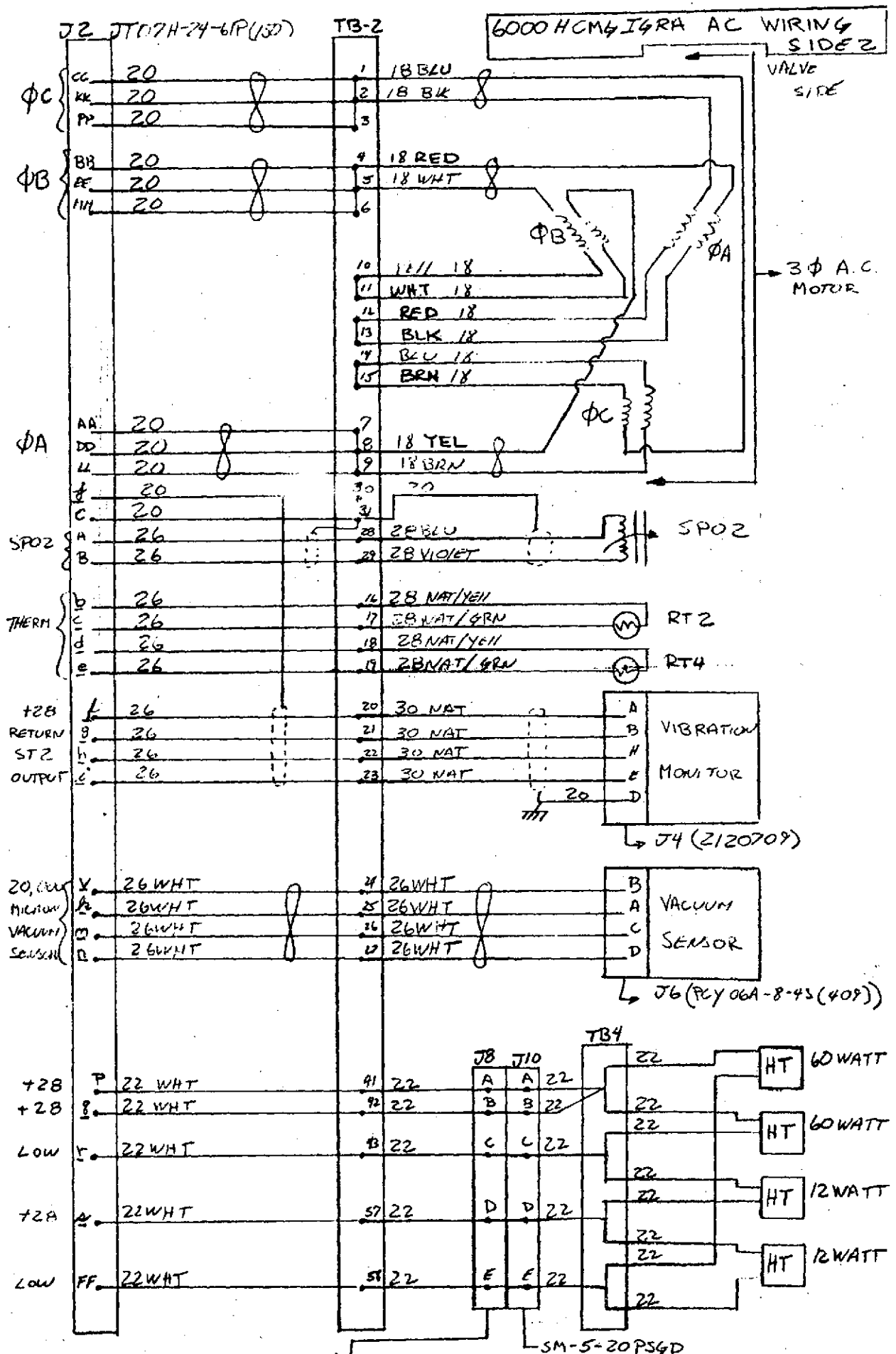2-9

The gimbal ring for the inner gimbal assembly was an elliptical shape with welded box cross ribbed sections fabricated from 2219 T-6 aluminum. This gimbal ring was configured so that optimum rotor performance was maintained throughout ambient and internal temperature and pressure changes. A principal contributor to this capability was the employment of a stiffening strut which connected the two sides of the gimbal through the center of the wheel. The gimbal for this unit featured the following design characteristics:

Material	2219 T-6 Aluminum
Material Tensil Stress (psi)	42,000
Weight (pounds)	54
Gimbal depth (in)	8.312
Gimbal Width Spin Axis (in)	15.625
Gimbal Length (in)	29.250
Wall Thickness(in)	.312
In Plane Torsional Stiffness Ft-Lb/RAD	1×10^6
Out of Plane " " "	1×10^6

The gimbal was fitted with gasket sealed covers in order to provide the lowest operating pressure within the gimbal cavity. Since these covers were easily removed, and by removing just one cover, all sensing elements and the wiring harness were completely exposed, therefore, modification and maintenance was easily facilitated.

This particular unit was fitted with dual connectors of

The Flywheel in its final configuration was characterized by the following parameters:

Material	350 maraging steel
Ultimate tensil strength (PSI)	325,000
Endurance limit (PSI)	110,000
Wheel diameter (in)	26
Wheel weight (pounds)	305
Inertia spin axis in-lb-sec^2	86
Inertia cross axis in-lb-sec^2	44
Torsional stiffness Ft-Lb/Rad	3.25×10^6
Nominal speed (RPM)	8000
Centrifugal stress nominal speed (PSI)	63,100
Centrifugal stress safety factor	5.16
Fatigue stress at 200 ft-lbs (PSI)	1250
Fatigue stress safety factor	88
Max. precession torque (Ft-Lbs)	14,100
Max. operating speed (RPM)	12,000
Centrifugal stress-Max. speed (PSI)	142,000
Centrifugal stress safety factor	2.28
Design proof speed (RPM)	15,000
Design burst speed (RPM)	18,200

This rotor with its spin motors,was supported on each end by a single size specially modified 307 replaceable angular contact spin bearing.

different shell sizes, to avoid miswiring and single terminal boards on each side so that bearing replacement, assembly, and disassembly could be accomplished without removal of a single wire. This design feature also allowed for prewiring of both gimbal harnesses. The location of the terminal boards on each side of the gimbal in an upright position permitted easy solder attachment of the sensors to the harness assembly.

The bearing support housings which were fabricated from beryllium with a steel liner, when located within the elliptical gimbal, allowed the bearings to be properly aligned and move axialy, as limited by the belleville preload springs. This bearing housing also contained a labyrinth seal which maintained a slightly higher pressure in the bearing area. Attached to these bearing support housings were the two beryllium end caps which contained the bearing preload device. These end caps also supported the steel strut which runs through the wheel shaft and ties together both sides of the gimbal.

A manual evacuation valve similar to the one used on the ATM CMG engineering units was used for periodic evacuation.

The 6000 Ft-Lb-Sec of angular momentum (H) of this inner gimbal and rotor assembly was effected by a 26 inch diameter 305 pound maraging steel integral full web flywheel rotating at 8000 RPM. This wheel was capable of storing 9000 Ft-Lb-Sec of momentum at 12,000 RPM. In actual use the wheel was capable of operating at 3 speeds (4000, 8000, and 12,000 RPM) to obtain momentums of 3000, 6000, 9000 Ft-Lb-Sec respectively.

The modifications incorporated into the bearing design, as shown in Figure 2.2-3 were increased length of the inner race lands for addition of bayonet slots for easy removal, increased length of the outer race for better bearing alignment , and a special Bendix designed phenolic retainer for better retainer stability and acceptance of the Bendix active lubrication system. For long life requirements these spin bearings were initially lubricated with KG-80 oil. Whenever the unit was operated, lubricant (KG-80 oil) was supplied to the bearing separator by means of an open loop type system in which the same nut that locked the bearing inner race to the wheel shaft was made hollow and filled with lubricant. Two orifices in each system permitted the prescribed quantity (.3 MG/HR) of oil to be metered by means of centrifugal force into the phenolic retainer of each bearing. This lubrication method was used successfully on the ATM-CMG IGRA. The bearings used in this program were also characterized by the following parameters:

Bearing Type	307 H modified
Number of Balls	10
Ball Diameter (in)	.5625
Bore (in)	1.3780
Outer Diameter (in)	3.5000
Quality	ABEC 9
Basic Dynamic Load Rating (LBS)	7083
Limiting Speed (RPM)	23,544
Nominal Contact Angle (degrees)	15
Static Thrust Capacity (Lbs)	7,544
Static Radial Capacity (Lbs)	3,412
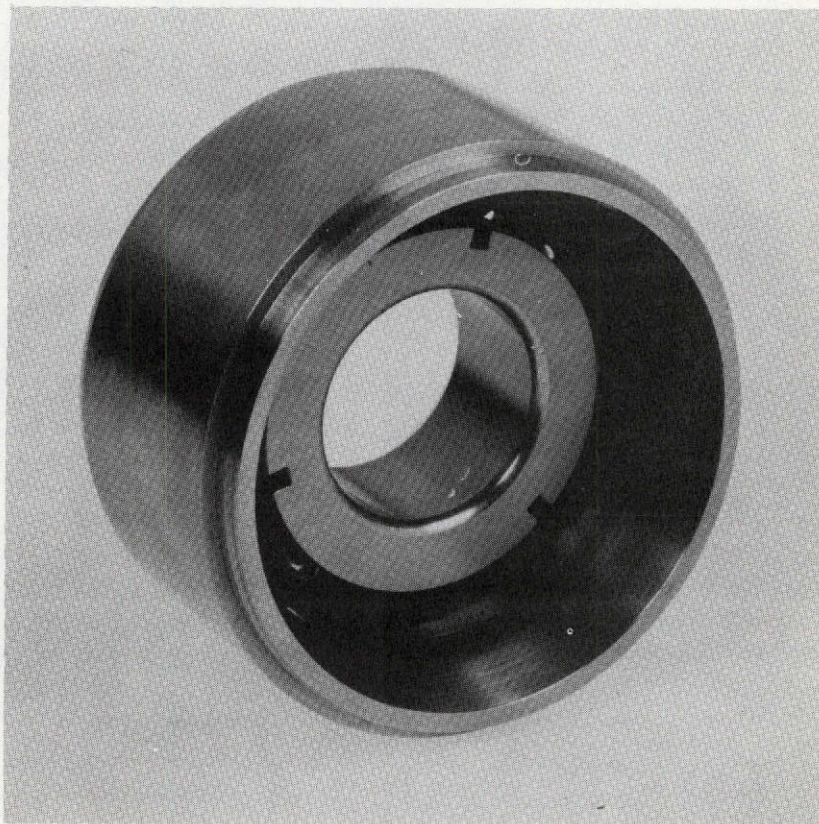
307H BEARING

FIGURE 2.2-3

Nominal Radial Load (Lbs)	160
Nominal Thrust Load (Lbs)	80
Dynamic Capacity at 8000 RPM (Lbs)	1138
Dynamic Capacity at 12000 RPM (Lbs)	995
Nominal Bearing Torque (oz-in)	4.0
Maximum Transient Radial Load (Lbs)	480
Calculated B-10 Life ATM Duty Cycle (Hrs)	$\approx$ 1,000,000
Reliability ATM Duty Cycle	.9999+

Bearing preload was accomplished using Belleville washers which were captured in adjusting nuts which were threaded into the Beryllium end caps. These washers applied a thrust load of 80 pounds on the outer race of each bearing. Since the length of the outer race was held to a very tight tolerance, bearing preload (axial end shake) never had to be readjusted after the initial settings were made.

In order to meet the bandwidth requirements, particular attention was paid to the stiffness and bearing slider clearances. Because the bearing design required a radial clearance of approximately .0001 inch to be functional, it became desireable to preload the bearing radially. A ball and spring device was inserted into each bearing support housing to radially load the bearing, thus removing all radial play while still allowing the bearing to be free axially. This allowed for a greater bandwidth by removing the bearing dead zone from the unit. This unit was instrumented with two accelerometers, two thermistors, two speed pick-offs, and two vacuum gauges. These sensors were utilized during testing to monitor wheel speed cavity vacuum level and bearing conditions.

2.3 SPIN MOTOR DESCRIPTION

To realize optimum performance characteristics of an AC induction motor, it is necessary to operate the motor near synchronous speed. Maximum efficiency and high torque are both available in this region. In order to operate in this fashion, the motor excitation is programmed such that voltage and frequency both increase with speed, resulting generally in a constant current. The AC induction motor characteristic then becomes similar to the more favorable DC machine but without the associated permanent magnet problems.

The spin motors for the 6000H IGRA are 3 phase, 4 pole, AC induction motors (See Figure 2.3-1). They were designed to exhibit very steep torque versus speed characteristics and high efficiency near synchronous speed.

The squirrel cage rotor is the inner member of the motor and is mounted on the shaft of the wheel. It consists of copper bars placed in slots in a stack of nickel-iron laminations and brazed to copper end laminations. One motor is located on each side of the wheel.

The stator is the outer member. It is wound for four poles and three phases. The machine has six windings to offer versatility to operate with windings in series or parallel and connections in wye or delta.

The basic motor dimensions are 2.387 ID x 6.000 OD x 2.45L. The motor can develop as high as 48 oz-in at 400 hertz at a peak power input of 530 watts. Torque versus speed characteristics
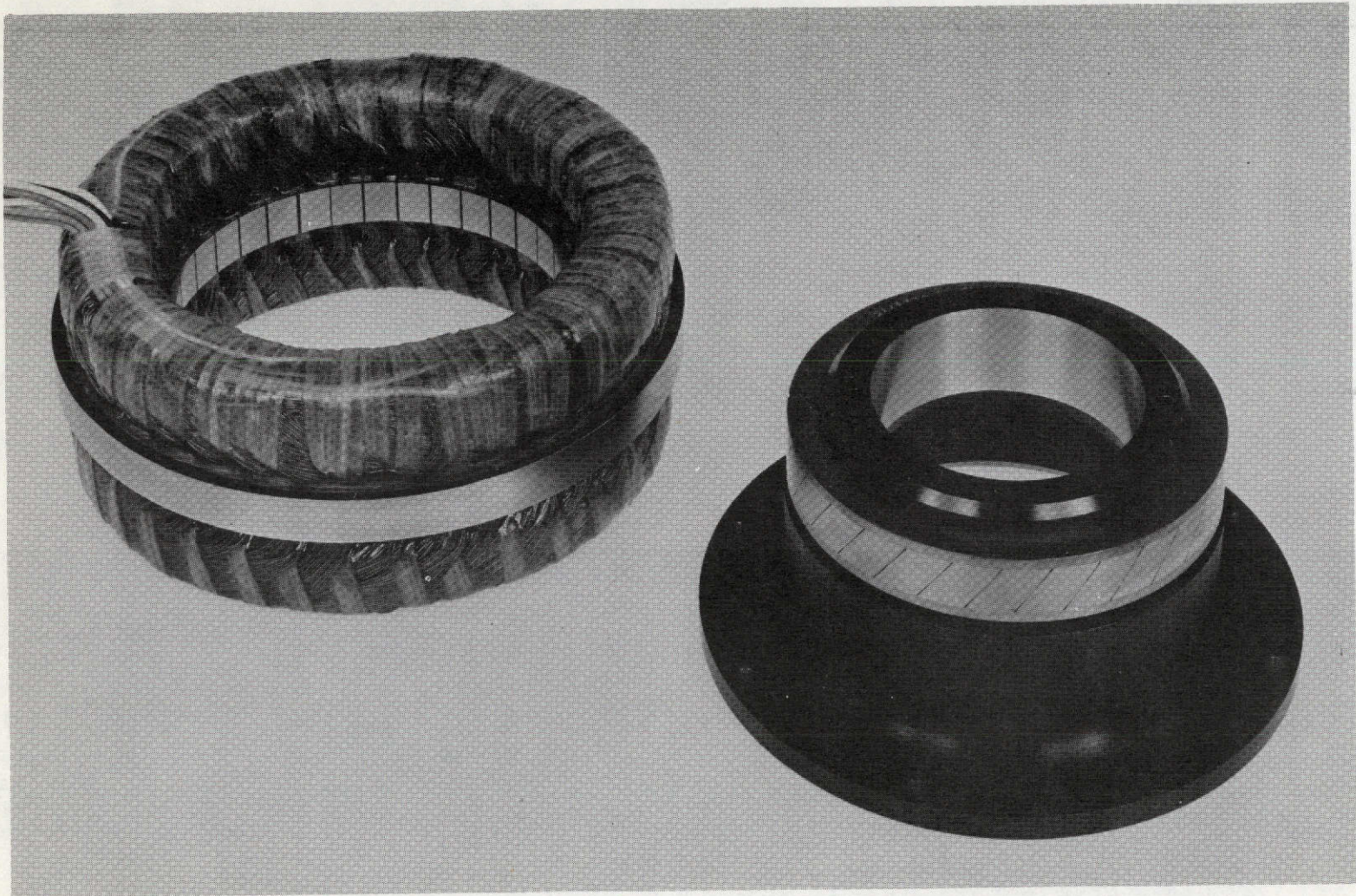
A C SPIN MOTOR

FIGURE 2.3-1

near synchronous speed are plotted in Figure 2.3-2 and power versus

speed are shown in Figure 2.3-3. The peak of each curve represents

the peak or pullout torque of the motor. The curves are plotted at

four different frequencies to show the general range of operation

of the motor. In the programmed input operating mode the torque

is relatively constant as indicated by the somewhat uniform height

of each torque curve and the power is rising with speed as indi-

cated by the progressively higher power curves as frequency is in-

creased. On the curves of Figure 2.3-2, some motor efficiencies

are indicated. It can be seen that for optimum operation the

torque level of this machine is between 15 and 30 oz-in.

AC SPIN MOTOR
STATOR 2123969-1
ROTOR 2123970-1
TORQUE VS SPEED CHARACTERISTICS
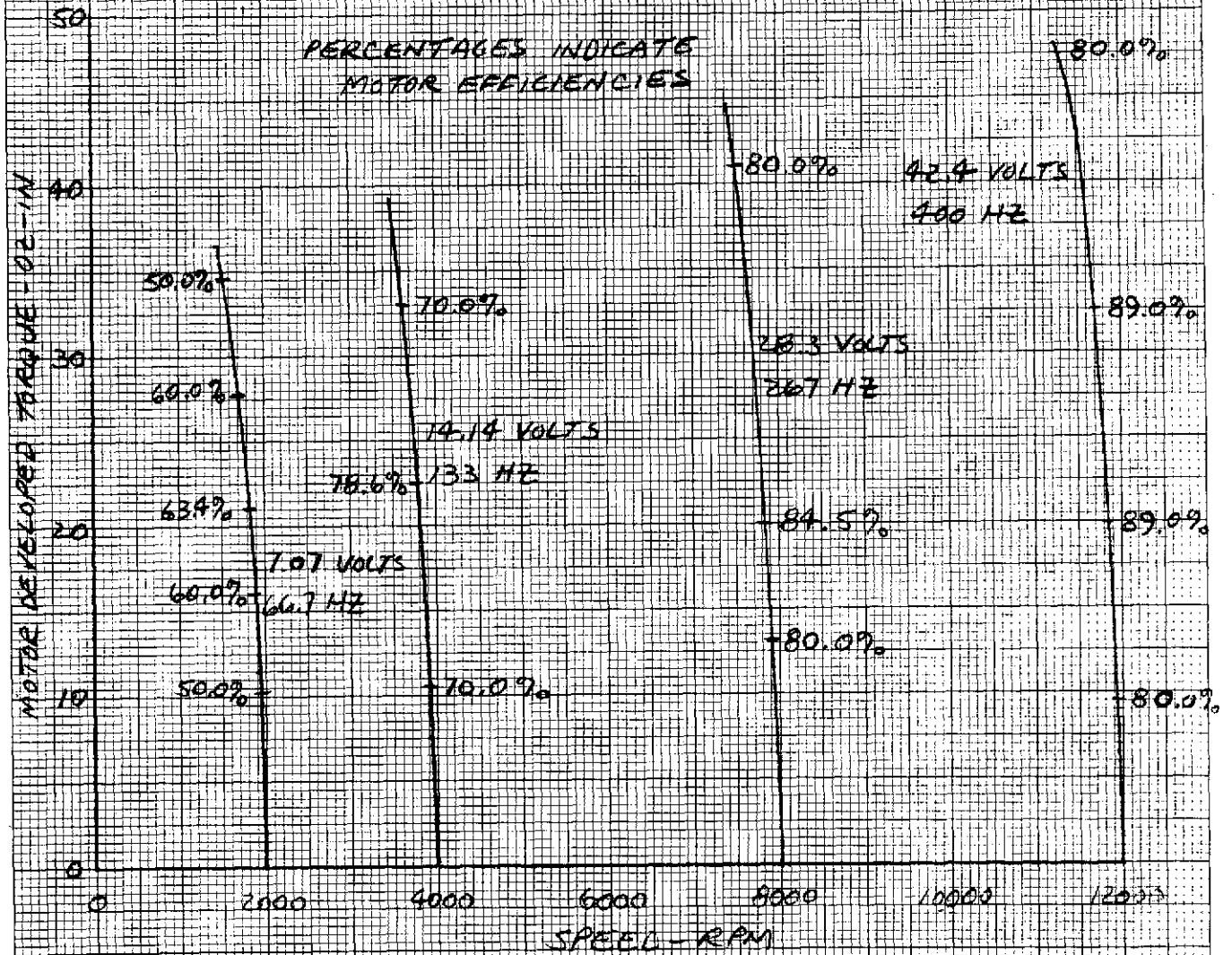NEAR SYNCHRONOUS SPEED

WINDINGS IN SERIES WYE CONNECTION

PERCENTAGES INDICATE
MOTOR EFFICIENCIES

FIGURE 2.3-2

AC SPIN MOTOR
STATOR 2123969-1
ROTOR 2123970-1
POWER VS SPEED CHARACTERISTICS
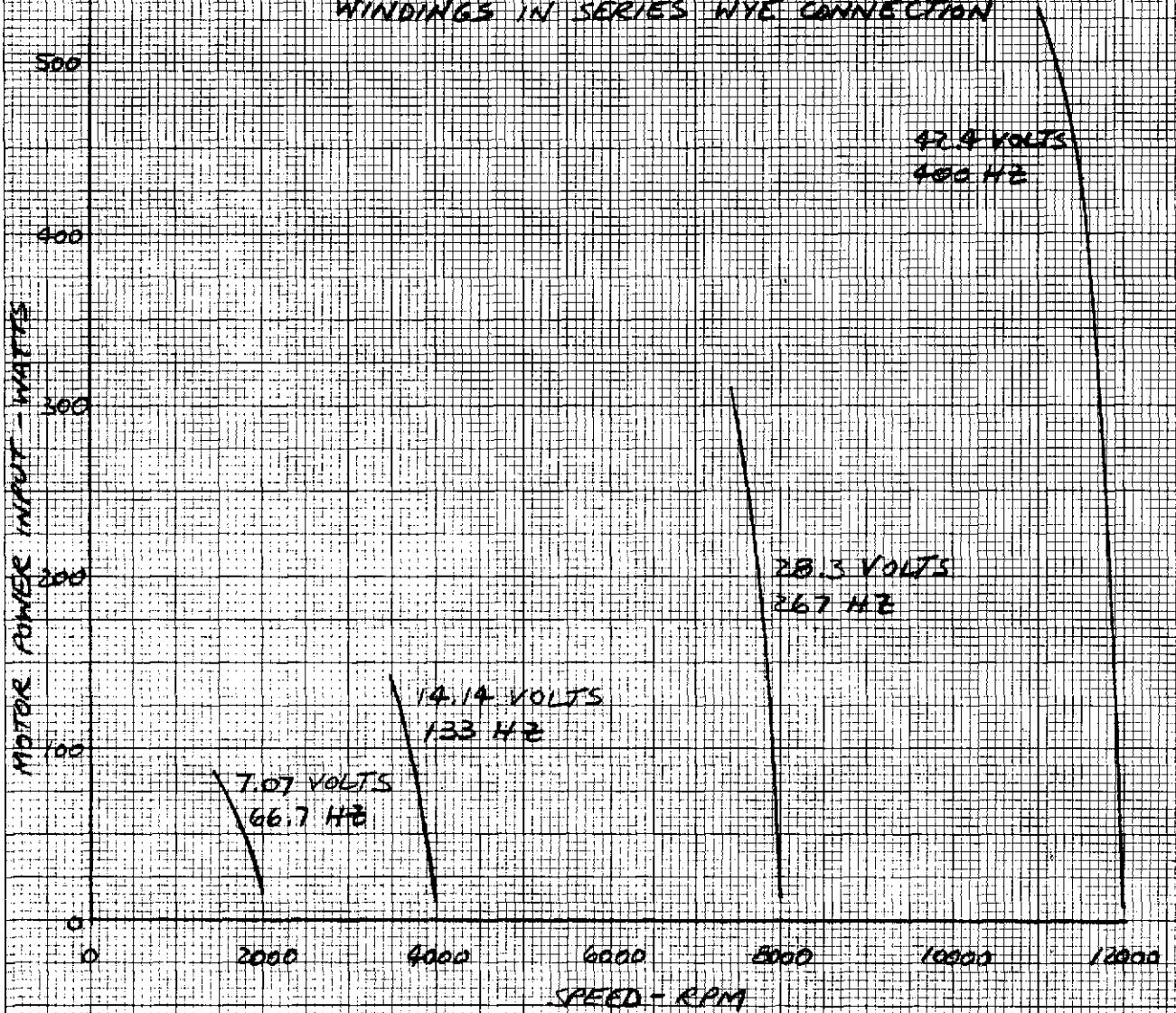NEAR SYNCHRONOUS SPEED

WINDINGS IN SERIES WYE CONNECTION

42.4 VOLTS
400 HZ

28.3 VOLTS
267 HZ

14.14 VOLTS
133 HZ

7.07 VOLTS
66.7 HZ

MOTOR POWER INPUT - WATTS

SPEED - RPM

FIGURE 2.3-3

2.4 WHEEL CONTROL SYSTEM DESCRIPTION

2.4.1 GENERAL

The general block diagram of the 3-phase AC variable frequency motor drive electronics is shown in Figure 2.4-1. To generate the variable frequency drive, rotor speed is sensed via a magnetic speed pick-off which produces 1 Hz per RPM. This speed information serves a dual purpose; as a feedback for speed control, and as a feedback for motor drive voltage-frequency generation. The voltage-frequency applied to the motor as a function of rotor speed is shown in Figure 2.4-2. A constant frequency slip is utilized since this results in a maximum run-up torque characteristic. The slip frequency used is approximately 27 Hz.

To generate the 3-phase AC voltage across the motor lines, a stepped-square approach was used. The advantage of this method is that it requires only six power transistors; and no multiplier circuits are utilized. The waveforms generated are shown in Figure 2.4-3. Such a waveform contains zero third harmonic.

To vary the motor voltage amplitude, pulse-width control is utilized. This results in maximum run-up efficiency. An on-off, digital type speed control is included with settability for 4000 RPM, 8000 RPM and 12,000 RPM operation. A DC braking scheme is also utilized. This is accomplished by grounding two motor lines, and switching the remaining line

FIGURE 2.4-1

MOTOR DRIVING FREQUENCY VS SPEED   FIG 2.4-2

3 PHASE AC SPIN MOTOR

PWM EXPANDED

V_A

3 PHASE POWER
BRIDGE OUTPUT
VOLTAGE

V_B

V_C

V_{AB}

LINE TO LINE
VOLTAGE

V_{BC}

V_{CA}
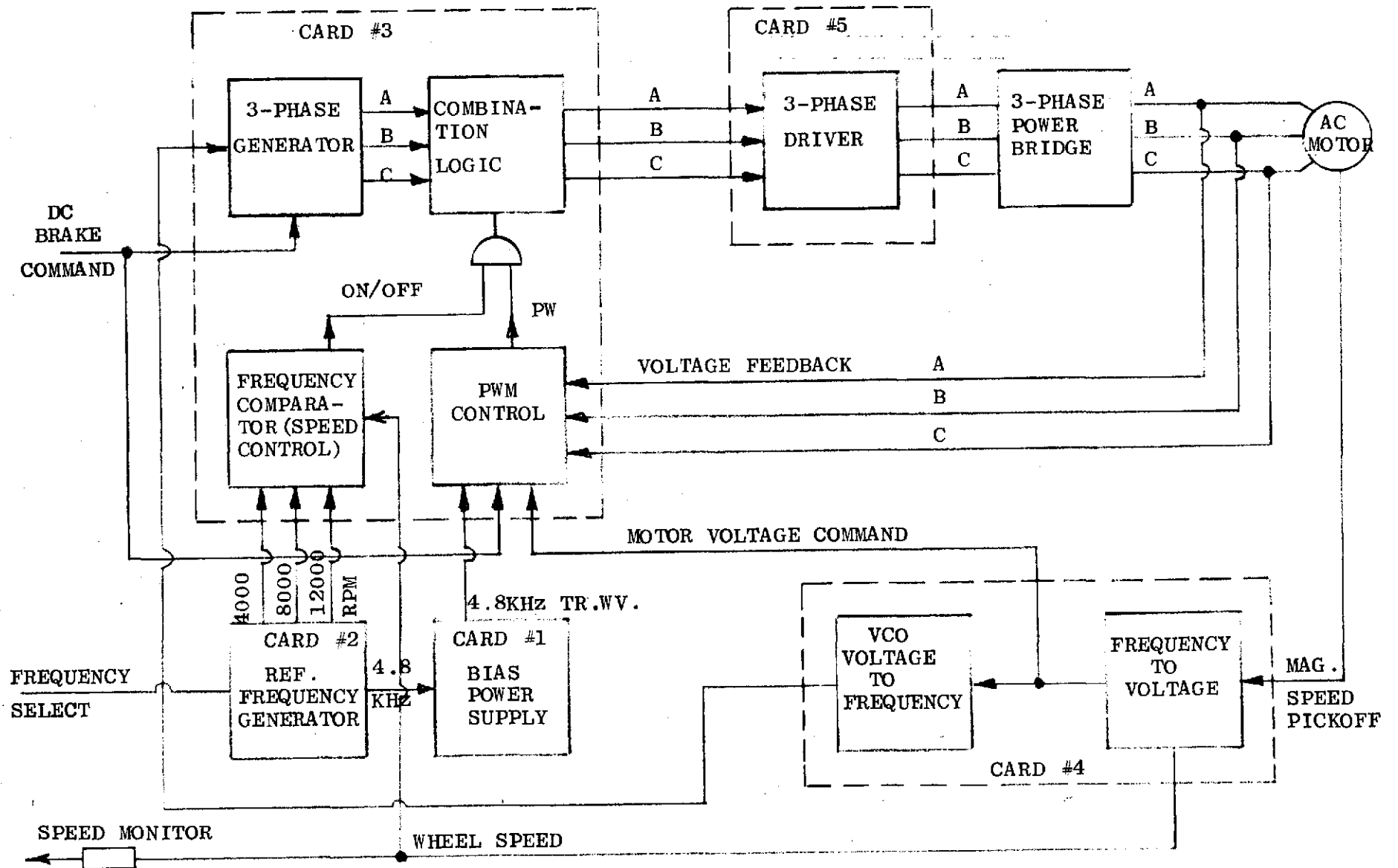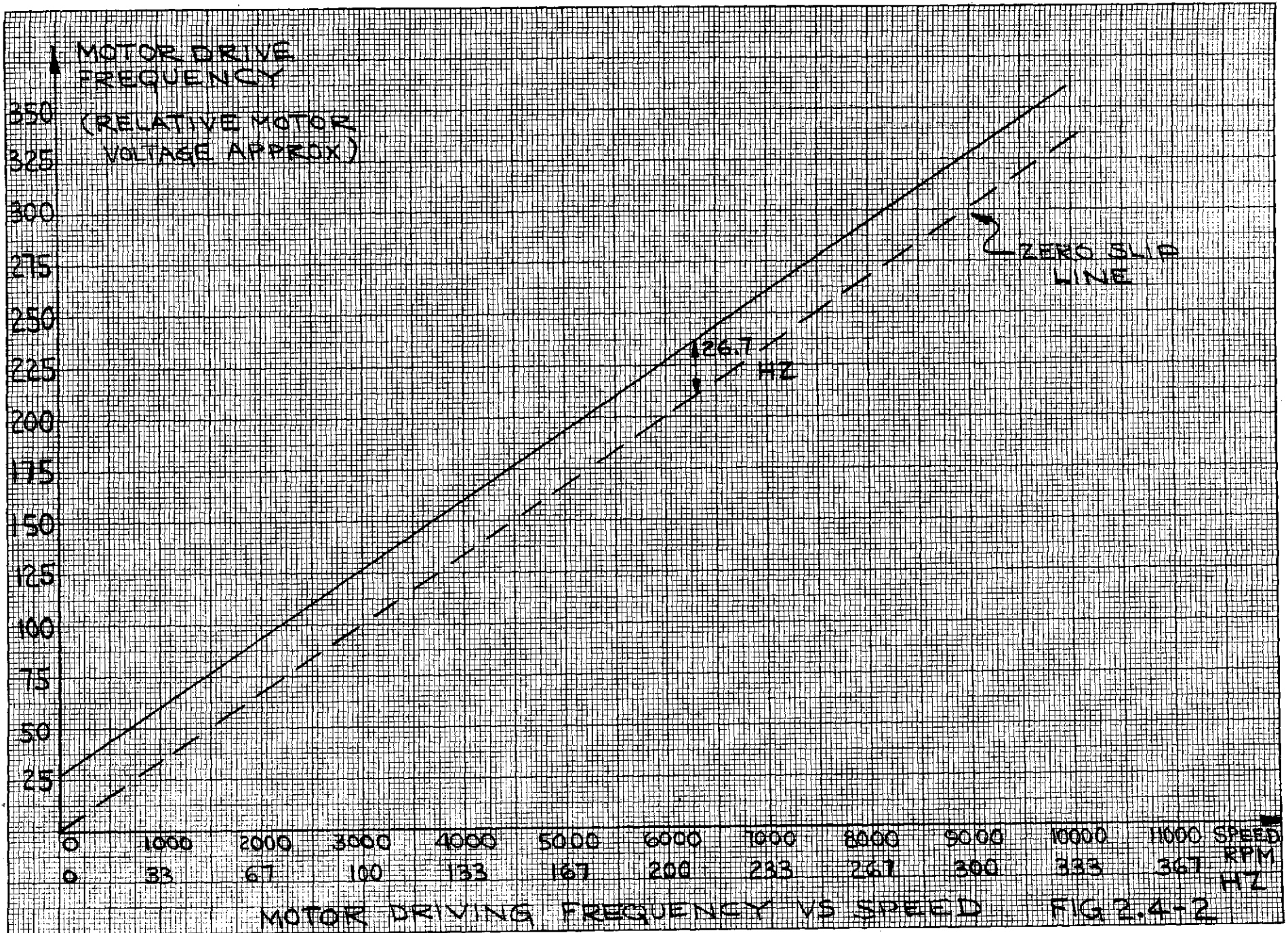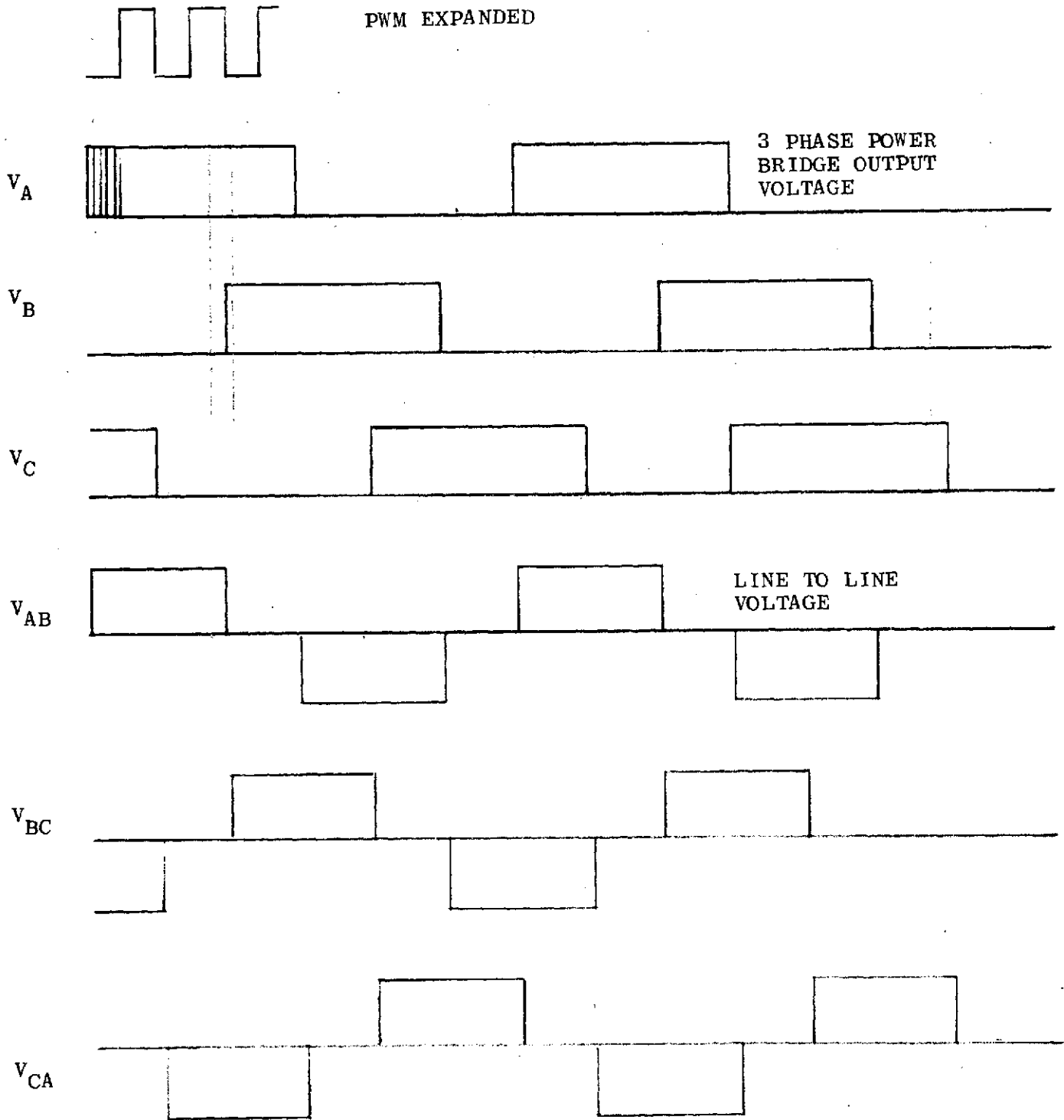
FUNDAMENTAL RMS CONTENT = 78% OF PEAK VALUE

FIGURE 2.4-3

between +28V and ground.

2.4.2   FREQUENCY-TO-VOLTAGE AND VOLTAGE-TO-FREQUENCY CONVERTER

The function of the frequency-to-voltage converter is to
provide a motor voltage DC command as a function of motor
speed (Figure 2.4-4). The sinusoidal output of the magnetic
speed pick-off is "squared-up" via a Schmidt trigger circuit,
whose output is used to trigger the monostable. The output
of the monostable is amplitude controlled and fed to a low-
pass filter. A voltage offset is included here to generate
the slip function. This particular circuit results in a
±1% accuracy of conversion.

The voltage output of the frequency-to-voltage converter
is fed to a voltage-to-frequency converter whose function
is to generate the keying frequency from which the motor
driving waveform is derived (Figure 2.4-5). The circuit
is essentially an integrator whose slope is controlled by
the input voltage. When the output reaches a predetermined
amplitude, the direction of integration is reversed. Thus,
a triangular wave, whose frequency is proportioned to the
input voltage is generated. A logic level square wave of
the same frequency is derived to produce the keying output.

2.4.3   3-PHASE GENERATOR AND PWM VOLTAGE CONTROL (FIGURE 2.4-6)

The 3-phase waveform generator is a synchronous divide by
6 counter whose input is the square wave from the voltage-

FREQUENCY TO VOLTAGE CONVERTER
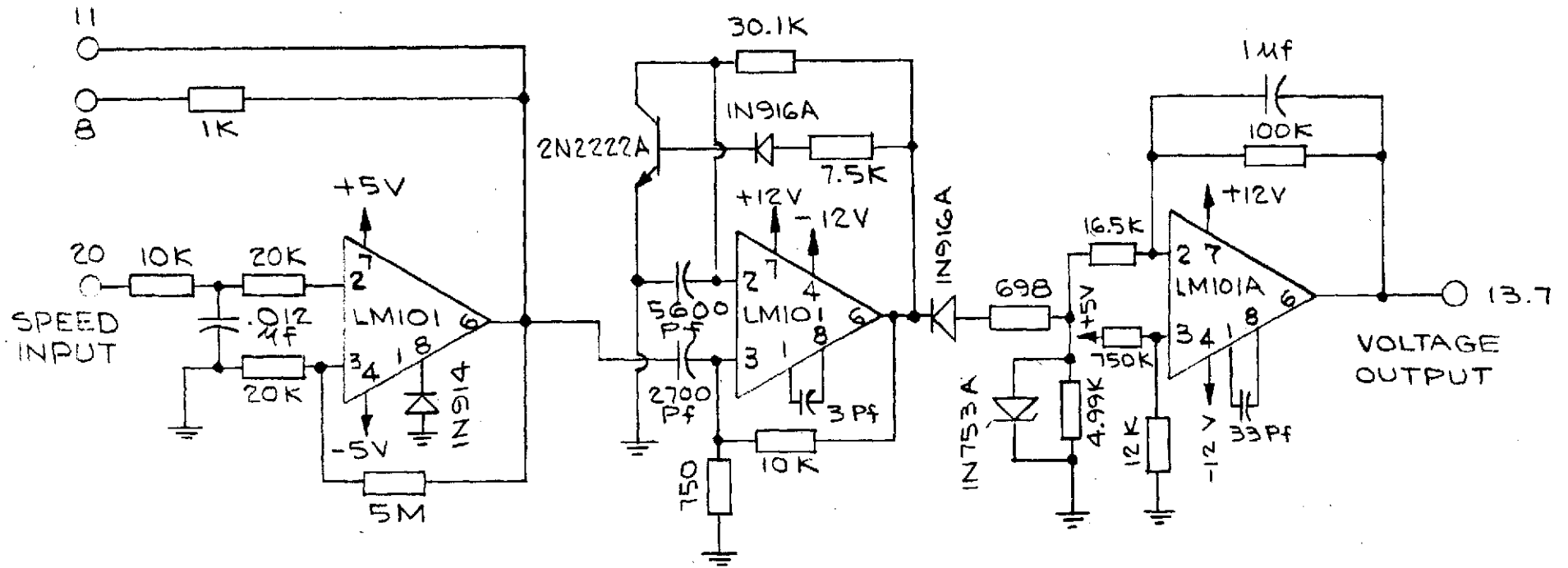## (1/2 CARD # 4)

OUTPUT TO SPEED CONTROL

FIGURE 2.4-4

VOLTAGE TO FREQUENCY CONVERTER
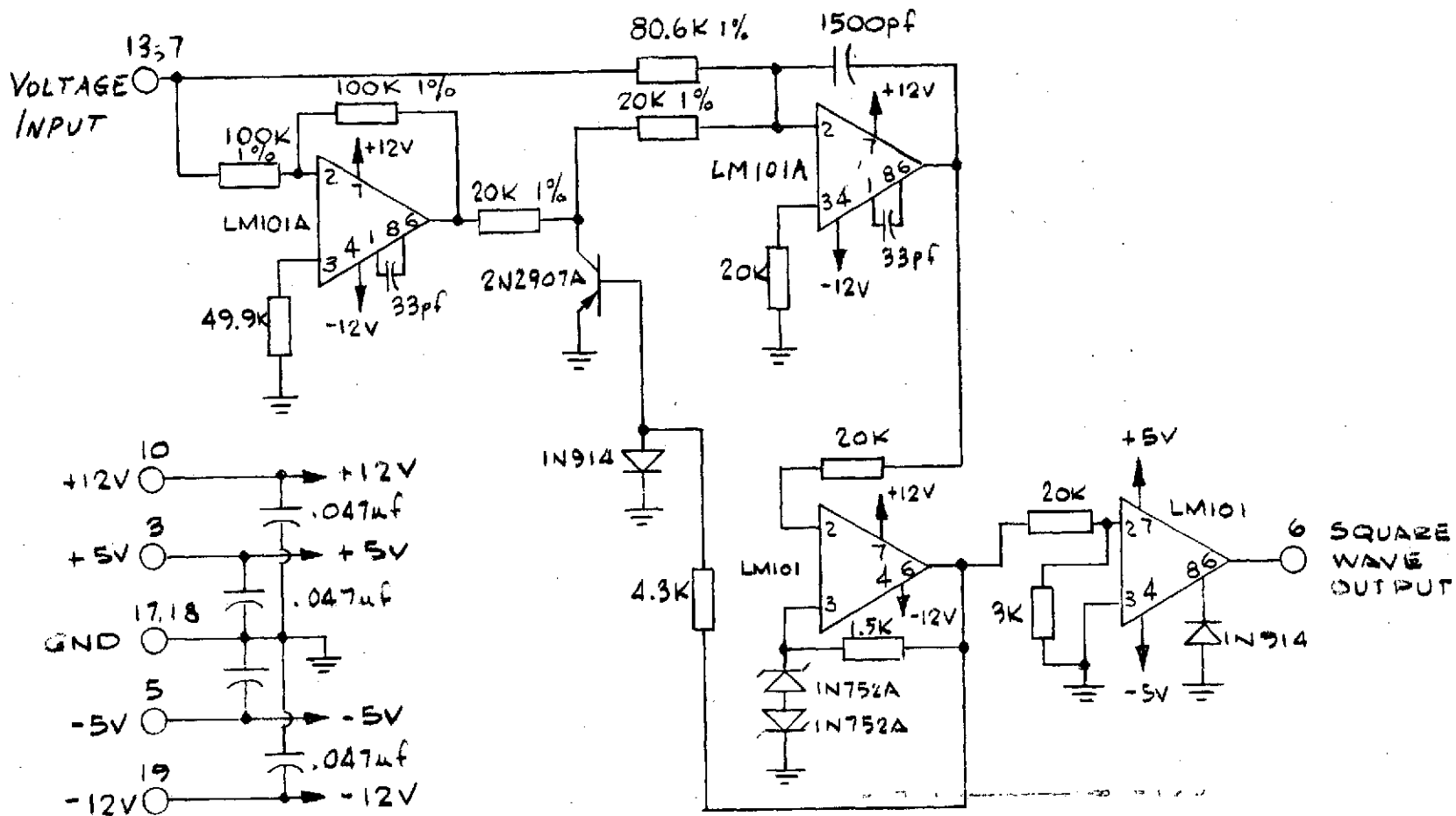## (1/2 CARD #4)

FIG 2.4-5

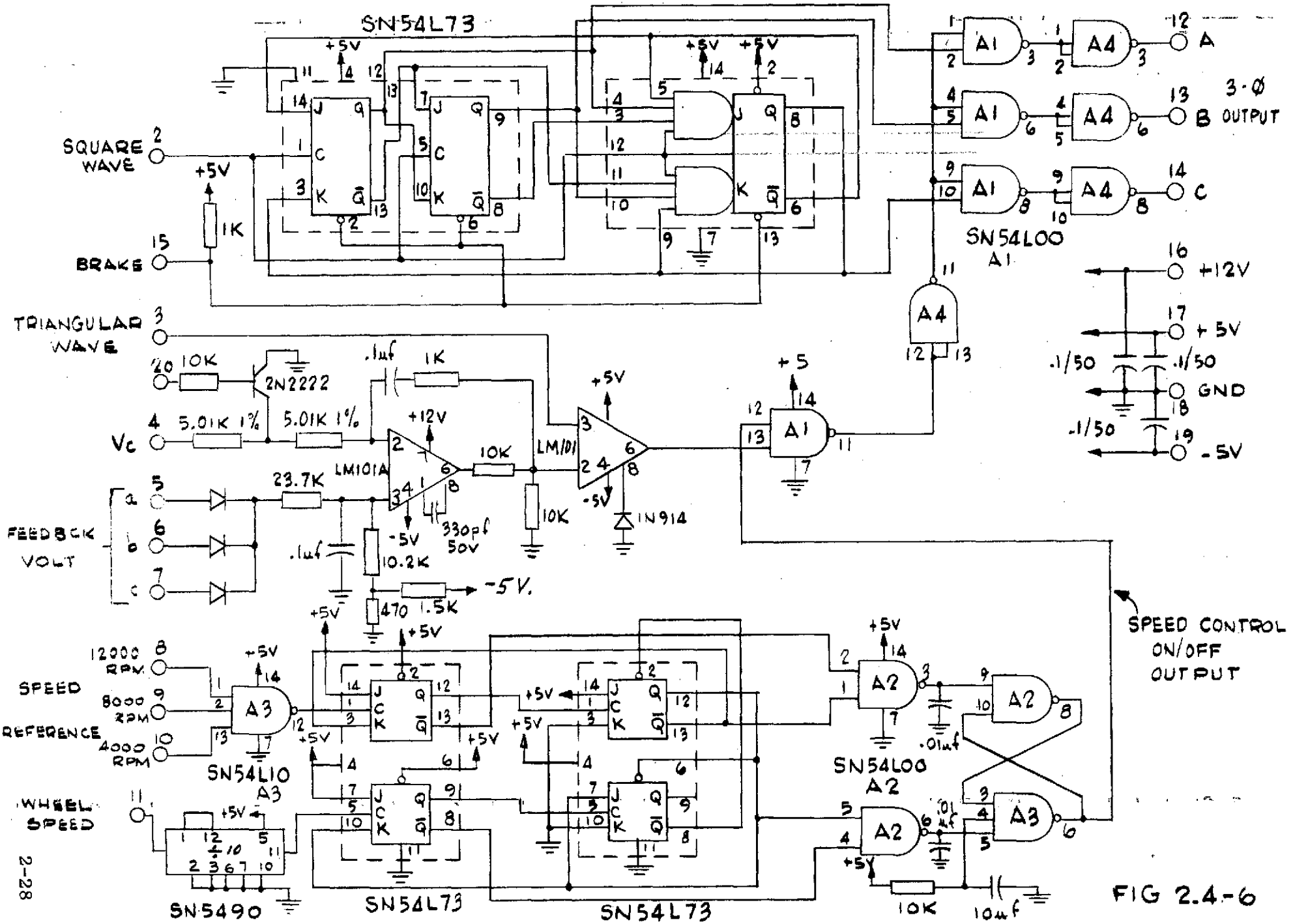# 3 PHASE GENERATOR, PWM, AND SPEED CONTROL II - CARD #3

FIG 2.4-6

to-frequency converter, and whose outputs are three square waves spaced 120° apart. All three outputs are gated with the output of the pulse-width modulator.

The pulse width modulator consists of a high gain summing amplifier stage and a voltage comparator stage. The motor voltage command (from the frequency-to-voltage converter) is algebraically added to the feedback voltage which is obtained by gating the three motor line voltages via diodes. The resultant error signal is compared with 4.8KHz triangular wave (derived from the bias power supply). The output is a PWM waveform, which is gated with the 3-phase waveform.

During the DC braking mode, the counter is preset so that only one motor line is high. The DC voltage command is removed via a transistor switch. The offset voltage in the summing amplifier results in a pulse-width which is used for DC braking.

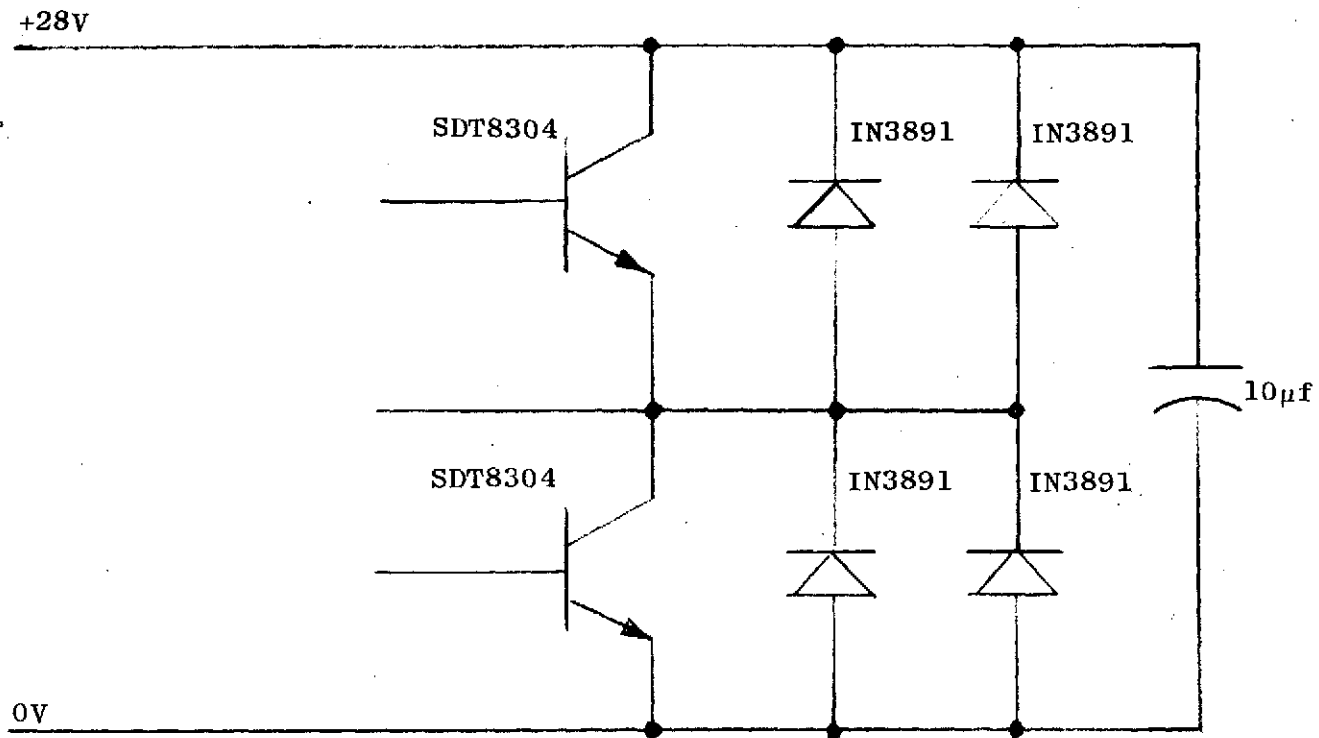2.4.4   3-PHASE POWER BRIDGE (FIGURES 2.4-7 AND 2.4-8)
The bridge consists of three identical sets of driver and power switch. The driver includes the timing capacitors to eliminate large current spikes. Since the peak line current is about 15A, a 30A transistor (SDT8304) and two 12A diodes in parallel (IN3891) were used.
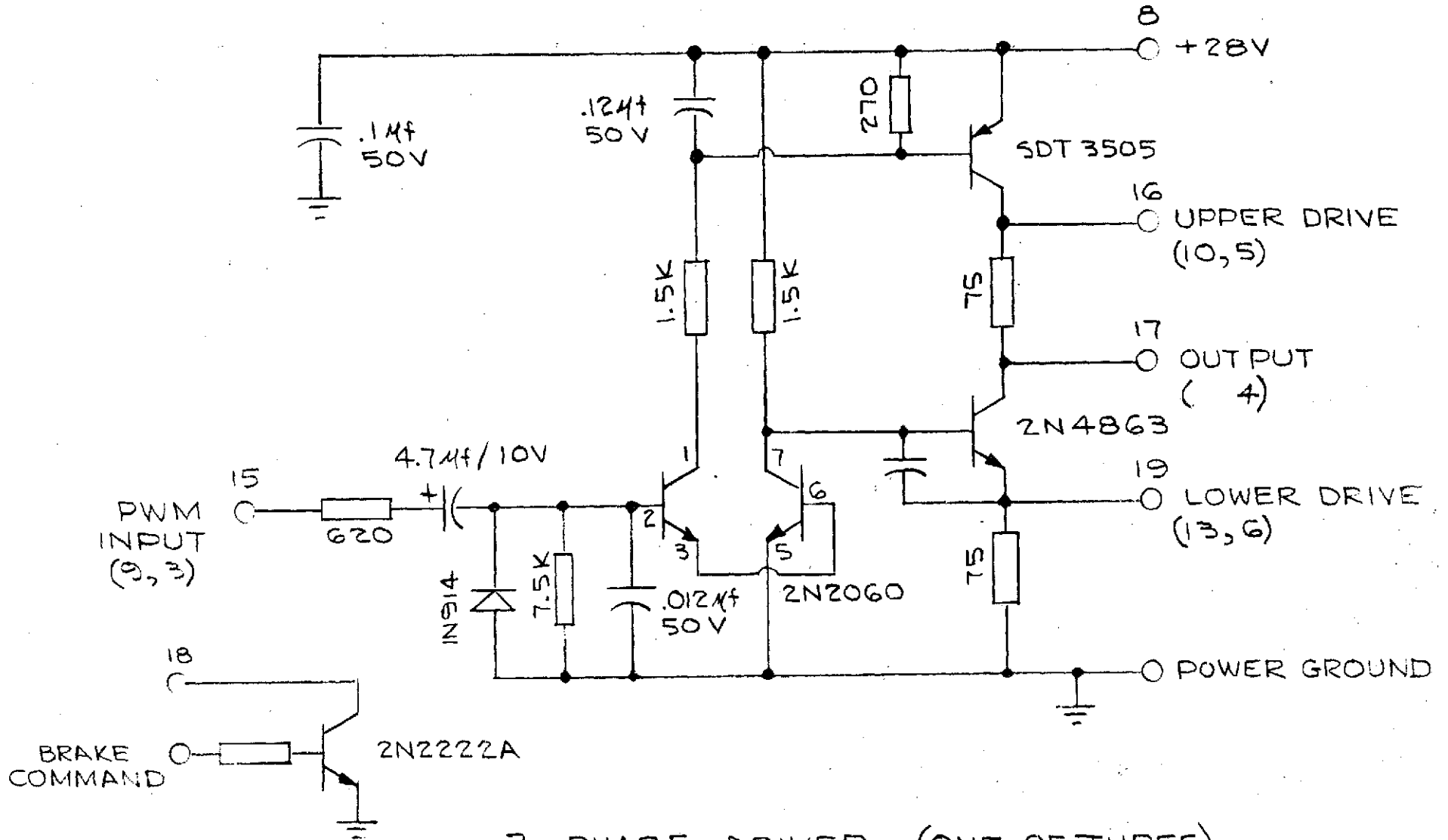
3-PHASE DRIVER (ONE OF THREE)

FIGURE 2.4-7

POWER SWITCH (ONE OF THREE)

FIGURE 2.4-8

2.4.5   SPEED CONTROL (FIGURES 2.4-6 AND 2.4-9)

The speed control circuitry consists of a reference

frequency generator, and a digital frequency comparator.

The crystal oscillator frequency is divided to obtain three

reference frequencies, one for 4000 RPM, one for 8000 RPM,

and one for 12,000 RPM. The operating speed is selected

via an external switch which enables the desired frequency.

The frequency comparator compares the reference frequency

with the frequency subdivided from the wheel speed output

of the magnetic pick-off. The comparator's output is used

to enable the PWM output via logic.

2.4.6   BIAS POWER SUPPLY (FIGURE 2.4-10)

The bias power supply is used to generate the $\pm$12V, +5V

and -5V bias power. It consists of a +5V switching

regulator, and a DC to DC converter. The +5V output is

used to energize the logic which in turn generates the

4.8KHz to key the DC to DC converter.

2.4.7   SYSTEM PERFORMANCE

2.4.7.1 Test Setup

To measure the motor torque, a setup as shown in

Figure 2.4-11 was utilized. The motor was placed in a

test fixture. The rotor shaft was connected to the strain

gage via a flexible coupling. On the other side of the

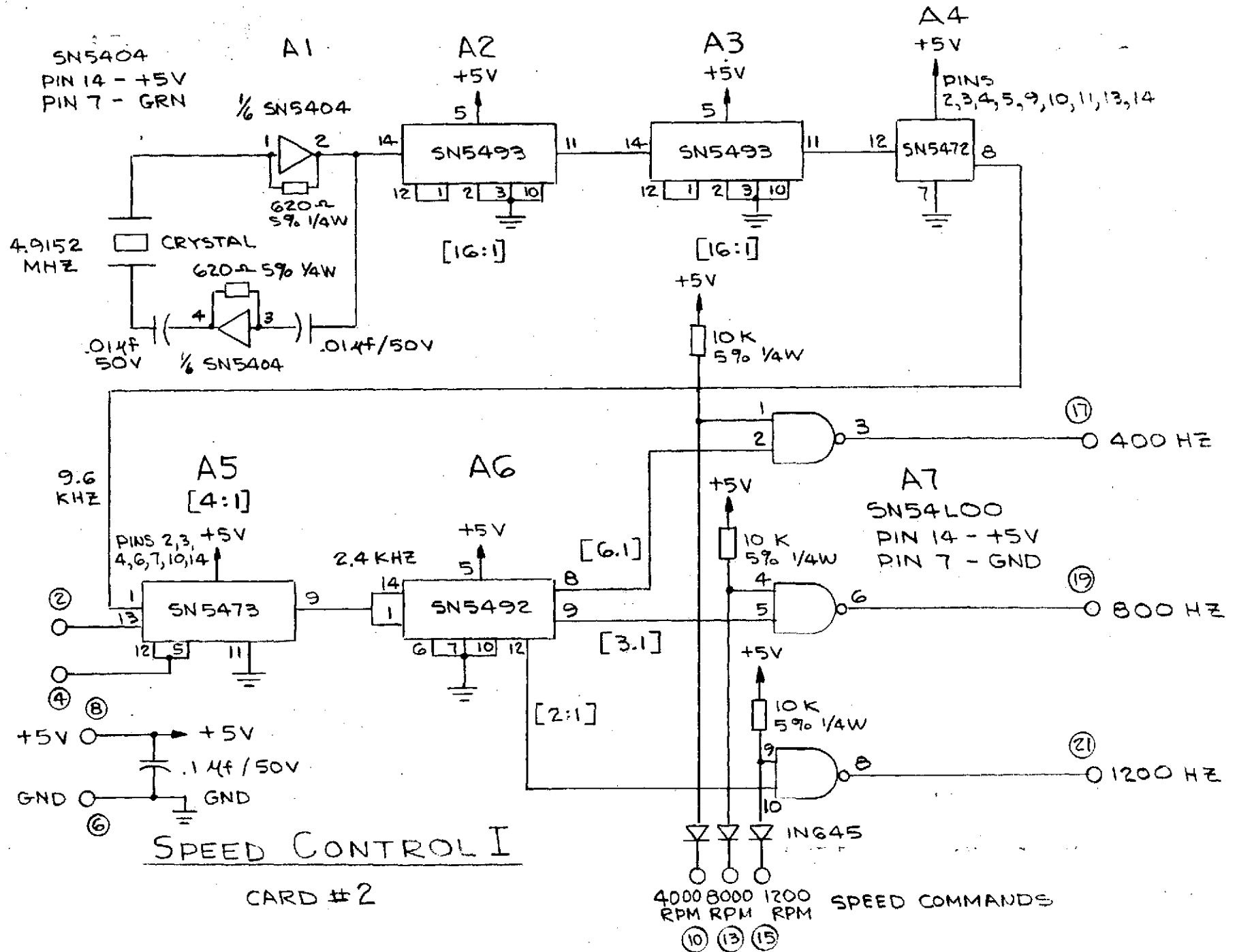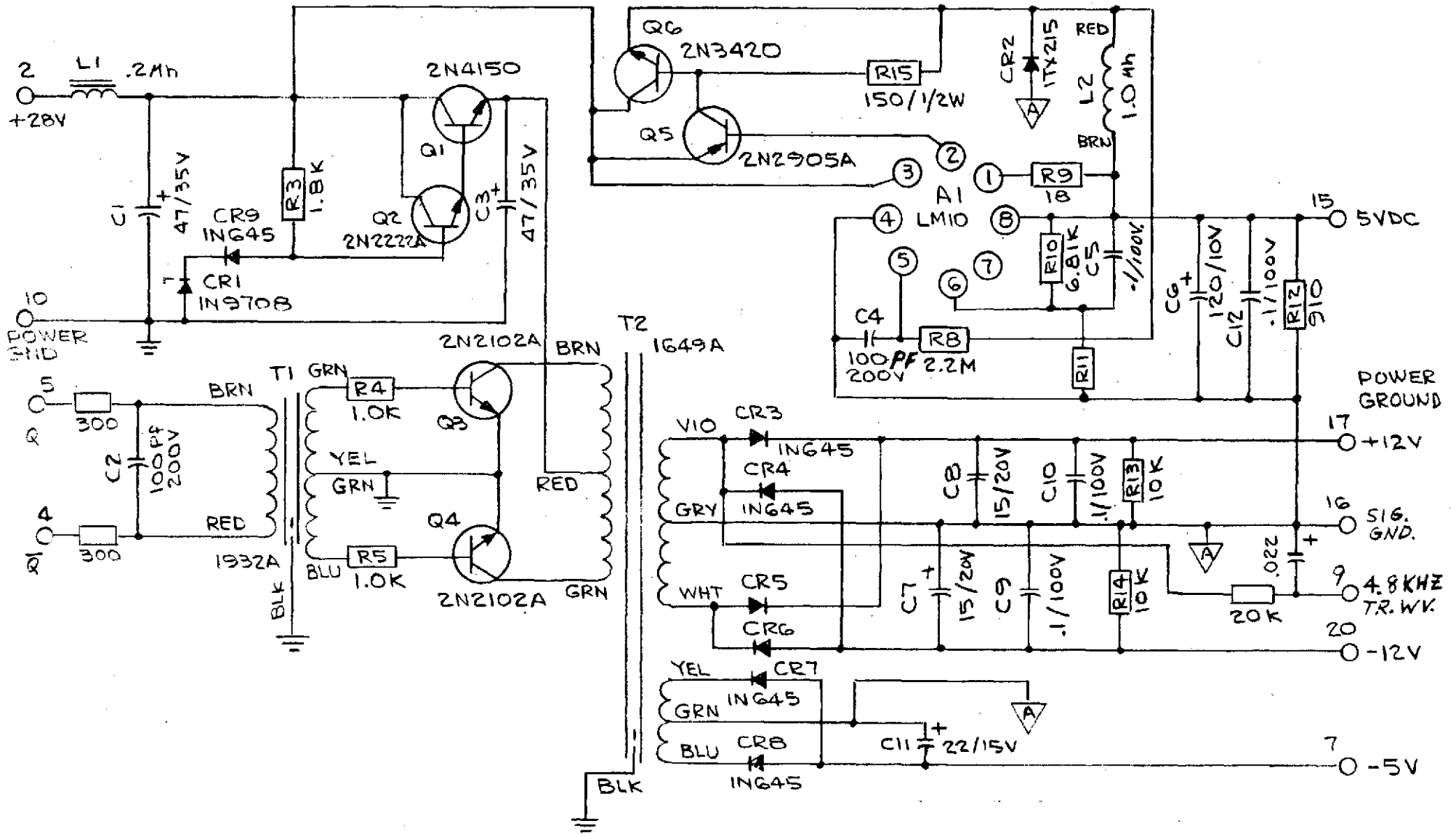gage, a dynamic brake was connected. During the test, the
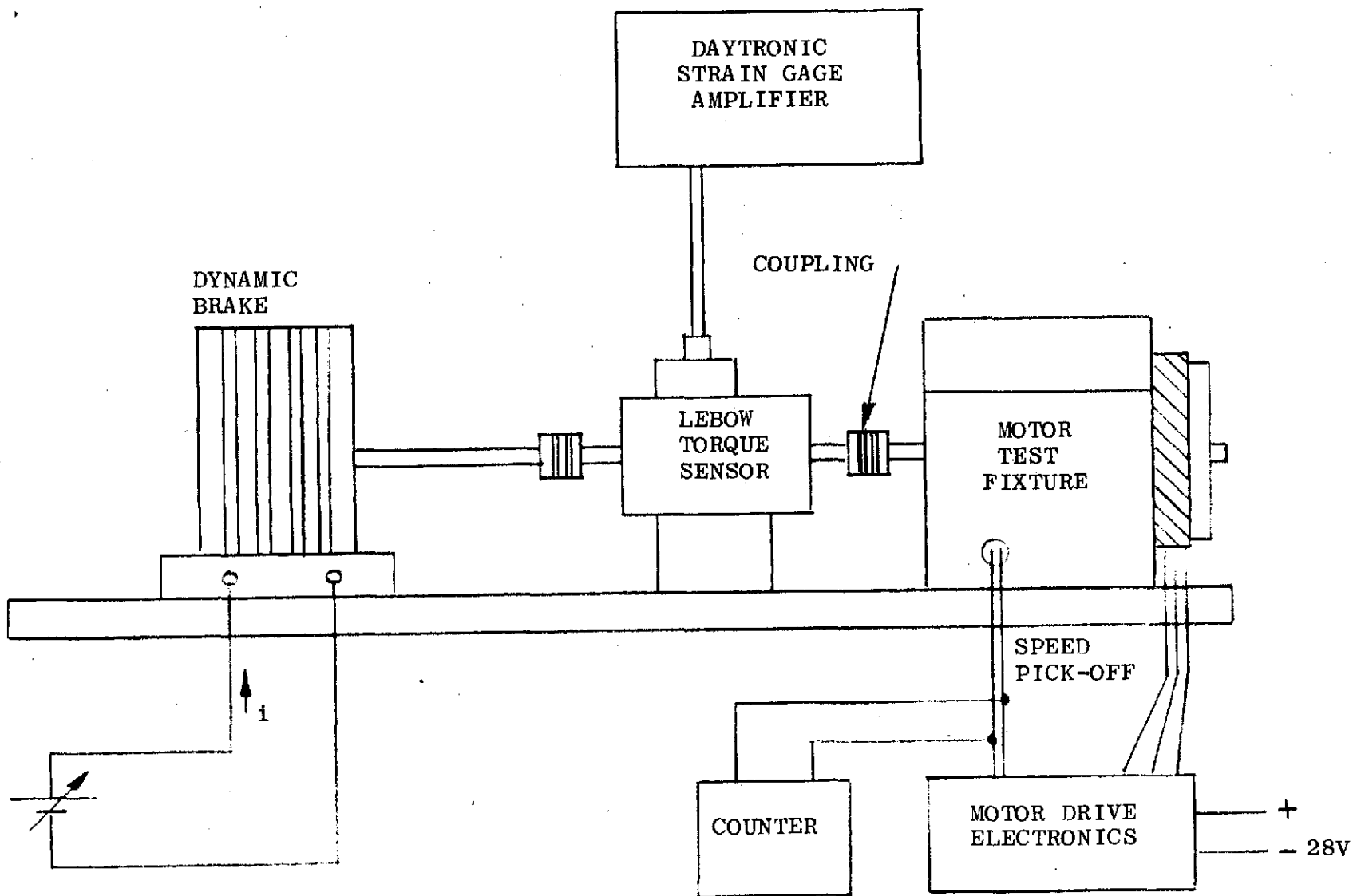
FIGURE 2.4-9

BIAS POWER SUPPLY

FIGURE 2.4-10

FIGURE 2.4-11

motor was run-up to the desired speed, then the brake current was adjusted until the motor stabilized at that speed. The strain gage reading is thus the motor developed torque plus the fixture torque for a given speed.

Motor fixture torque (friction and windage) was measured in another set-up where the motor in a fixture was driven by a drive motor through the strain gauge (Figure 2.4-12). The gage reading is the fixture torque for a given speed.

The electrical test connection is shown in Figure 2.4-13. The +28V DC power into the electronics was measured by a wattmeter. A DC voltmeter was placed across the line to monitor the +28V. To measure the motor input power, a two wattmeter method was used. In addition, line current and line to line voltage were monitored.

2.4.7.2   Test Results

The results of the tests were tabulated and plotted. Figure 2.4-14 shows torque vs speed and overall efficiency vs speed. With the line current set to approximately 10A RMS, the starting torque was 45.5 oz-in. At about 6000 RPM, the amplifier attained saturation, hence for higher speed, the line current and torque dropped off to 8A RMS and 24 oz-in at 8000 RPM. The efficiency at 8000 RPM for the full torque condition was 70.2%. This includes the losses in the EMI filter capacitor, but does not include

FIGURE 2.4-12

'WESTON 329'

+28V

DC
VOLTMETER

WATT
METER

− V +

0V

− +

'SENSITIVE RESEARCH'

AC MOTOR

A

CURRENT
POTENTIAL

W1

MOTOR

DRIVE

ELECTRONICS

WATTMETER

B

I_L

AC AMMETER

WATTMETER

W2
POTENTIAL
CURRENT

V_L

THERMOCOUPLE
VOLTMETER

C
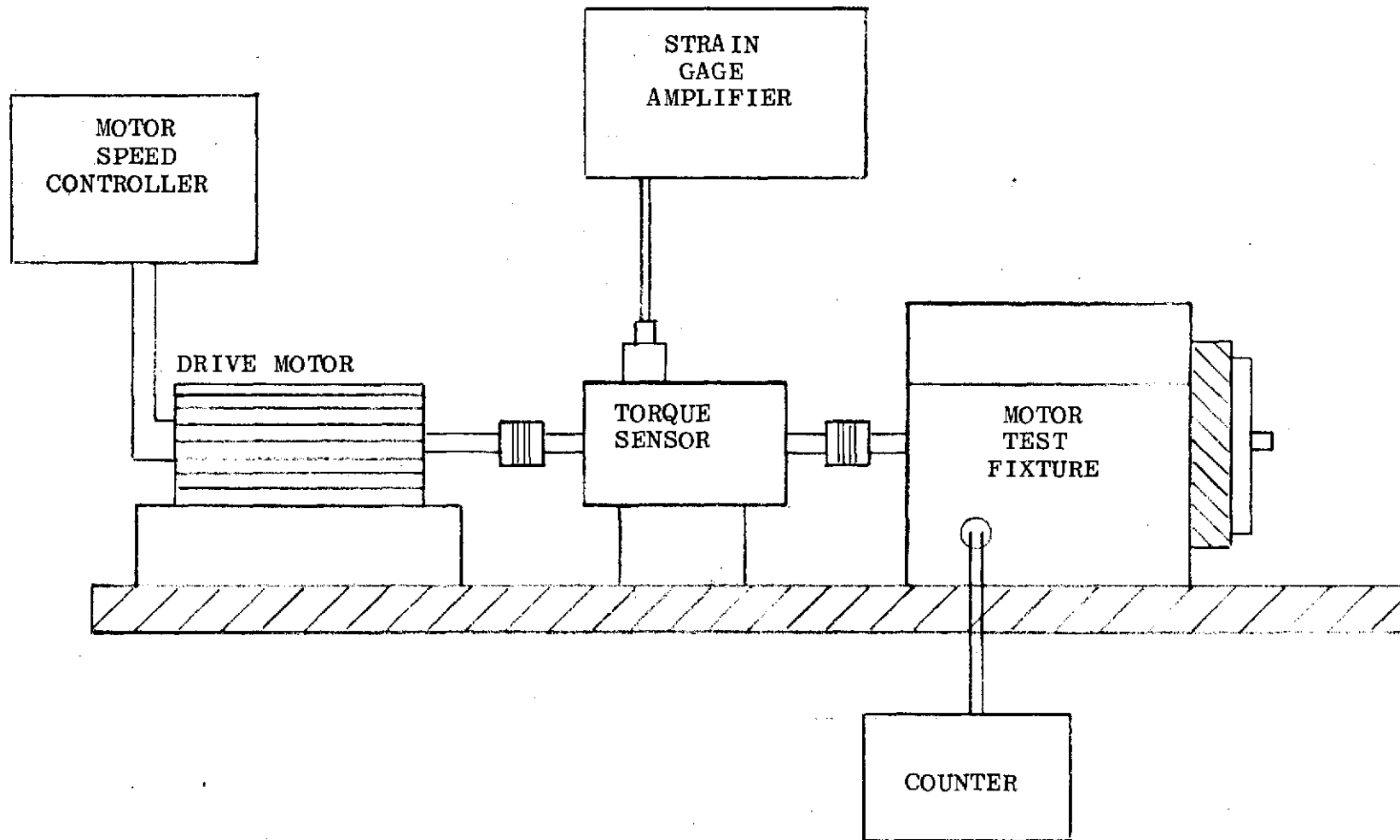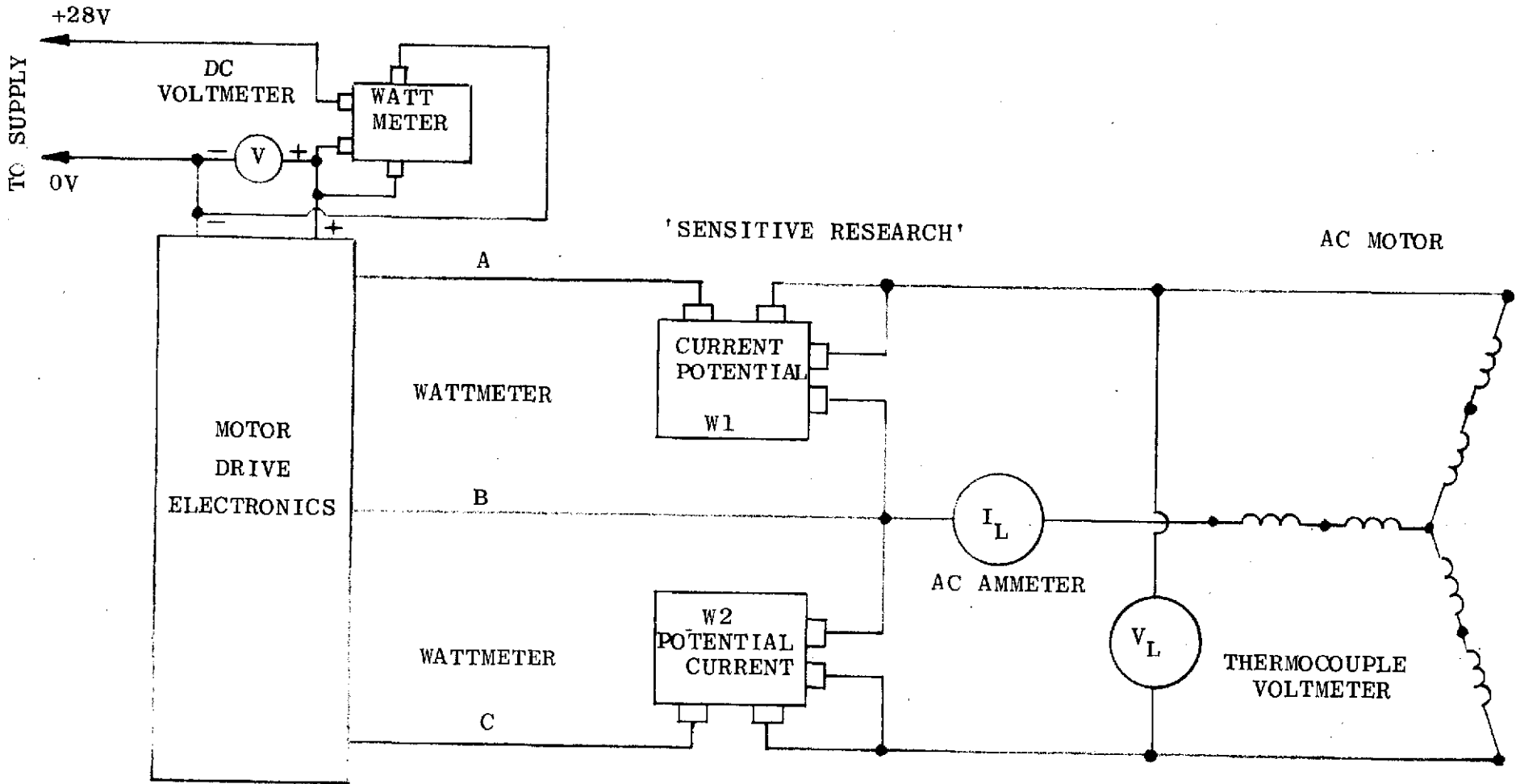
TEST EQUIPMENT CONNECTION

FIGURE 2.4-13

RUN-UP TORQUE

RUN-UP SYSTEM EFFICIENCY
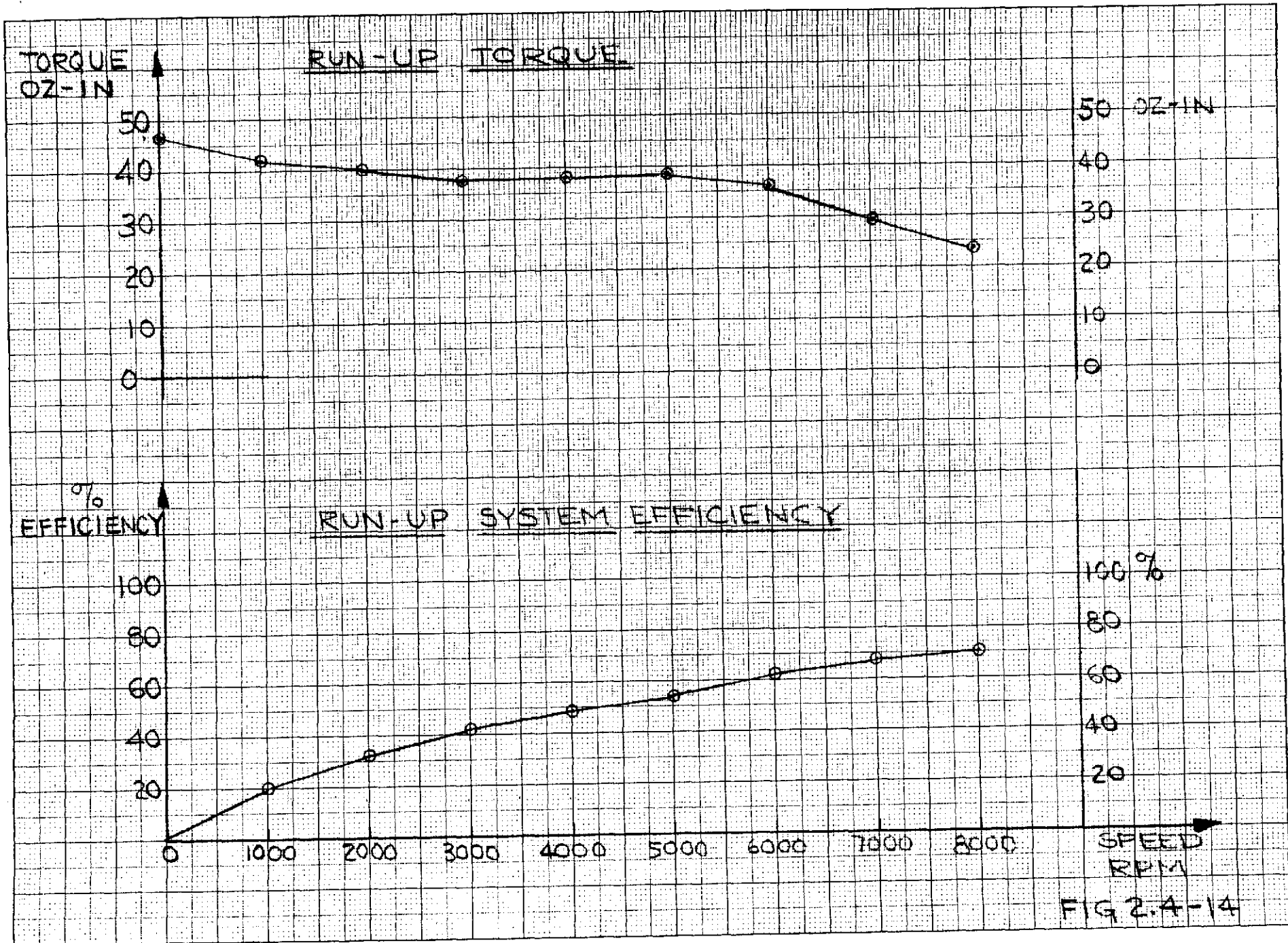
FIG 2.4-14

bias power. The bias power was not minimized in this design, hence it is not meaningful to include it in the system power consumption.

Figure 2.4-15 shows efficiency vs torque at 8000 RPM. For the purposes of this test, the motor voltage command was adjusted by external means until the desired torque was obtained. Efficiency at 24 oz-in is 70%. At a lower torque level the efficiency drops off as anticipated. The jump in the curve between 17 oz-in and 24 oz-in is attributed to a change in electronic efficiency as the amplifier goes from the switching to a saturated mode.

SYSTEM % EFFICIENCY
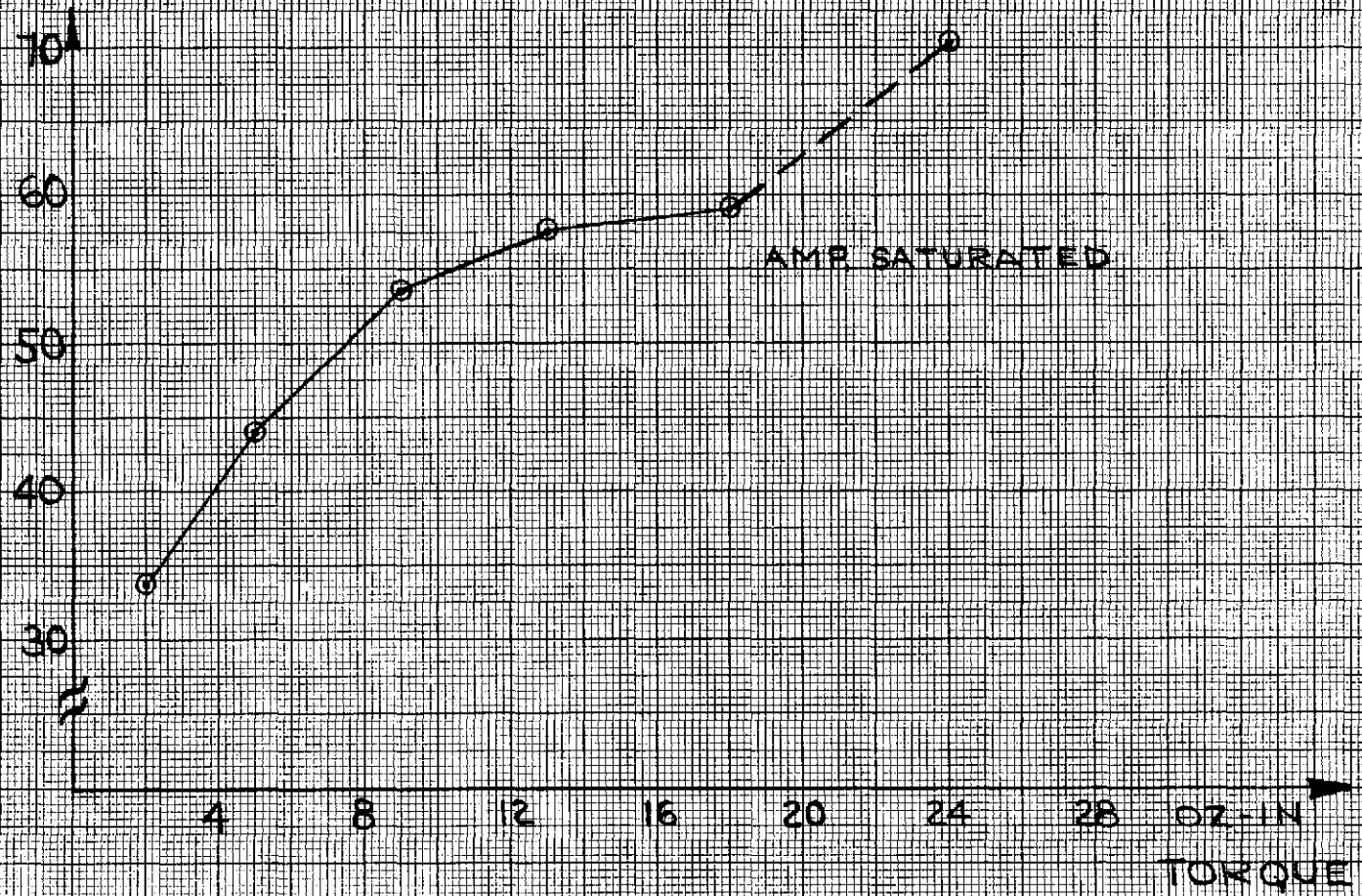
8000 RPM EFFICIENCY VS TORQUE

FIG. 2.4-15

AMP. SATURATED

2-41

2.5 IGRA TESTING

The advanced inner gimbal and rotor assembly was completed during the month of August 1972, at which time performance testing and engineering evaluation commenced. During any operation of the unit the following performance parameters were always monitored:

1. Running Time

2. Wheel Speed

3. Power Supply Voltage

4. Power Supply Current

5. Bearing Vibration Side 1 & Side 2

6. Bearing Temperature Side 1 & Side 2

7. Cavity Pressure

Initial testing of the inner gimbal and rotor assembly was performed at 4000 RPM. The unit was accelerated from zero RPM to 4000 RPM in 2.5 hours. Once the unit achieved stability at 4000 RPM, a measurement of windage and bearing drag torque was made in the spin axis horizontal position. This drag torque was found to be 6.0 oz-in, well within the design goals for the unit. The unit operated at this speed for 500 hours. During this operational time, torque tests were taken in all three spin axis positions; i.e., spin axis up, spin axis down, and spin axis horizontal. After each 100 hours of operation, the unit was run down for bearing visual inspections. During these periods of testing, various lube system flow rates were experimented with to find the optimum lube system flow rate. Once the lube flow rate was optimized, unit testing began at 8000 RPM.

Acceleration from zero RPM to 8000 RPM was achieved in 6 hours. When the unit was stabilized at 8000 RPM, dynamic balance and bearing drag torque were measured in each of the spin axis positions. Bearing drag torque was $\approx$ 7.0 oz-in in the horizontal position and $\sim$ 15 oz-in in the spin axis vertical positions. Dynamic balance was measured to be less than 0.1G's in all positions. After 200 hours had been accumulated at 8000 RPM the unit was decelerated to zero speed for a bearing visual inspection. This inspection revealed that the bearing showed no signs of degradation. The unit was accelerated to 8000 RPM and allowed to accumulate 1000 hours at this speed to gain further confidence in the units performance before testing at 12,000 RPM began.

After approximately 1500 hours of operational time had been accumulated at 8000 and 4000 RPM, testing was to begin at 12,000 RPM. After a bearing visual inspection the unit was accelerated to 8000 RPM and allowed to run at this speed for several days with bearing drag torque and dynamic balance being monitored daily to obtain a baseline set of data before accelerating to 12,000 RPM. During the acceleration from 8000 RPM to 12,000 RPM the following parameters were monitored every 10 minutes.

Wheel Speed

Volts from DC Supply

Current from DC Supply

Cavity Pressure

Bearing Vibration Side 1 & Side 2

Bearing Temperature Side 1 & Side 2

Also, during this transition period, panoramic pictures were taken of the units accelerometer outputs at 500 RPM intervals. The peak unbalance output occured at 8500 RPM (χ 0.4 G 's). At a wheel speed of 11,933 the unit flywheel burst without prior warning. Unit performance at 4000 and 8000 RPM was perfect, and the performance as monitored from 8000 RPM to the point of failure was perfect.

2.6   Conclusions and Recommendations

2.6.1   Inner Gimbal and Rotor Assembly (6000H)

An IGRA of this size is practical, however, in light of

the explosion accident where the wheel burst, several

basic areas of further state-of-the-art development should

be pursued relative to materials to be considered for use

in this type of application. These include:

1.   The "Fracture Mechanics" design and analysis discipline.

2.   Materials K_{IC} values available for engineering use.

3.   Improvement in Non-Destructive Inspection/Testing

      techniques involving flaw definition.

4.   Improved proof test criteria for wheel overspeed

      testing.

The failure of the MA-6000 rotor was investigated by

both NASA/MSFC and BGSD personnel in an effort to deter-

mine why the failure occurred and what measures can be

taken in the future to avoid such catastrophic failures.

The Failure Analysis Report was submitted to MSFC under

separate cover. The 18 Ni 350 material chosen for rotor

fabrication was not previously used by BGSD but was a

commercially available product. The reasons behind the

choice of the material centered around its higher

strength qualities versus the 18 Ni 300 used in other
Control Moment Gyro (CMG) rotors. The techniques
applied in material fabrication and inspection and rotor
fabrication and inspection followed past BGSD practice
using qualified vendors whose performance on previous
CMG efforts were judged as quality efforts. The review
of the failed rotor pieces indicated a small flaw near
the rim was the cause of failure.

Based on a review of the findings, the following conclu-
sions are drawn:

1. The failure was caused by a flaw in the web at the
    9" station near the neutral axis of the section.
2. The stress analysis performed was satisfactory and a
    re-analysis confirmed earlier calculations. The "g"
    load capabilities of the rotor are in the order of
    > 1000 g magnitude and therefore transportation
    induced loads could not have produced the stresses
    necessary for failure.
3. The failure is related to the "Fracture Mechanics"
    Discipline where a small flaw is caused to grow until
    at some later date a lower stress field is of such a
    magnitude as to cause fracture of the hardware. This

is a relatively new analysis technique that was
not applied at the time of original design.

4. Non-Destructive Inspection techniques (NDT; "Non-Destructive Testing") appear to be adequate in scope
but somewhat limited in flaw definition. Ultrasonic,
X-Ray and Magnaflux were all applied before and after
overspeed testing but, in view of the flaw size in
question, the resolution available is unsatisfactory
for the 6000H IGRA 18 Ni 350 rotor.

2.6.2   Wheel Control System

A variable frequency/voltage control electronics technique
for a 3 phase CMG spin motor has been demonstrated
successfully with performance within the goals required.
The selection of a CMG wheel control system from among a
large variety of schemes (involving two or three phase
AC or Brushless DC motors and their corresponding con-
trollers) should depend on more detailed application
requirements and, as can be expected, is continually
affected by new development in motors as well as electro-
nics.

A general comparison of AC and DC motor schemes indicates
that either wheel control system will perform equally well

in a CMG. In applications where the ultimate in weight and efficiency are required, the permanent magnet motor scheme is superior. The only significant motor loss is in the copper of the stator. In the induction motor, however, the copper losses associated with the squirrel cage rotor are significant. From a mechanical standpoint, the induction motor is the most rugged of the two systems. The squirrel cage rotor is less limited in size and speed when compared to a permanent magnet rotor. This has been minimized by titanium banding around the periphery of the permanent magnet.

SECTION 3

SPACE REPLACEABLE SPIN BEARING DEVELOPMENT

3.1   General

In order to provide for Control Moment Gyro spin axis
ball bearings capable of meeting any future space system
life requirements greatly beyond those of the 270 day
mission in the Skylab ATM Program, a ball bearing con-
figuration was developed that is easily replaceable in
space. This design feature insures that the CMG units
will be able to meet future life extension requirements
(numbered in years) by replacing the bearings in space.
The spin axis bearings developed were incorporated in
the 2000H DG CMG and the 6000H IGRA described in sections
1 and 2 of this report.

Two possibilities which would require a bearing change
are an increase in bearing torque after extended periods
of operation due to either increased friction torque or
inreased viscous drag associated with the continuous
flowing lubrication system, or a "hard" bearing failure.

Rather than expend the additional power resulting from
increased bearing torques, it would be advantageous to
change the bearings. A change in bearing torque of 2 oz
inches at 8000 RPM corresponds to an increase in mechanical
power requirement of approximately 12 watts. For 10,000

hours this would be 120,000 watt hours. Without the space replaceable bearings, it would be necessary to live with this additional power or shutdown. With the replaceable bearing scheme, a short shut down period of approximately 2 hours would allow for replacement of the bearings.

3.2   Bearing Description

The space replaceable ball bearings used in the advanced inner gimbal and rotor assemblies have the following design characteristics:

ITEM	6000H IGRA	2000H DG CMG
Bearing Type	Modified 307H	Modified 107H
Number of Balls	10	15
Ball Diameter	0.5625	.3125
Bore (In)	1.3780	1.3780
Outer Diameter (In)	3.500	3.00
Quality	ABEC 9	ABEC 9
Basic Dynamic Load Rating (lbs)	7083	3510
Limiting Speed (RPM)	23544	25823
Nominal Contact Angle (Degrees)	15	15
Static Thrust Capacity (lbs)	7544	2908
Static Radial Capacity (lbs)	3412	2509

ITEM	6000H IGRA	2000H DG CMG
Nominal Radial Load (lbs)	160	75
Nominal Preload (lbs)	80	40
Dynamic Capacity At 8000 RPM (lbs)	1138	564
Dynamic Capacity at 12,000 RPM (lbs)	995	493
Nominal Bearing Torque (oz-in)	4	2
Maximum Transient Radial Load (lbs)	480	275
Calculated B-10 Life (hrs) ATM Duty Cycle	$\approx$1,000,000	122,000
Reliability ATM Duty Cycle	.9999$^+$	.998

Suppliers	Barden Corp.
	Split Ball Bearing Co.
Metal Parts - Material	CEVM 52100 Steel
Retainer - Material	Cotton Phenolic Synthane with Post Cure
Special Procedures	TCP Soak Smooth Ractor Test
Lubricant	KG-80 Super Refined Mineral Oil
Lubrication Method	Dynamic Lubrication System
Nominal Operating Temperature	$90^{\circ} \pm 30^{\circ}F$
Preload Method	Belleville Spring

The modifications designed into the standard angular contact ball bearings to make them easily replaceable both on earth and in orbit were rather unique. The inner race was lengthened to accommodate three bayonet type slots on the inner race land diameter. The slots were incorporated so that the bearing could be removed with a single tool pulling on the inner race while jacking against the wheel shaft. The outer race was also lengthened to accommodate the special preload mechanism that was assembled to the bearing cartridge end caps. This preload, once set for proper bearing loading, would not have to be readjusted after a bearing change was accomplished. This bearing design also uses the same retainer and lubrication system used with the standard bearing. This bearing design also incorporates a felt reservoir in close proximity to the bearing outer race to collect excess lubricant.

3.3   Tools Required

Only simple standard wrench type tools are required to gain access to the ball bearing of the inner gimbal and rotor assembly. The tools consist of a one size allen wrench to remove the side covers and end caps, one socket wrench to remove the strut nut, and one spanner wrench

to remove the lubrication nut. Two special tools are needed to complete a bearing change. One tool is a specially designed bearing puller, and the other is a specially designed bearing inserter. Figure 3.3-1 is a layout of the bearing extraction tool and Figure 3.3-2 is the layout of the bearing insertion tool. The bearing extraction tool has three pins which engage the three bayonet slots in the inner race, and the bearing is removed by jacking it out against the wheel shaft with the turn screw. The bearing insertion tool utilizes a heater within a brass slug that fits the bore of the bearing and a teflon pusher. The inner race is heated to overcome the shrink fit and the bearing is seated with the pusher.

Both bearings, with these tools, have successfully been changed at Bendix in less than two hours.

3.4   Maintainability Considerations
3.4.1   Determination of When to Replace Ball Bearings
With the replaceable design now incorporated into the CMG, one of the first questions to be asked is how often should the spin axis ball bearings be replaced? In some cases, if a definite figure can be established for the bearing fatigue limitations, a life expectance figure
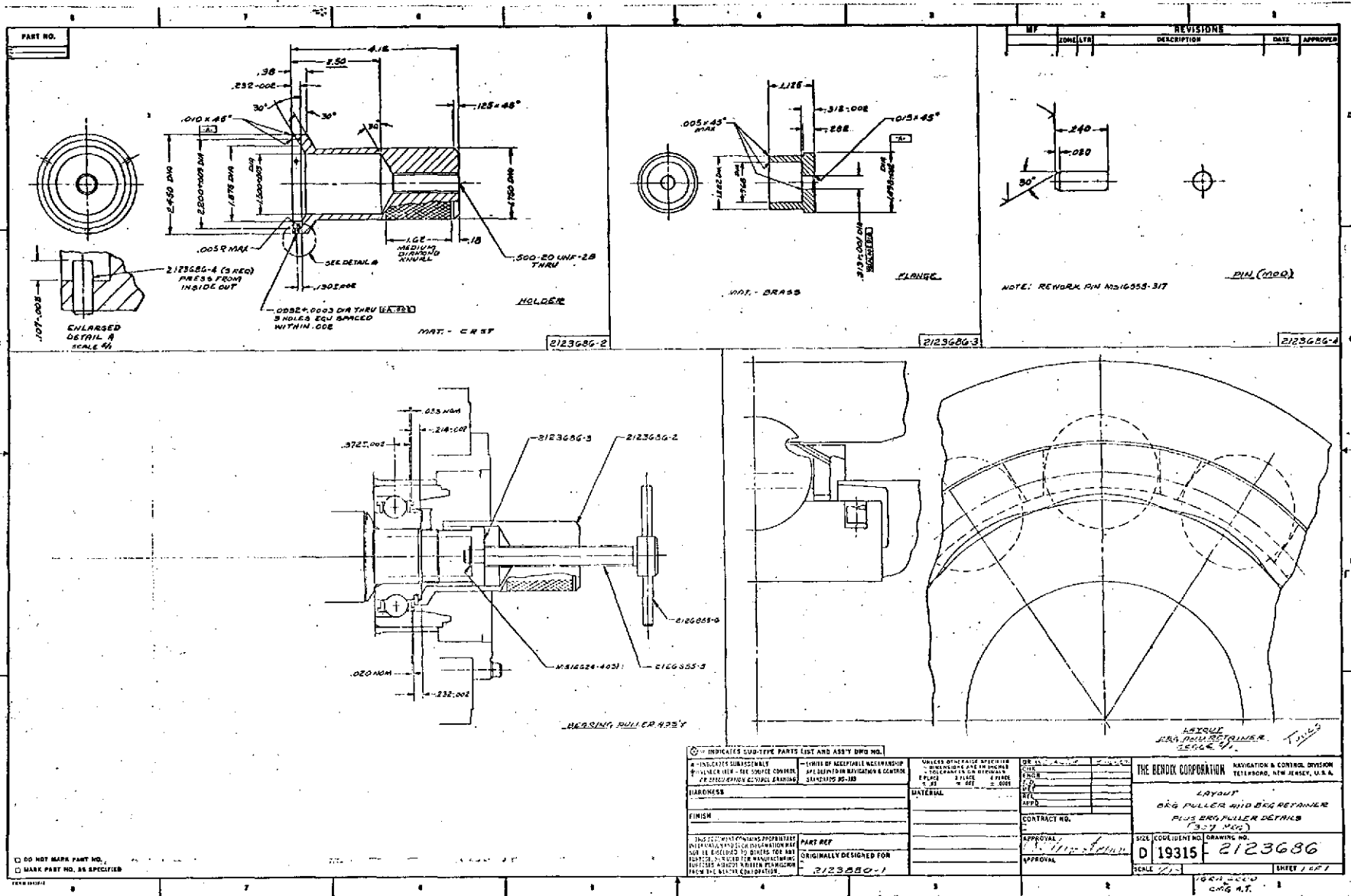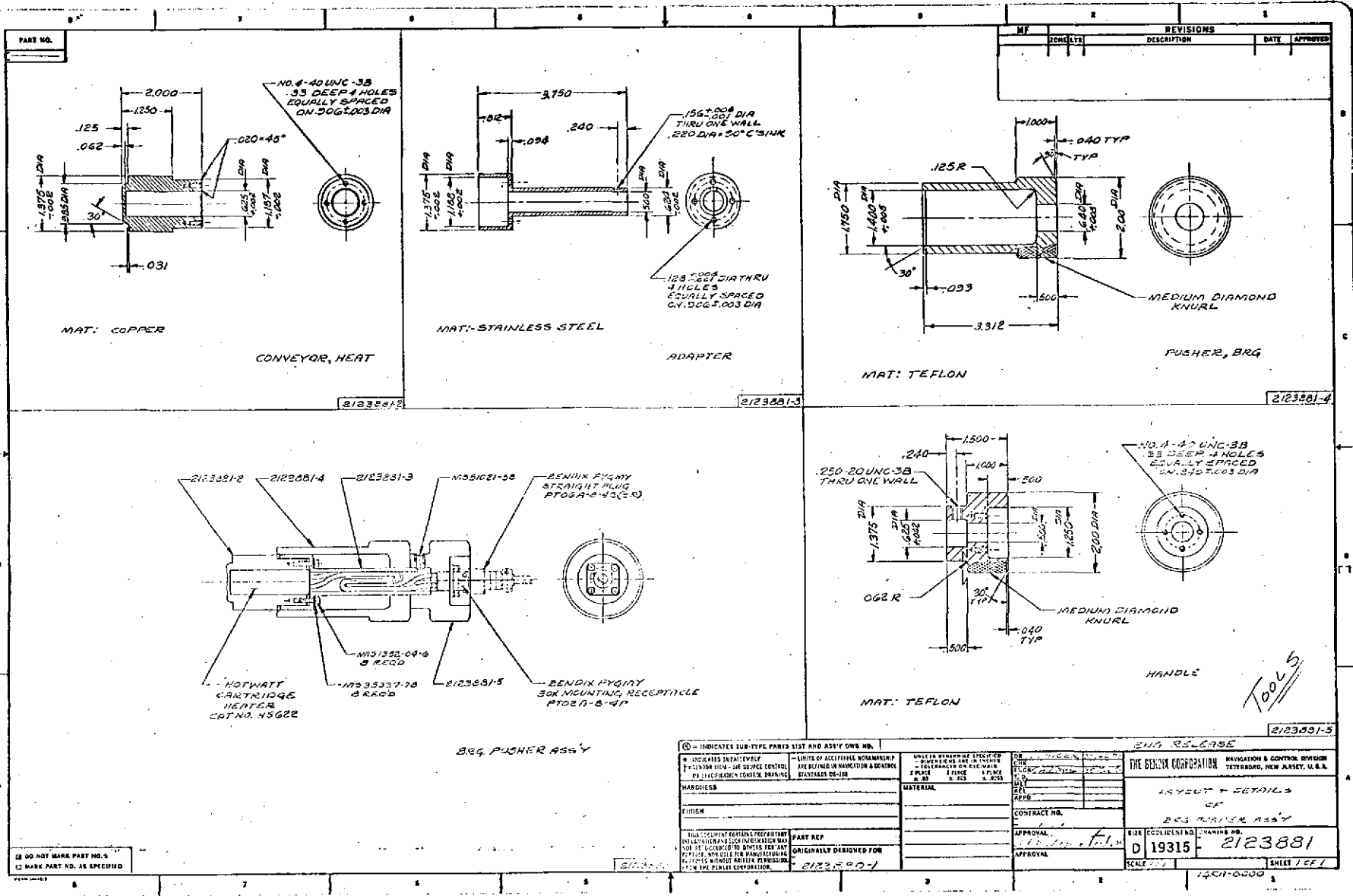
FIGURE 3.3-1

FIGURE 3.3-2

for the ninetieth percentile can be established and may
be used for determining bearing replacement. However,
in many cases, the bearing fatigue life calculations
predict an infinite life span provided lubrication is
available. To date there is no existing system available
to predict the eventual failure of gyro type ball bear-
ings. Work is proceeding in this area but nothing
conclusive appears imminent. With that in mind, two
alternatives are still available, one is programmable
maintenance (i.e., change the bearings after finite
time periods regardless of whether the change is required)
or the alternate is to choose a power limitation (i.e.,
when the bearing torque exceeds a certain value, replace
the bearing). The desirability of either approach should
be determined in a separate system reliability study
which would determine the advantage of one method over
the other based on consideration of all the system sub-
components.

3.4.2   Astronaut Maintenance Activities Associated with
        Replaceable Bearings

The replaceable bearing design is such that an individual
with a normal mechanical aptitude could replace the bear-
.ings in a two hour period. This has been demonstrated at

BGSD. The individual will be required to remove simple items such as snap-lock rings and ordinary screws. Bearing removal and insertion is accomplished with simple tools. These tools are actually socket wrenches specifically designed for the job of either inserting or removing bearings. It is the assumption at present that all operations will be performed under zero "G" environments. This will require that all wrenches be adptable to the various reactionless tools being developed for space use.

3.4.3   **Tools Required for Replacing Bearings in Space Under Zero "G"**

As mentioned above, no special skills or tools are required in order to replace bearings in space. The only tool not of wrench type is the bearing heater insertion tool. In order to insure proper dynamic balance and for improved bearing performance, the ball bearings are press fit on the wheel shaft. In order to do this, the bearing insertion tool was equipped with heaters.

The means of powering the heaters would be determined after considering the types of power NASA feels will be available on orbit. Again, this should present no particular problems. Because of the zero "G" environment, all

removable parts were captive, and the number of parts
to be removed was minimized.

3.4.4   Procedure for Replacing Spin Axis Ball Bearings
Listed below is an abbreviated procedure for replacing
spin axis ball bearings.

1. Remove vacuum sealed end covers from sides of unit.
2. Remove end caps,which contain the preload devices,
   and strut lock nuts from both sides.
3. Remove thru strut.
4. Remove felt oil collection reservoirs from both sides.
5. Remove lubrication system locknut and snap ring.
6. Jack out ball bearing side 1.
7. Install ball bearing side 1.
8. Put back lubrication system locknut and snap ring.
9. Repeat steps 5 through 8 for side 2 bearing.
10. Repeat steps 1 thru 4 in reverse to complete replace-
    ment.

It should be noted that bearing insertion is simply the
replacement of the parts removed in reverse. Resetting
of preload is not required because during the bearing
change, the preload setting was not disturbed.

3.5   Conclusions and Recommendations

From the experience gained with replaceable bearings
on this advanced inner gimbal and rotor assembly, it can
be concluded that replaceable spin bearings are a practi-
cal design feature and that all future CMG's have replace-
able spin bearings as part of their design.

SECTION 4

ELECTRONIC DATA TRANSMISSION

ACROSS A GIMBAL PIVOT

4.1   General

The requirement for unlimited CMG gimbal freedom leads
to implementations for carrying signals and power across
gimbal pivots either by slip rings or by some electronic/
magnetic/optical technique. Slip rings were chosen for
incorporation in the prototype advanced CMG (Section 1)
because of state of the art simplicity with the obvious
ability to provide redundant slip rings for reliability
and long life if required by application details. A
multiplexed electronic/magnetic technique might provide
a life and reliability advantage, has fewer lines (wires),
would eliminate rings subject to ultimate noise and/or
wearout and would reduce the total friction torque about
the gimbal pivot.

This section deals with an effort to show feasibility of
electronically multiplexing typically required CMG signals
across a gimbal pivot through a rotating signal trans-
former. Carrying power across a pivot through a rotating
transformer was not included in this task. A breadboard
circuit was designed, built, tested and delivered to
MSFC for evaluation in February 1972.

The breadboard consisted of a rotary signal transformer and associated electronics designed to process the following primary advanced CMG signals associated with the Inner Gimbal and Rotor Assembly and the Inner Gimbal rate control:

4 Spin Motor Speed Signals	– Square Wave
4 Spin Motor Currents	– DC
4 Spin Bearing Temperatures	– Resistance
1 Inner Gimbal Tach Signal (Motor Side)	– DC
1 Inner Actuator Rate Command Signal	– DC
4 Spin Motor Disconnect Signals	– Discrete
1 Accel/Decel Signal	– Discrete

The list of signals was selected from a consideration of all signals planned in the advanced CMG configuration. A list of signals not included in this design and the rationale for their exclusion is provided below.

Signal	Rationale For Exclusion
Spin Bearing Accelerometers	Engineering ground test use only.
IGRA Vacuum Gages	"

Signal	Rationale for Exclusion
Torquer Currents	Engineering use only – experimental
Gimbal Tachs (Brush Type)	(Same)
Resolver Signals	(Same)
Ext. Speed Ref, (Oscillator to varry speed)	(Same)

Multiplexing Electronics

The use of rotary transformers for multiplexed signal transfer is outlined in the block diagram of Figure 4.1-1. The configuration approach was to multiplex the analog signals for the various information sensors, modulate them at a fixed keying frequency ($\approx$10 KHz) and transfer them across the transformer in a successive pattern of rates necessary to meet system bandwidth requirements. The processed information across the transformer is demodulated and channeled into applicable sample and hold amplifiers which retain the information. Keying frequencies and sync commands are likewise fed into an additional transformer winding. The signals which are fed in the direction from the master to slave section are designated as command signals. These are:

1. Inner Actuator Rate Command - DC to 50 Hz

4. Spin Motor Disconnect Discretes

1. Accell/Decel Discrete

These signals are of a form to be readily multiplexed.

The signals which are fed from the slave section to the master are designated as status signals. They include:

4. Spin Motor Speed Signals - Conditioned to DC

4. Spin Motor Currents - DC

1. Inner Gimbal Tach Signal (Motor Side) - DC to 50 Hz

4. Spin Bearing Temps - Conditioned to DC

The motor current and tach signal are of the form to be processed. However, the speed signals are frequency signals generated from the hall devices in the spin motor. These signals must be conditioned for multiplexing by frequency to DC conversion. The DC which is multiplexed provides an output magnitude which is proportional to speed. The bearing temperature sensors are thermistors which must also be conditioned. The conditioned signal is a DC voltage proportional to temperature.
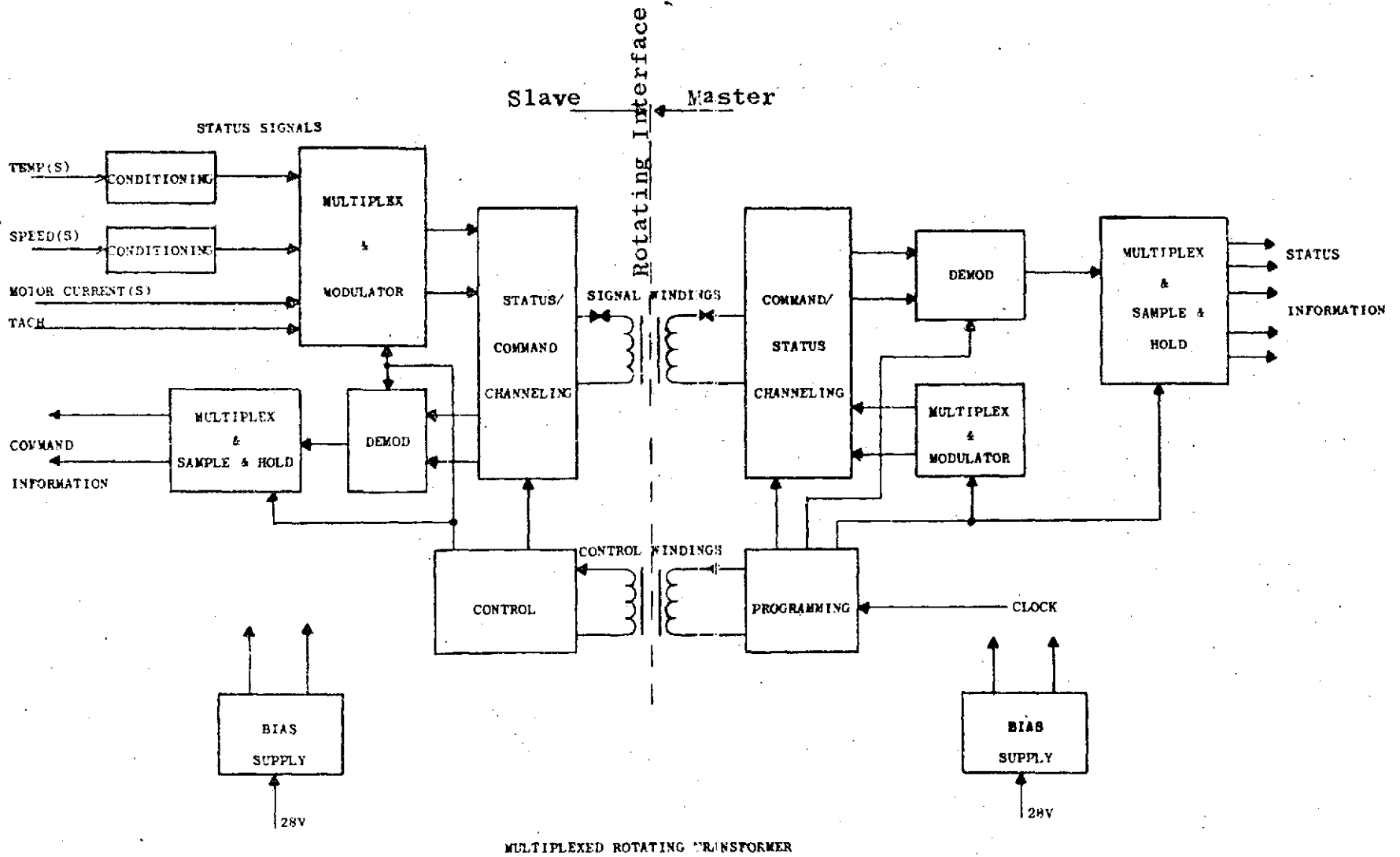
MULTIPLEXED ROTATING TRANSFORMER

FIGURE 4.1-1

4.2   Description of Breadboard Circuits

4.2.1   Rotating Transformer

In order to minimize the transformer size and weight, minimize power losses and maximize radial gap for application on a CMG gimbal pivot axis, the signal transformer operating frequency was chosen as 9.6 KHz. This selection was also commensurate with the bandwidth requirements of the signals to be multiplexed through the transformer. The characteristics of the signal transformer successfully produced and used are as follows:

Excitation:	20V pk-pk, 9.6 KHz
Input Impedance:	39+j2220 ohms
Load:	No load to 1000 ohms
Ratio (no load):	0.992
Regulation:	1.3% no load to 1000 ohms
Efficiency:	94% at 1000 ohms load
Radial Gap per Side:	0.005"
Size:	1.75"OD 0.50" ID, 0.75" Wide
Construction:	See Figure 4.2-1

ROTATING SIGNAL TRANSFORMER

TYPICAL CONSTRUCTION

USING

FERRITE CORE MATERIAL

FOR

SIGNAL AND POWER APPLICATION

STATOR BOBBIN (NYLON)
AND WINDING ASS'Y

STATOR CORE
(FERRITE)

AIR GAP
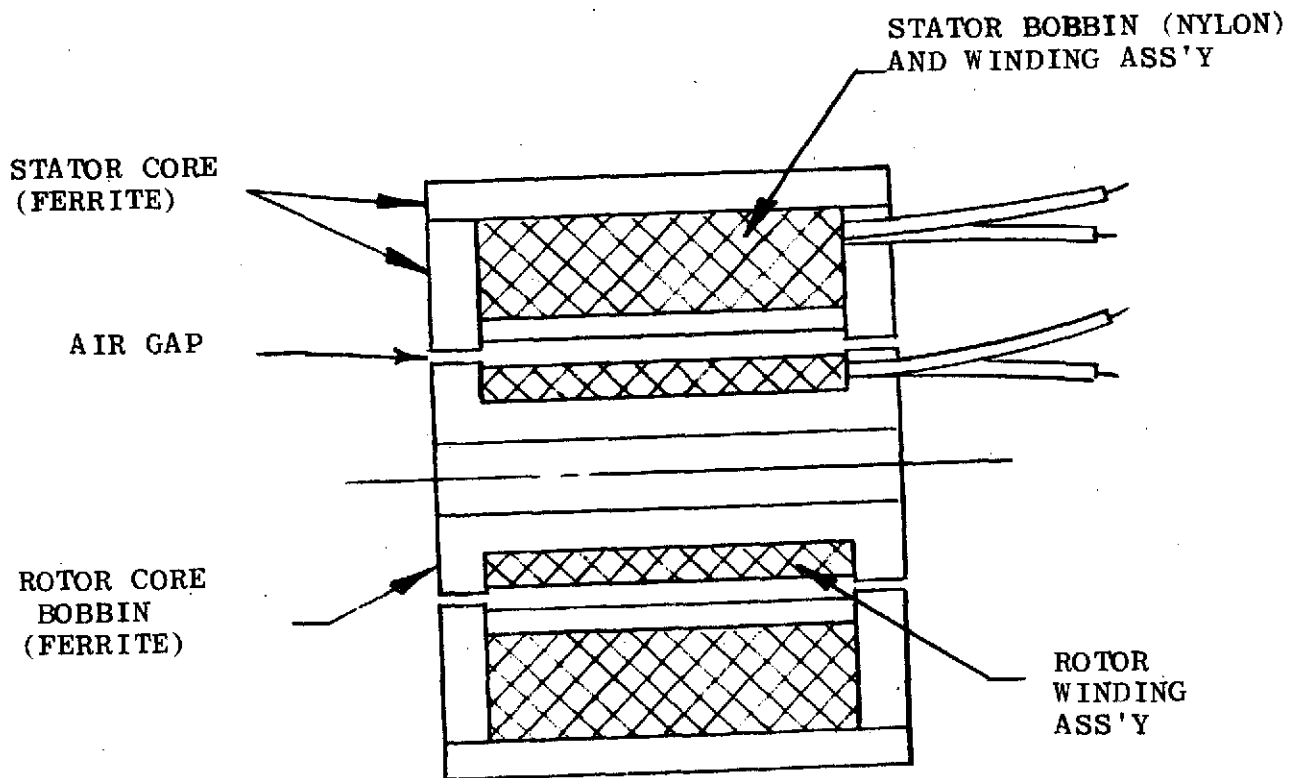
ROTOR CORE
BOBBIN
(FERRITE)

ROTOR
WINDING
ASS'Y

FIGURE 4.2-1

Although this task did not require demonstration of carrying power across a pivot with a rotating transformer, Bendix designed and constructed one compatible with the typical CMG requirements under this study. The measured performance of this prototype transformer was as follows:

Power Rating: 450VA, 90% power factor, 9.6 KHz

Efficiency: 97.5%

Radial Gap per Side: 0.005"

Size: 1.5" OD, 0.25" ID, 1.25" Wide

Weight: 184 grams

4.2.2   Electronic Circuits

The basic principle of system operation is as follows. Given a number of analog signals generated within the CMG inner gimbal assembly, the system will transfer these signals to the outer gimbal assembly using two rotary transformers – a signal transformer and a synchronizing transformer. This is accomplished using time sharing and modulation techniques. The system consists of a transmitter located on the inner gimbal assembly and a receiver located on the outer gimbal assembly, and associated power supplies. The transmitter consists of a signal multiplexer and a modulator. The receiver con-

sists of a synchronous demodulator and a de-multiplexer. Bi-directional multiplexing is included by providing for the signals from the outer gimbal assembly to the inner gimbal assembly. The general schematic scheme is illustrated in Figure 4.2-2.

The breadboard consisted of 13 Inner-Outer signals and 6 Outer-Inner signals as follows:

a. Inner-Outer Signals

4 speed signals   S1, S2, S3, S4 - DC

4 current signals   C1, C2, C3, C4 - DC

4 temperature signals T1, T2, T3, T4 - DC

1 tachometer signal DC to 50 Hz

b. Outer-Inner Signals

4 motor disconnect

 signals   D1, D2, D3, D4 - Discretes

1 accelerate/

 decelerate signal   Discrete

1 rate command sig. DC to 50 Hz

The sampling rates chosen for the breadboard were: Tach and Rate Comm. Signals - 1200 per sec, all other signals-
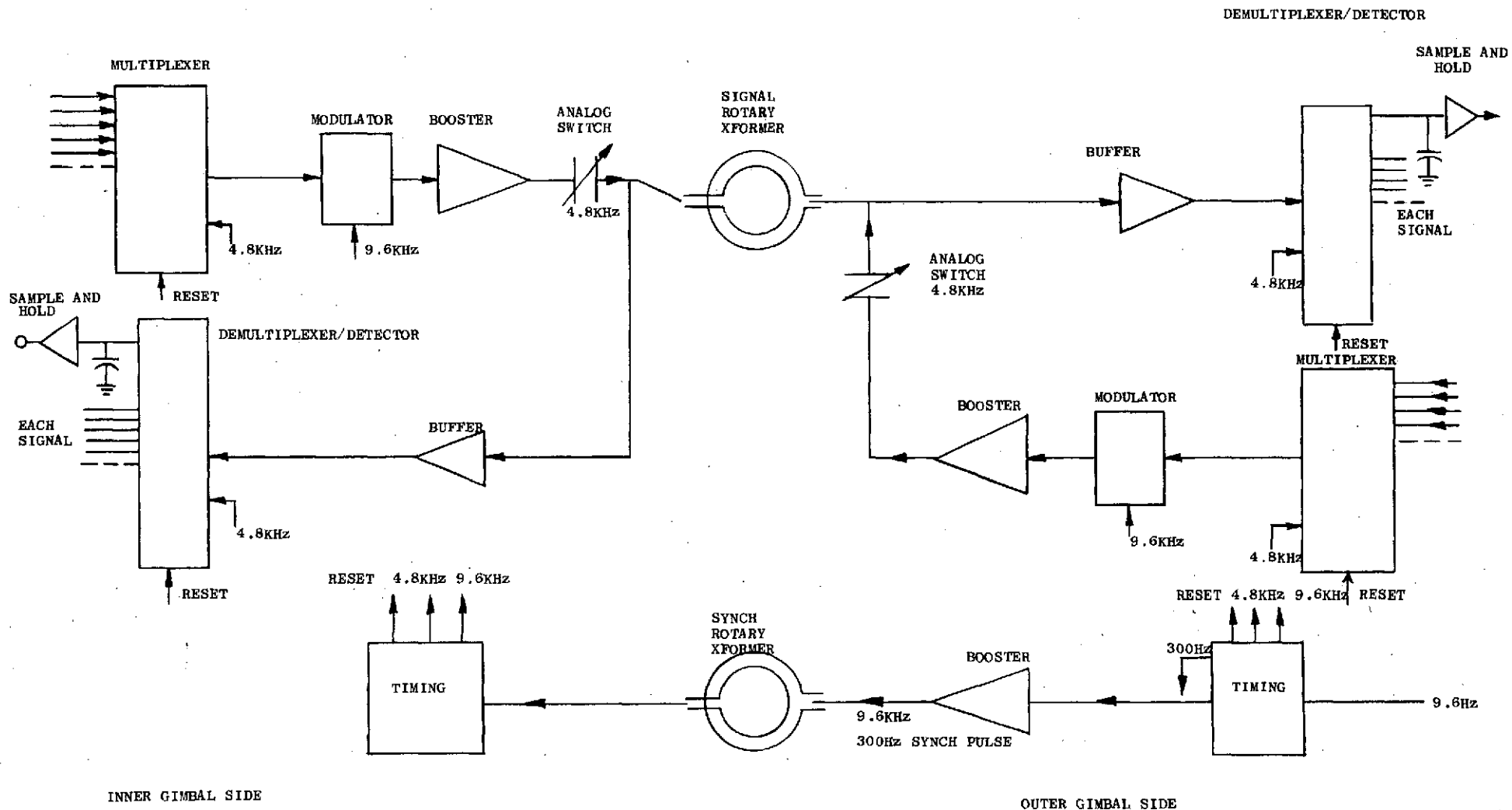
BREADBOARD SYSTEM BLOCK DIAGRAM

FIGURE 4.2-2
4-11

300 per sec. Figure 4.2-3 illustrates the timing speed.

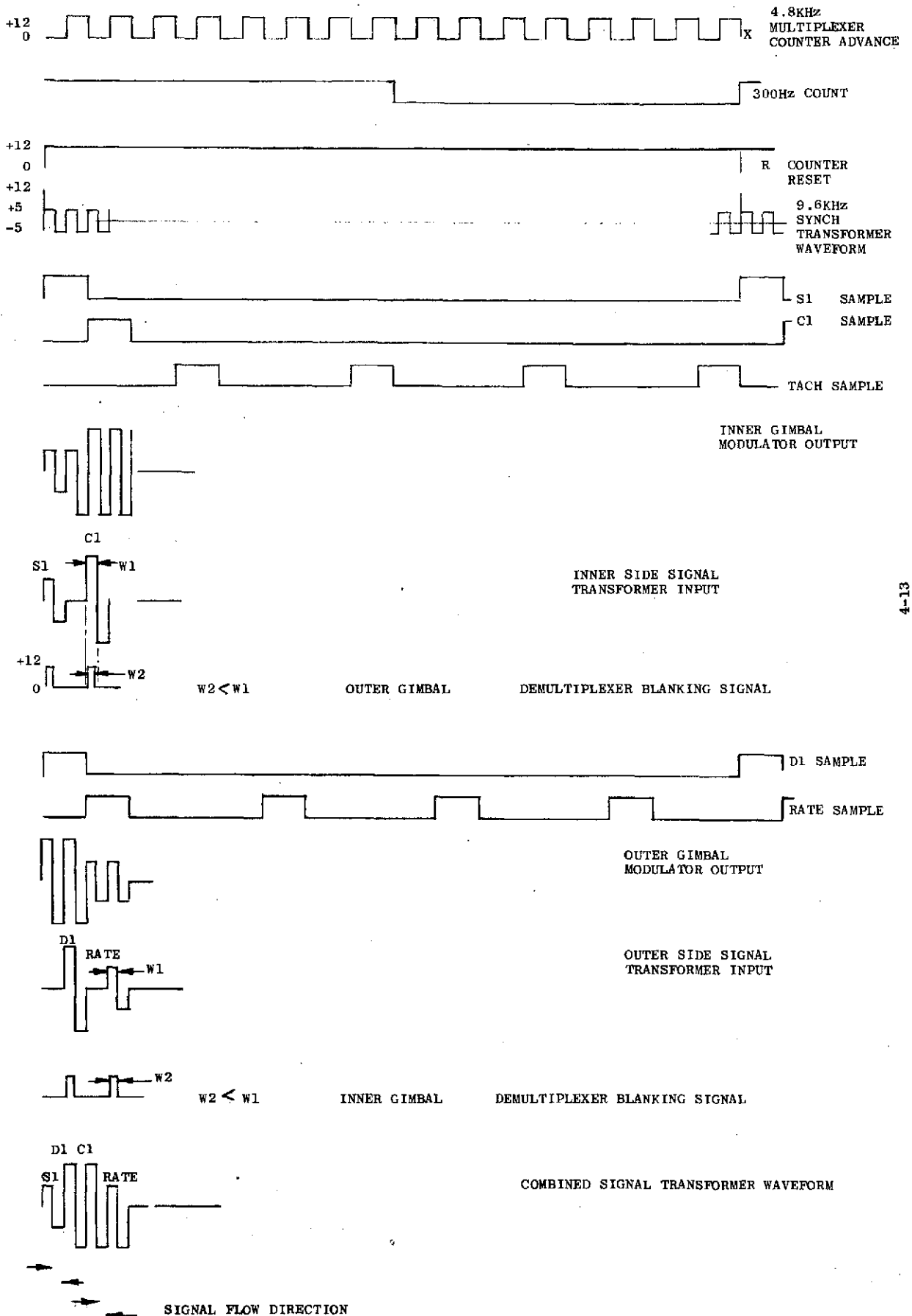Figures 4.2-4 and 4.2-5 are schematics of the detail
breadboard circuits.

Prior to delivery to MSFC for further evaluation, the
measured performance for all signals was summarized as
follows;

Signal range:	$\pm7V$, -25^oC to $+70^oC$
Offset:	$<0.05V$ "
Gain linearity:	1 ± 0.02 "
Accuracy:	$\pm0.1V$ at $\pm7V$ "
	$\pm0.05V$ at $\pm1V$ "
Cross Talk:	less than 0.05V room temp
Phase shift:	Tach and rate comm -6° lag at 40 Hz
	All other signals -4° lag at 5 Hz
Power Reqmt:	5W (not optimized)
Rotational Signal	
Stability:	±5 mv, 0° to 360°, over full sig. range

4.3   Conclusions and Recommendations

The replacement of signal slip rings for unlimited gimbal

+12
0 X 4.8KHz MULTIPLEXER COUNTER ADVANCE

300Hz COUNT

+12
0 R COUNTER RESET

+12
+5
-5 9.6KHz SYNCH TRANSFORMER WAVEFORM

S1 SAMPLE

C1 SAMPLE

TACH SAMPLE

INNER GIMBAL MODULATOR OUTPUT

C1
S1 W1

INNER SIDE SIGNAL TRANSFORMER INPUT

+12
0 W2

W2 < W1 OUTER GIMBAL DEMULTIPLEXER BLANKING SIGNAL

D1 SAMPLE

RATE SAMPLE

OUTER GIMBAL MODULATOR OUTPUT

D1
RATE W1

OUTER SIDE SIGNAL TRANSFORMER INPUT

W2

W2 < W1 INNER GIMBAL DEMULTIPLEXER BLANKING SIGNAL

D1 C1
S1 RATE

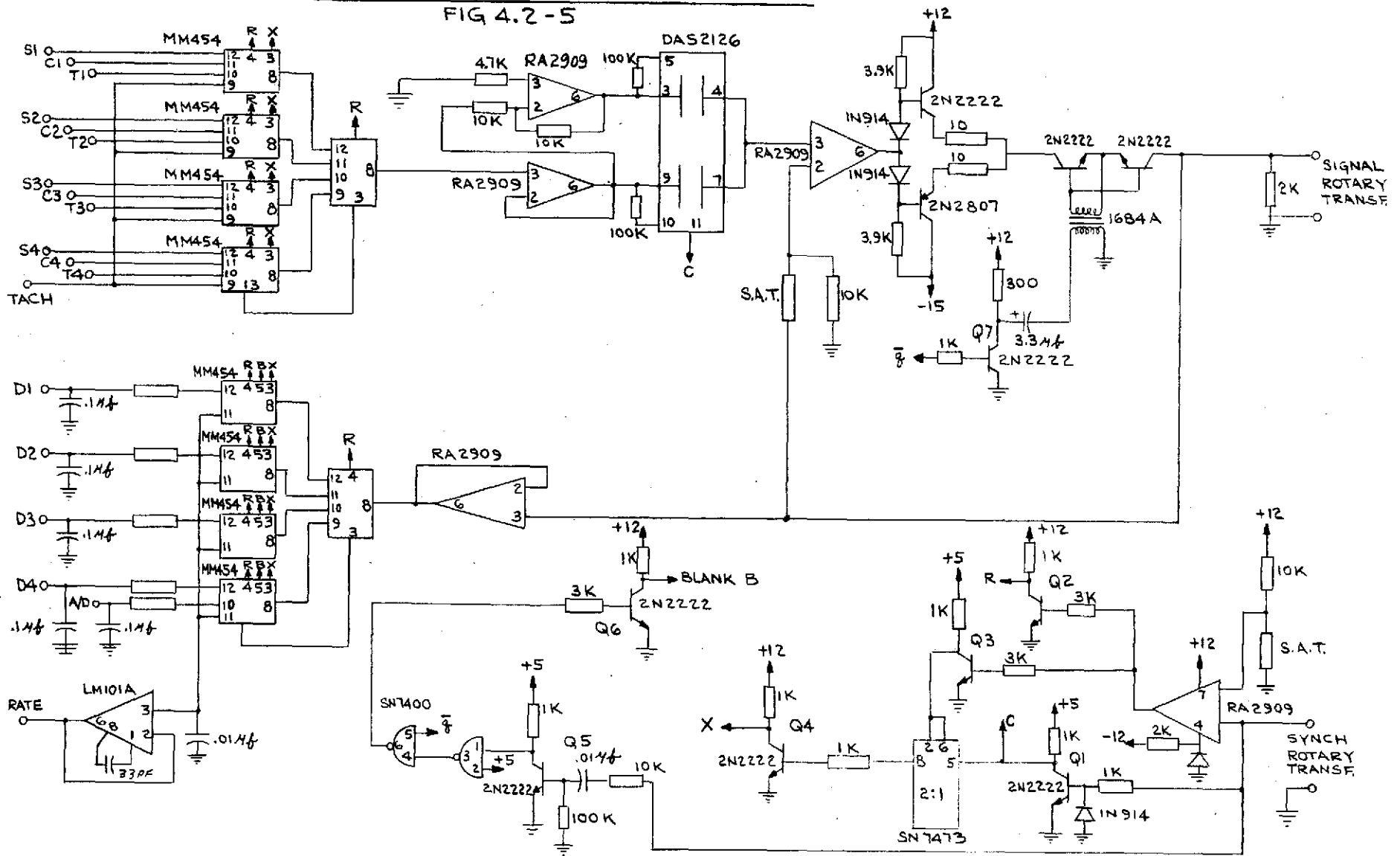COMBINED SIGNAL TRANSFORMER WAVEFORM

SIGNAL FLOW DIRECTION

4-13

OUTER ELECTRONICS SCHEMATIC
FIG 4.2-4

4-14

INNER ELECTRONICS SCHEMATIC
FIG 4.2-5

freedom CMGs with a multiplexed transformer technique has been shown to be feasible. Additional development work should be conducted to design a rotating transformer, and associated modulator and demodulator, to carry spacecraft DC input power across the CMG pivots. This should be combined with the signal level circuits and implemented in a full CMG system for evaluation. The ultimate decision whether or not to eliminate slip rings should be the result of a tradeoff study for each application involving cost, reliability, redundancy configuration of the CMG set used for 3 axis control, the need to eliminate the slip ring contribution to pivot friction (CMG small signal bandwidth) as well as life and in-orbit maintenance and replacement possibilities as is ultimately planned for the Space Shuttle Payloads.

An optical signal transmission technique, employing devices such as light emitting diodes and silicon detectors, is also recommended for study and comparison to the rotating transformer technique studied here. This technique would not require modulation, would have a very high optical bandwidth and would have no cross coupling since multiple paths must be provided.

For the implemented configuration studied in this program, it is recommended that further development work be done to minimize offset and improve gain accuracy by AGC and to eliminate the synch transformer using a phase locked loop.